NIST-GCR-92-603

Concurrent Flow Flame Spread Study

Hai-Tien Loh

United States Department of Commerce
National Institute of Standards and Technology

NIST-GCR-92-603

Concurrent Flow Flame Spread Study

Hai-Tien Loh
University of California
Department of Mechanical Engine
Berkeley, CA 94720

Issued March 1992

Sponsored by:
U.S. Department of Commerce
Barbara Hackman Franklin, ***Secretary***
Technology Administration
Robert **M.** White, ***Undersecretary*** of ***Technology***
National Institute of Standards and Technology
John W. **Lyons, *Director***
Building and Fire Research Laboratory
Gaithersburg, MD 20899

Notice

This report was prepared for the Building and Fire Research Laboratory of the National Institute of Standards and Technology under grant number 60NANB7D737. The statements and conclusions contained in this report are those of the authors and do not necessarily reflect the views of the National Institute of Standards and Technology or the Building and Fire Research Laboratory.

CONCURRENT **FLOW** FLAME SPREAD STUDY

Hai-Tien Loh

Ph.D

Mechanical Engineering

A. C. Fernandez-Pello

Chairman of Committee

ABSTRACT

An experimental study has been performed of the spread of flames over the surface of thick PMMA and thin filter paper sheets in a forced gaseous flow of varied oxygen concentration moving in the direction of flame spread. It is found that the rate of spread of the PMMA pyrolysis front is time independent, linearly dependent on the gas flow velocity and approximately square power dependent on the oxygen concentration of the gas, The experimental data with thin filter paper sheets shows that the flame spread rate is independent of the flow velocity for forced flow conditions and linearly dependent on the oxygen concentration of the flow. In both experiments, it was found that the flame spread rate data can be correlated in terms of parameters deduced from heat transfer considerations only. This indicates that heat transfer from the flame to the condensed fuel is the primary mechanism controlling the spread of flame. Finite rate chemical kinetic effects have apparently a small influence on the flame spread process itself.

Analytical and numerical methods were also employed to study theoretically the flame spread process over thermally thick fuel and the influence on the flow field behavior in the presence of a flame. It is found that an analytical model based on a quasi-steady analysis and the flame sheet approximation predicts a square power law dependence of the flame spread rate on the flow oxygen concentration and a linear dependence on the flow velocity . The correct and encouraging qualitative descriptions of the flow structure and surface fluxes in the region downstream from the pyrolysis front.

Table of Contents

Nomenclature

A Pre-exponential factor

B Mass transfer number

C Sonic nozzle calibration constant

C_p Specific heat of the gas

C_s Specific heat of the solid

D Diffusivity

D_c Nondimensional heat of combustion or sonic nozzle orifice diameter

E Activation energy of the gas phase reaction

F Normalized energy-species function

f Normalized stream function

G Normalized species-species function

g Acceleration of gravity

h Specific enthalpy

L_v Heat of vaporization of fuel

M Molecular weight

$\dot{m}''$ Local mass flux per unit area

$\dot{m}'''$ Mass generation rate per unit volume

P Pressure

P_r Prandti number

$\dot{q}''$ Local heat flux per unit area

$\dot{q}'''$ Heat generation rate per unit volume

Q Heat of combustion

R Universal gas constant

R_e Reynolds number

S Solid phase transformation variable

T Temperature

t time

U Velocity component of gas mixture in the x direction

V Velocity component of gas mixture in the y direction

X_b Burn-out length

X_f Flame length

X_p Pyrolysis length

z Coordinate parallel to the fuel surface

Y_i Mass fraction of species i per unit mass mixture

$Y_{o\infty}$ Oxygen mass fraction in main stream

y Coordinate normal to the fuel surface

Greek

β Shvab-Zeldovich variable

γ Shvab-Zeldovich variable

η Local similarity variable

δ Boundary layer thickness

Λ Ratio of flame length to pyrolysis length

λ Thermal conductivity

w Vorticity in Main Flow

μ Dynamic viscosity

ν **Kinematic viscosity or stoichiometric soefficient**

ξ **Nondimensional coordinate normal** *to* **the fuel surface**

ρ **Density**

σ **Nondimensional coordinate parallel** *to* **fuel surface**

ψ **Stream function**

τ **Fuel thickness** or **dummy integration variable**

Subscripts

f **Fuel**

g **Gas phase**

i **Species**

o Oxygen

p **Pyrolysis or product**

s Solid **phase**

v **vaporization**

w **Wall**

∞ **Ambient value**

Superscripts

$''$ **Per unit area**

$'''$ **Per unit volume**

$\dot{}$ **Per unit time**

Chapter 1 Introduction

1.1 General Problem Statement

The threat of uncontrolled fire has been a problem to societies for centuries. However, an understanding of how fire behave and how environmental factors play a role has still yet to be determined. The need to prevent and control fire hazard thus motivated an active research area aimed at the understanding of the controlling mechanisms leading to the spread of flames as well as its interactions with the surroundings.

Natural fires normally involve diffusion flames spreading over the surface of solid combustibles and result from the complex interactions of transport and chemical processes that occur in the vicinity of the boundary separating the burning and non-burning regions. A very simplified mechanism that describes the initial growth of fire over a horizontal fuel surface in an forced flow environment is illustrated in Fig. 1.1. For the flame to spread over the surface of the solid combustible, sufficient amount of heat must be transferred from the reaction zone to the virgin fuel ahead of the flame via conduction, convection and radiation to cause the fuel to pyrolyze. Once the fuel pyrolyzes, the fuel vapor must react with the gaseous oxidizer from surroundings in order to maintain the flame propagation process. In the concurrent mode of flame spread, the fuel vapors generated upstream of the pyrolysis front are not completely consumed by the upstream diffusion flame . The excess pyrolyzate that exists between the flame and fuel surface is driven ahead of the pyrolysis front where they keep reacting with the oxidizer, thus extending the diffusion flame downstream from the pyrolysis front. The hot, still reacting gas mixture favors the heat transfer to the unburnt material due to its proximity to the fuel surface, as a result, the flame spread process is more rapid and hazardous than in other flow

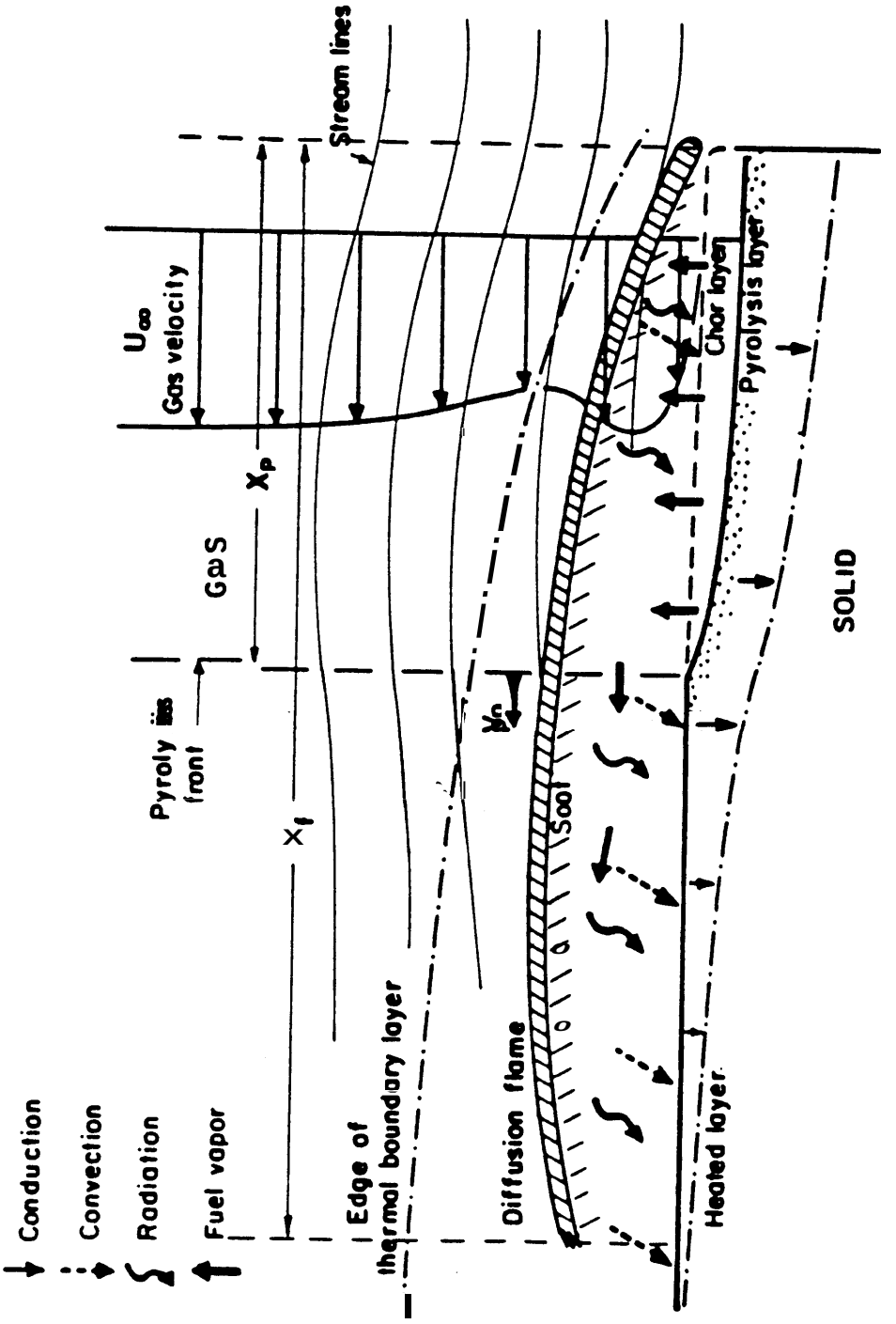
Conduction
Convection
Radiation
Fuel vapor
Edge of thermal boundary layer
Diffusion flame
Soot
Heated layer
Char layer
Pyrolysis layer
SOLID
Stream lines
U_∞ Gas velocity
X_p
Gas
Pyrolysis front
X_f
y_n

Fig. 1.1

configurations. This downstream flame is practically independent of the existence of a spreading process, except that its length is a function of the length of the pyrolysis region. For this reason, this mode of flame spread appears to be controlled primarily by the rate of heat transfer from the downstream flame to the unburnt fuel surface through conduction, convection and radiation. The downstream flame involves and is close to the unburnt fuel surface and, once the fuel starts to pyrolyze, the fuel vapors incorporate themselves in the diffusional process that initially established the flame. Thus, the flame spread process consists primarily in the spread of a pyrolysis or sublimation front. The rate of flame spread will depend on how fast the surface temperature of the solid is raised to its pyrolysis temperature. This will depend, in its turn, on the length of the flame and the heat flux from the flame to the combustible. Gas phase chemical kinetics appears to be unimportant in the flame spreading process itself. It is important, however, in the establishment and length of the flame.

1.2 Objective of The Study

Although the problem of flow assisted type of flame spread has been extensively studied, only very limited amount of information about the concurrent mode of flame spread process is available in the literature. Current interest was motivated by a lack of understanding concerning the flame spread process in a concurrent flow environment and is aimed at identifying the controlling mechanisms of the flame spread process, especially the effect of external flow velocity and oxygen concentration on the flame spread rate.

The present work will follow a progressive path as follows:

(1) An experimental measurement is carried out on the flame spread rate under varied flow velocity and oxygen concentration for two different kinds of

fuels. One is a thermally thick fuel where the temperature gradient along the longitudinal direction is negligible and the dominant mode of heat, transfer path in the solid is in the normal direction, the other is a thermally thin fuel where the fuel is thermally thin enough that the temperature gradient across the thickness of the fuel can be neglected, This experimental information could help the determination of the controlling mechanisms for the flame spread rate.

(2) A simplified mathematical model based on heat transfer considerations alone for the concurrent mode of flame spread over a flat surface is proposed. The analytical approach makes use of an infinitely fast chemical reaction rate and quasi-steady approximation for the gas phase process, which provides an analytical expression for the rate of flame spread in terms of the fuel properties and the ambient conditions.

(3) A numerical study is carried out on the flow assisted type of flame spread to identify the gas phase transport process, the dynamic structure of the flow field and their interactions with the surroundings due to the presence of a flame.

Chapter 2 Experimental Procedure and Apparatus

2.1 Introduction

The flow assisted type of flame spread is characterized by a flame spreading over the surface of the condensed fuel in a gaseous oxidizer that flows, either naturally induced or forced, in the same direction of flame propagation. The hot, still reacting and the post-combustion gases generated in the burning region of the fuel move ahead of the pyrolysis front enhancing the transfer of heat to the unburnt material and consequently the spread of flame. The resulting flame spread process is generally very rapid and hazardous, and therefore of great interest in the fire safety fields.

The realization of the practical importance of the flow assisted type of flame spread has motivated the development of test methods that involve this mode of flame spread, and recently the concentration of research efforts in this area. However, the early interest in the opposed mode of flame spread and difficulties associated with the experiments have resulted in a scarcity of fundamental information about the controlling mechanisms of the flame spread process. Most of the work performed to date has been for vertically upward flame spread in a natural convective atmospheric environment [1-7], and only very limited preliminary data is available for flame spread in a concurrent forced flow [8]. The reader is referred to the recent reviews of reference 9 and 10 for an overview of the current status of the research in this area.

In the present work an experimental study is presented of the spread of flames over the surface of both thermally thick and thin fuels in a forced gaseous flow moving in the direction of flame spread. The objective of the study is to provide basic information that could help the determination of the controlling mechanisms of the flow assisted mode of flame spread. The success in

obtaining this type of experimental information in studies of flame spread in opposed flows by analyzing the combined effects of gas velocity (or gravity) and oxygen concentration on the flame spread rate [9, 11-13], moved us to perform similar experiments in a concurrent forced flow. In the flow assisted mode of flame spread, the spread process can be viewed as the spread of a pyrolysis or burning front. The rate of flame spread will depend on how fast the surface temperature of the solid downstream from the pyrolyzing front is raised to its pyrolysis or vaporization temperature. Once the combustible material is gasified the fuel vapors are incorporated by convection and diffusion into the flame, which sustains the spread process through heat transfer to the unburnt fuel. Through our experiment, it is found that the experimental measurements of the rate of flame spread over thick PMMA sheets for different flow velocities and oxygen concentrations can be correlated in terms of a single nondimensional parameter that describes the heat transfer mechanisms from flame to fuel, and that finite rate chemical kinetic effects have apparently a small influence on the flame spread process.

Most experimental studies of the flow assisted mode of flame spread have been performed with thick fuels [3,4,6,8,9,23]. The only studies performed with thin fuels are the experiments of Markstein and de Ris [1,2] with cotton sheets and Hirano and Sato [5] and Hirano et al [24] with paper sheets. In all cases the flame spread in an air flow. Thus, in our study, a second experiment is carried out on the spread of flames over the surface of thin filter paper sheets in a forced flow environment with varied flow velocity and oxygen concentrations moving in the direction of flame spread to simulate a thermally thin fuel experiment. The objective of this study is to investigate the flame spread rate when the temperature gradient across the thickness of the fuel can be neglected. Of particular importance is the study of the influence of the burn-out

process of the fuel on the flame spread rate. **A** similar non-dimensional parameter was found to be able to correlate the experimental measurements when the steady state spreading rate was achieved.

2.2 Instrumentation

2.2.1 Wind Tunnel Design

A schematic diagram of the wind tunnel design is shown in fig.2.1. It includes four parts:

(1) **A** mixing chamber with dimension **12** inch **x 5** inch **X 7** inch: It has two intake tubes, each of 1/2 inch in diameter oriented perpendicular to the main flow direction. This provides the necessary mixing of the oxidizer with the flow.

(2) **A** laminated section of dimension 12 inch x **5** inch x **16** inch filled with glass beads of **6** mm in diameter and two mesh screens at inlet and outlet. It serves to reduce the local reynolds number and thus partially laminate the flow.

(3) Convergent section: which was shown in **fig.2.2.** It has dimension of 12 inch x 5 inch at its inlet and **3** inch x **5** inch at its outlet. This section serves to laminate the flow and stretch the vorticities generated in the upstream flow according to formula

$$\frac{\omega_{in}}{L_{in}} = \frac{\omega_{out}}{Lout} \tag{2.1}$$

where ω_{in} is the vorticity at inlet, ω_{out} vorticity at outlet, L_{in} the characteristic length at inlet, L_{out} the characteristic length at outlet.

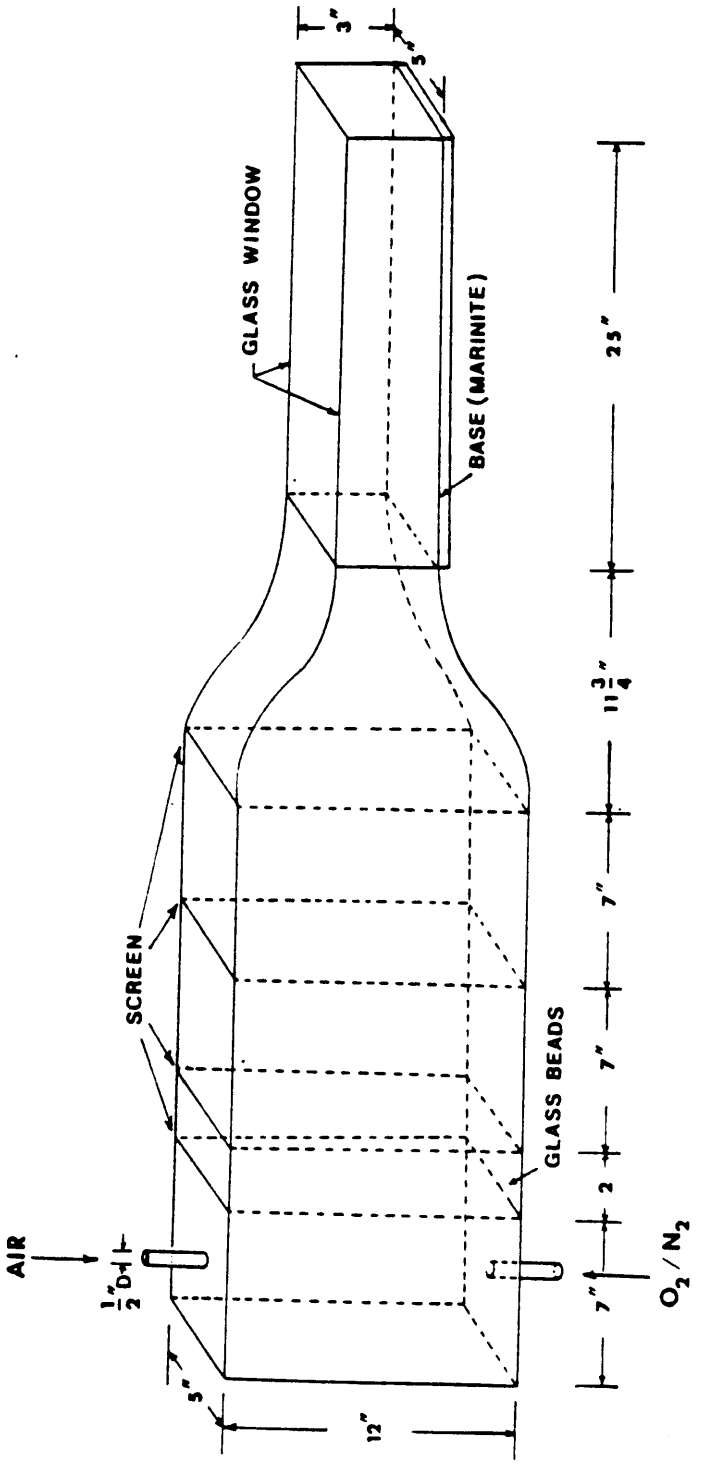
GLASS WINDOW
BASE (MARINITE)
SCREEN
GLASS BEADS
AIR
$\frac{1}{2}$"D
O_2 / N_2
3"
3"
25"
$11\frac{3}{4}$"
7"
7"
2
7"
12"
3"

Fig. 2. 1

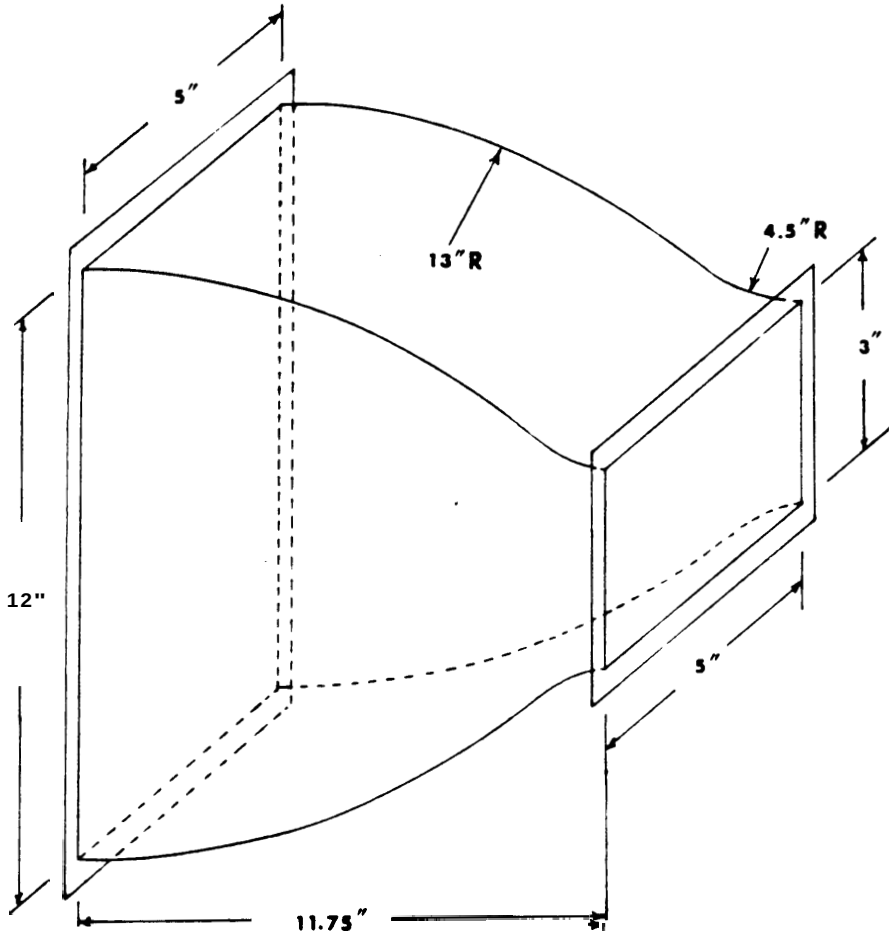

Fig. 2. 2

(4)Test section: This section has a dimension of **3** inch **x 5** inch **x 25** inch with two **1/4** inch thickness pyrex glass along the narrow sides to provide optical access to the test area during the flame spread experiments. It has a movable base **made** of marinite and a hollowed rectangular section where the fuel sample **is** inserted. This arrangements prevents the possible heat transfer path along the side ways.

With present setup, the flow velocity attainable in the test section is between 0 to 4 m/s and a turbulence level $\frac{\Delta V}{V} < 0.5\ \%$.

2.2.2 Flow Control System

2.2.2.1 Sonic Nozzle

Fig.2.3 shows the schematic diagram of the sonic nozzle design used to control the flow rate in the wind tunnel. There are two sonic nozzles used in our experiment, one for the oxidizer and the other for either nitrogen or air. Each of the nozzles has four orifices with dimension 0.0625 inch, 0.1 inch, 0.2 inch and **0.3** inch. Proper choice of the combinations of the orifices with its upstream pressure could choke the **flow** and yield velocity in the test section ranging from 0 to 4 m/s according to the following formula

$$V = (0.8856 D_{o_2}^2 P_{o_2}^o + 0.8284 D_{n_2}^2 P_{n_2}^o)(0.8755 - 0.1067 Y_{o_2})\ C \qquad (2.2)$$

$$Y_{o_2} = \frac{D_{o_2}^2 P_{o_2}^o}{0.9354 D_{n_2}^2 P_{n_2}^o + D_{o_2}^2 P_{o_2}^o} \qquad (2.3)$$

with

D_{o_2} :orifice diameter for oxygen.

D_{n_2} :orifice diameter for nitrogen.

$P_{o_2}^o$:stagnation pressure for oxygen.

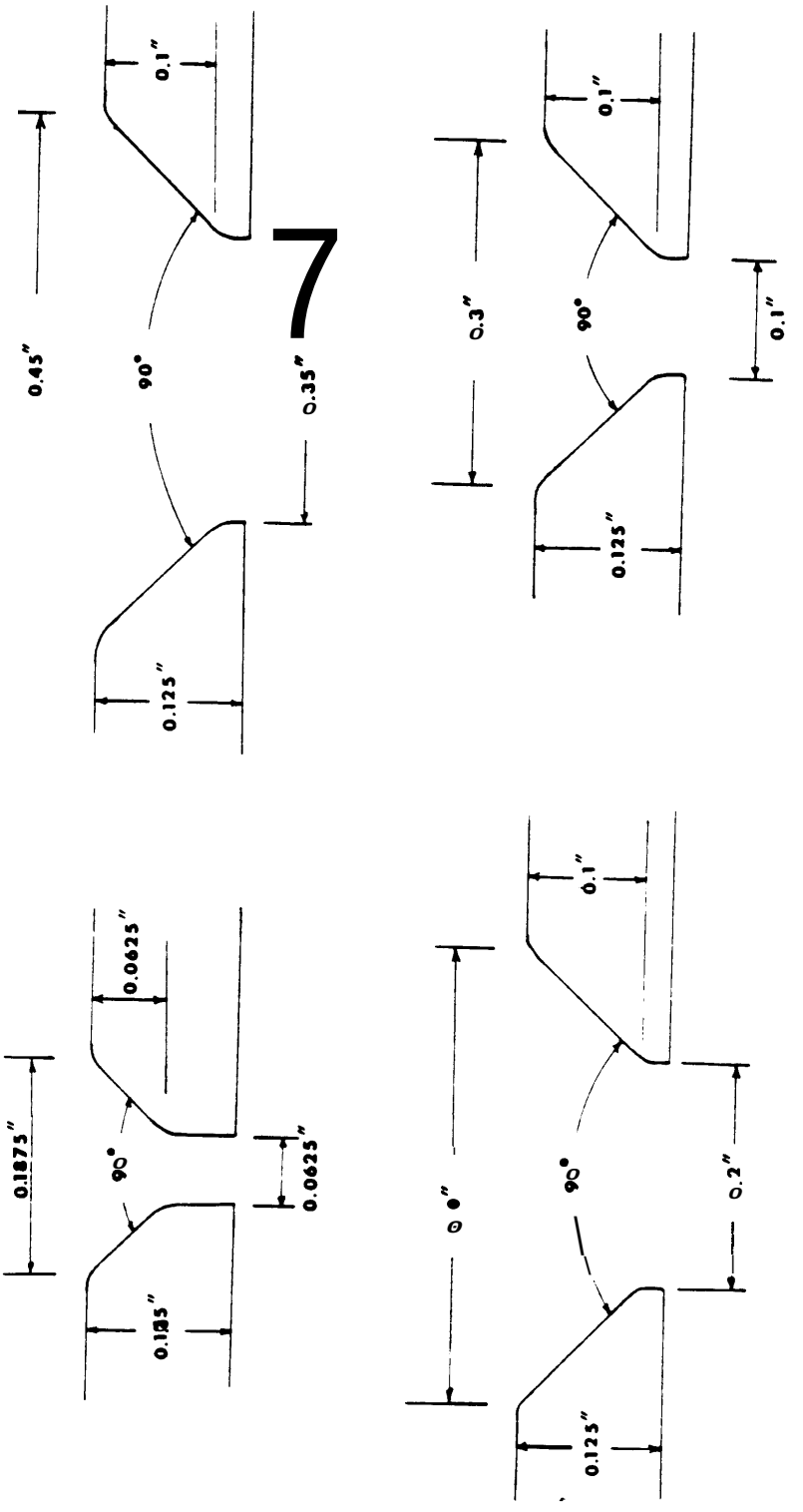
0.45"
90°
0.1"
0.35"
0.125"
0.3"
0.1"
90°
0.125"
0.1"
0.1875"
90°
0.0625"
0.0625"
0.125"
0.1"
90°
0.2"
0.125"

Fig. 2.3

Table **2.1**

			2	3	4
AIR/N_2	C	0.945	0.996	0.859	—
O_2	C	0.963	0.908	0.852	—

$P_{n_2}^{o}$:stagnation pressure for nitrogen.

Y_{o_2} :oxygen mass fraction in test section.

C is a calibration constant to be determined from flow rate measurements. Table 2.1 shows the measured calibration constant C through a west test meter.

2.2.2.2 Flow Field Measurements

A constant temperature compensated hot wire anemometer model TSI-1010 with linearizer model TSI-1005B was used to determine the flow behavior in the test section prior to perform the flame spread measurements. This system was carefully calibrated in an wind tunnel which capable of measuring velocity down to 5 m/s. The calibrated curve of Fig. 2.4 was extrapolated to the flow range of 0 to 4 m/s attainable in our experiment The maximum error of the measured flow velocity was estimated to be 1.5 % and with an average error of 0.5 %. The heart of this system is a voltage controlled heat flux system which utilizes a bridge circuit to maintain a resistance element at essentially constant resistance by varying the current that passing through it. This, in its turn is then related to the changes in the environment conditions. The flow field behavior was established by sweeping the sensor probe through the crosection area at the inlet, of the test section.

2.2.3 Fuel Sample Arrangement

2.2.3.1 Thermally Thick Fuel

The fuel sample used was polymethylmethacrylate(PMMA) with a dimension of 3 inch x 12 inch x $\frac{1}{2}$ inch. Fig.2.5 shows the fuel sample arrangement in the test section, it was clamped and bolted into place on a bed of metal of

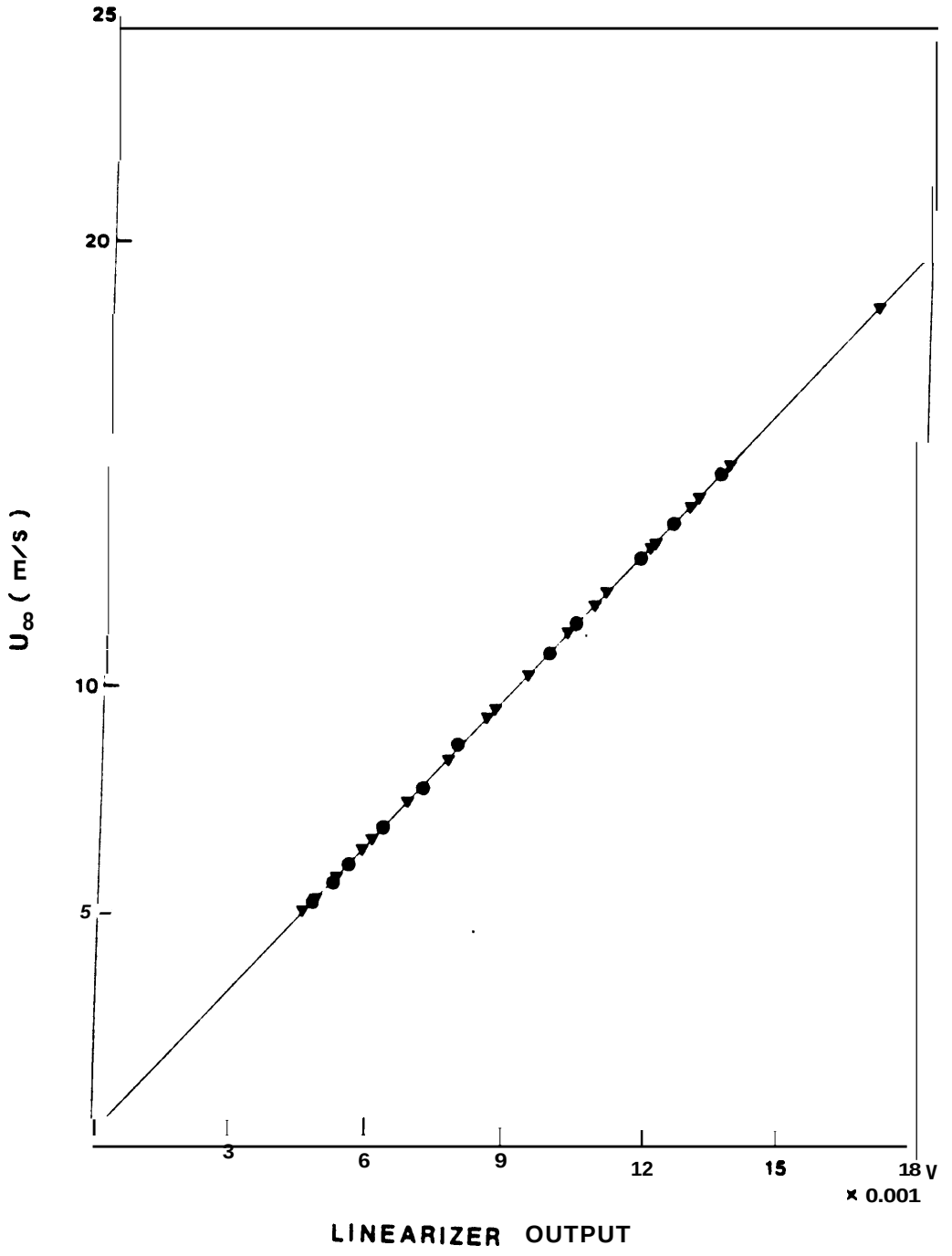

Fig. 2. 4

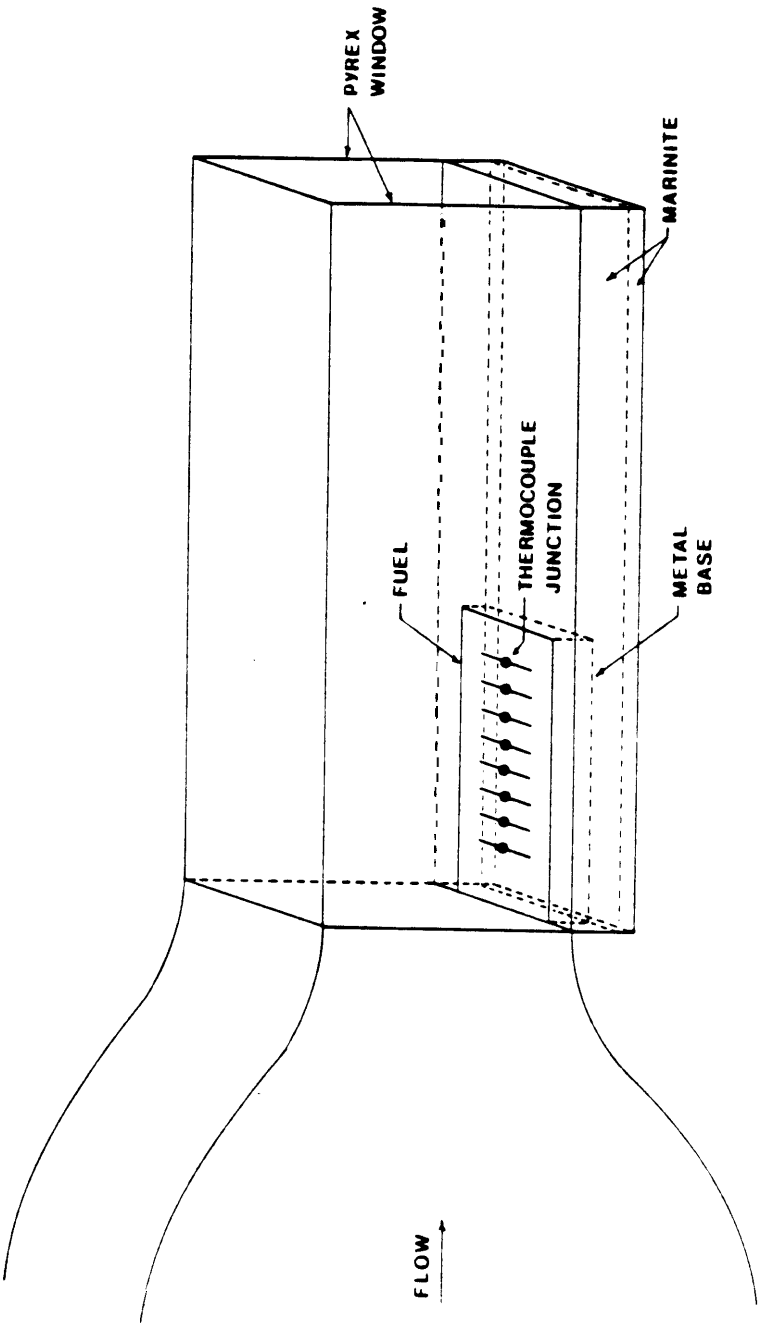
PYREX WINDOW
MARINITE
THERMOCOUPLE JUNCTION
FUEL
METAL BASE
FLOW

Fig. 2. 5

dimension 3 inch x 12 inch x $\frac{1}{4}$ inch which was hollowed in its center to allow the thermocouples passing through. The clamping was to minimize the effects of fuel buckling encountered during the burning process. There are eight pairs of holes of dimension $\frac{1}{16}$ inch in diameter spacing 2 inch apart drilled on the fuel sample to allow the pass of thermocouples. The thermocouples are 0.005 inch diameter Chromel-Alumel wires with its junction beads soldered flush on the fuel surface to provide the temperature reading during the experiments. The output from thermocouples are then feed through an amplifier and recorded by a minicomputer through an externally controlled clock. This provides the necessary informations for the measurement of flame spread rate.

2.2.3.2 Thermally Thin Fuel

Fig.2.6 shows the schematic diagram of the fuel sample arrangement for the thermally thin fuel experiment. The fuel specimen are 0.33 mm thick Whatman Chromatography filter paper, 0.076 m wide by 0.45 m long. The paper sheets are mounted in a metallic frame by inserting them in metallic spikes placed $\frac{1}{2}$ inch apart on the sides of the frame. The spikes are used to hold the paper in slight tension to provide a flat surface [5] and favor the ignition. The paper sheets are dried in an oven and kept in a dessicator for at least forty-eight hours prior to performing the flame spread measurements.

2.3 Thermally Thick Fuel Experiment

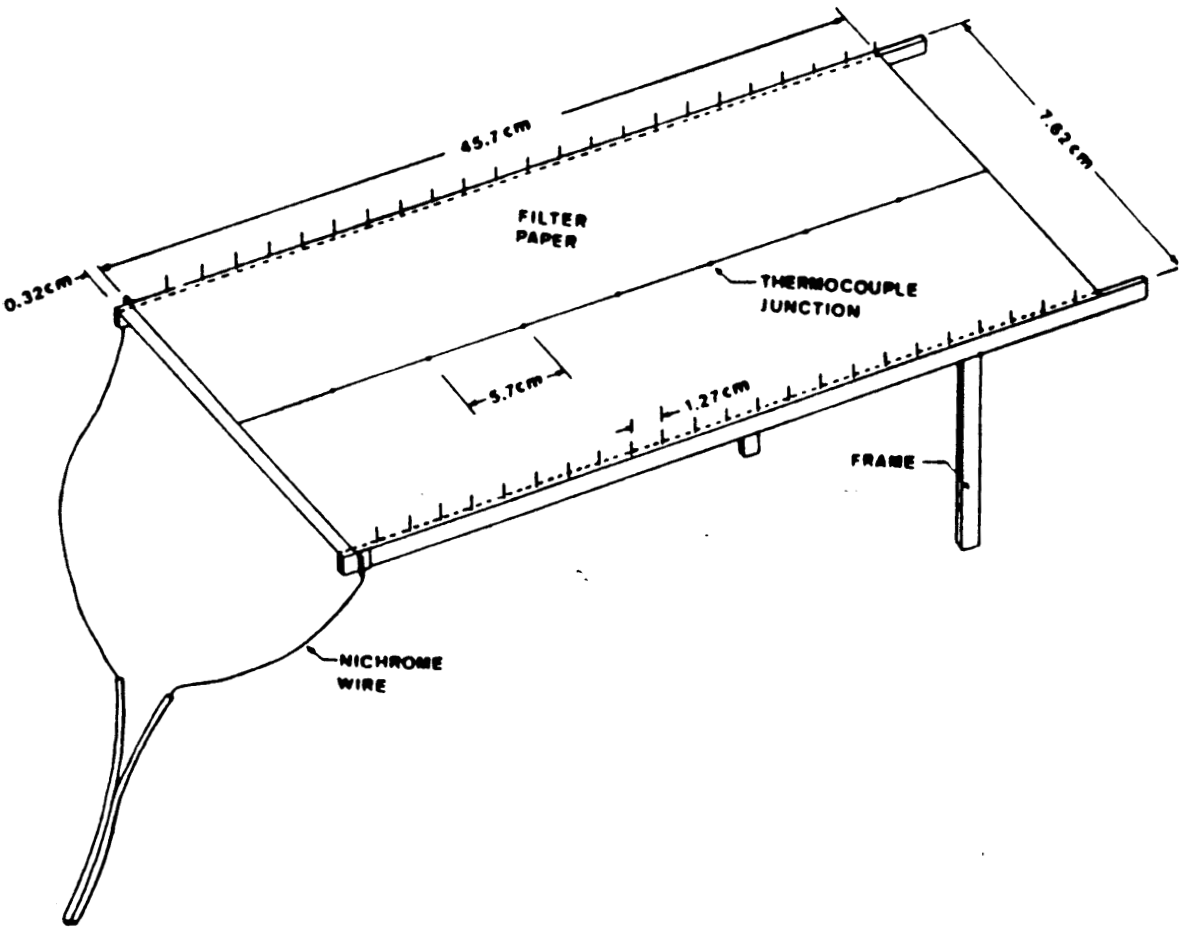
45.7cm
7.62cm
0.32cm
FILTER
PAPER
THERMOCOUPLE
JUNCTION
5.7cm
1.27cm
FRAME
NICHROME
WIRE

Fig. **2. 6**

2.3.1 Experiment

A schematic diagram of the experimental installation is shown in fig.2.7. The experiments are carried out in a small scale combustion tunnel with a test section 0.61 m long of rectangular cross section 0.127 m wide and 0.076 m deep. [23] The walls of the wide sides of the test section are made of 0.0254 m thick Marinite and the walls of the narrow sides of pyrex glass 0.006 m thick to allow optical access to the test area. The thick fuel specimens are 0.076 m wide by 0.3 m long, and are mounted flush in one of the Marinite walls with the upstream leading edge placed 0.015 m from the exit plane of the convergeht nozzle of the tunnel so that a flat plate flow is generated over the fuel surface. The combustible material used in the present experiments is polymethylmethacrylate (PMMA) sheets 0.0127 m thick as representative of a non-charring thermally thick fuel.

The gas flow in the tunnel is supplied either from a centralized compressed air installation or from bottles of compressed oxygen and nitrogen. The gas flows of the individual gases are metered with critical nozzles and mixed at the settling chamber of the tunnel. Oxygen and Nitrogen mixtures with concentration accurate to within 1 % are obtainable with the present arrangement. Maximum gas velocities attainable in the test section with the current installation are of the order of 5 m/s. The gas velocity is measured both with a pitote probe instrument capable of measuring velocities down to 0.4 m/s, and with a hot wire anemometer. Prior to performing the experiments, extensive measurements were made of the velocity profiles along several planes of the test section to determine the characteristics of the flow. For the range of gas velocities used in these experiments the flow over the fuel specimen was found to be laminar and of the flat plate type. Under combustion conditions the maximum flow reynolds number at the downstream edge of the fuel specimen is of the order of 10^4.

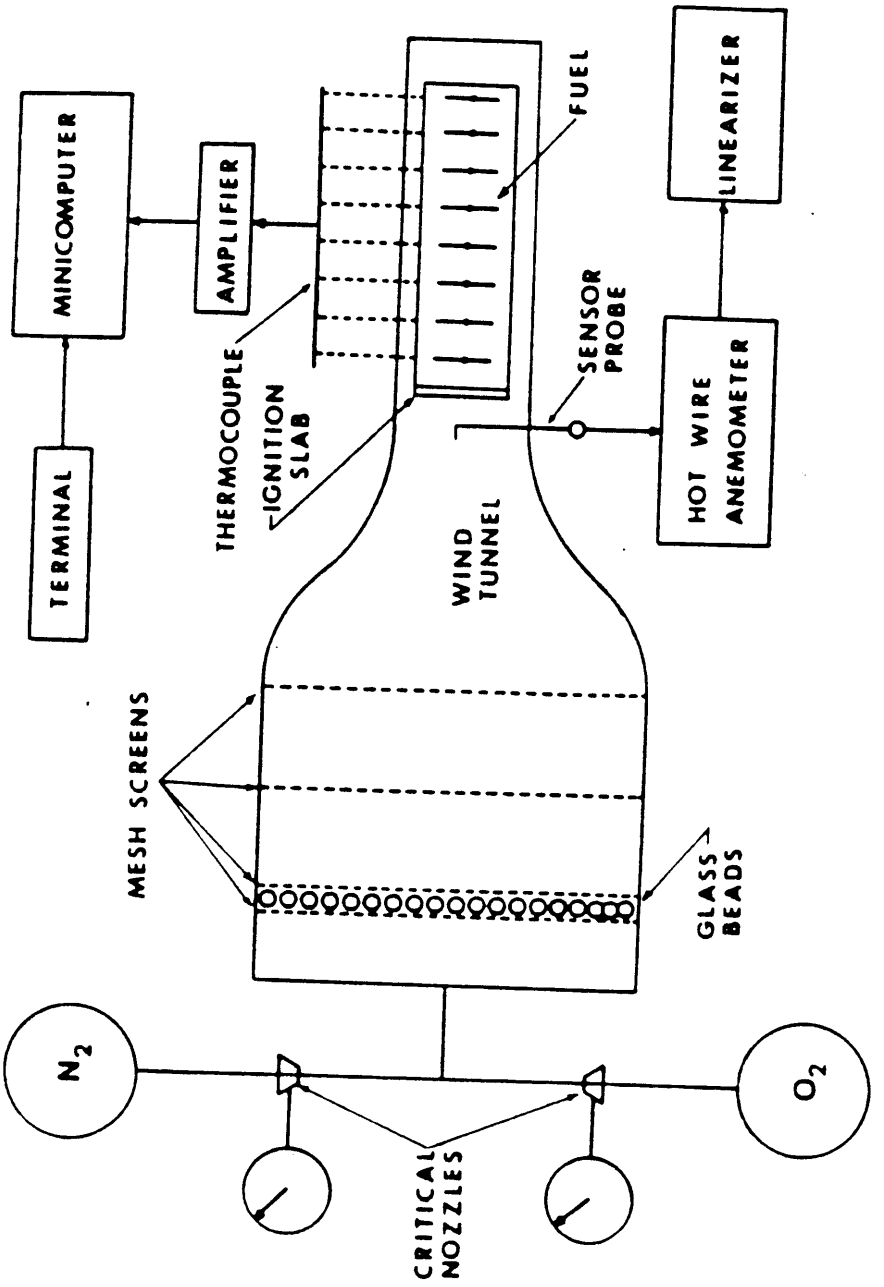
MINICOMPUTER
AMPLIFIER
LINEARIZER
FUEL
TERMINAL
THERMOCOUPLE
IGNITION SLAB
SENSOR PROBE
HOT WIRE ANEMOMETER
WIND TUNNEL
MESH SCREENS
GLASS BEADS
N_2
O_2
CRITICAL NOZZLES

Fig. 2. 7

In the flow assisted mode of flame spread it is very important to obtain a uniform and well defined (in time and space) initiation of the flame to simulate a two dimensional flame spreading process [14]. This is, however, difficult to accomplish because at the upstream leading edge region where the fuel is first ignited near-extinction conditions often prevail due to the Damkoller number effect, which makes the ignition of the fuel difficult particularly at high gas velocity or low oxygen concentrations. On the other hand, once the ignition of the fuel take place the flame spreads very fast due to the heat transfer from the post-combustion gas, which requires a very fast response to determine in practice the instant of flame spread initiation. The large spread rate and the fact that in this mode of spread the flames bath the unburnt fuel surface make also difficult the accurate measurement of the flame spread rate. To overcome theses difficulties and reduce the error in determination of the moment of ignition the following experimental procedure was followed. With the fuel sheet positioned in the test section, the gas flow is established at the predetermined velocity and oxygen concentration. During the process of fuel ignition the gas flow is by-passed to have a quiescent gas near the fuel surface and thus facilitate its ignition. The thick PMMA sheets are ignited by first igniting a thin PMMA strip which is placed along the upstream leading edge of the PMMA sheet. The thin PMMA strip is very easy to ignite and provide a consistent and uniform ignition source. Because the initiation of the PMMA burning is relatively slow, during the ignition process the PMMA surface is covered with a Mariuite sheet except for a narrow strip at the upstream edge of the sheet to prevent the preheating of the fuel and the uncontrolled spread of flames before a uniform ignition is accomplished. The length of the uncovered PMMA surface is increased from 0.01 m up to 0.04 m to overcome the extinction conditions [27,28] that occurred at low oxygen concentrations and high flow velocities.

Once it is considered that the PMMA has been ignited and is burning uniformly, the flow by-pass is rapidly closed, the insulation cover removed and the data acquisition process initiated.

The rate of flame spread is measured from the temperature histories of the thermocouples placed at fixed distances along the fuel surface [5]. Eight Chromel- Alumel thermocouples 0.127×10^{-3} m in diameter are enbeded on the PMMA with their beads flush with the PMMA surface at distances **0.03175** m apart. The output from the thermocouples is amplified through an amplifier and processed in a real time data-acquisition system (PDP-11 minicomputer). With the surface temperature histories recorded by the minicomputer, the rate of spread of the pyrolysis front is calculated from the time lapse of pyrolysis arrival to two consecutive thermocouples and the known distance between the thermocouples. The arrival of the pyrolysis front at the thermocouple position is characterized by the leveling of the temperature profiles when the approximately constant pyrolysis temperature of the fuel is reached. Fig.2.8 shows a typical surface temperature measurement from thermocouple output, it is seen that before the flame tip arrives the thermocouple location, the heat transfer from the post-combustion gases to the fuel surface is insignificant and the fuel remains at approximately the ambient temperature. As the flame extended its length along the burning process, the fuel surface are gradually heated up at approximately a constant rate until it reaches its vaporization temperature which record the arrival of the pyrolysis front, from then on the fuel surface remains at its vaporization temperature until the fuel surface has regressed an appreciable amount that the thermocouple beads were exposed to the ambient flow and finally burnt by the flame.

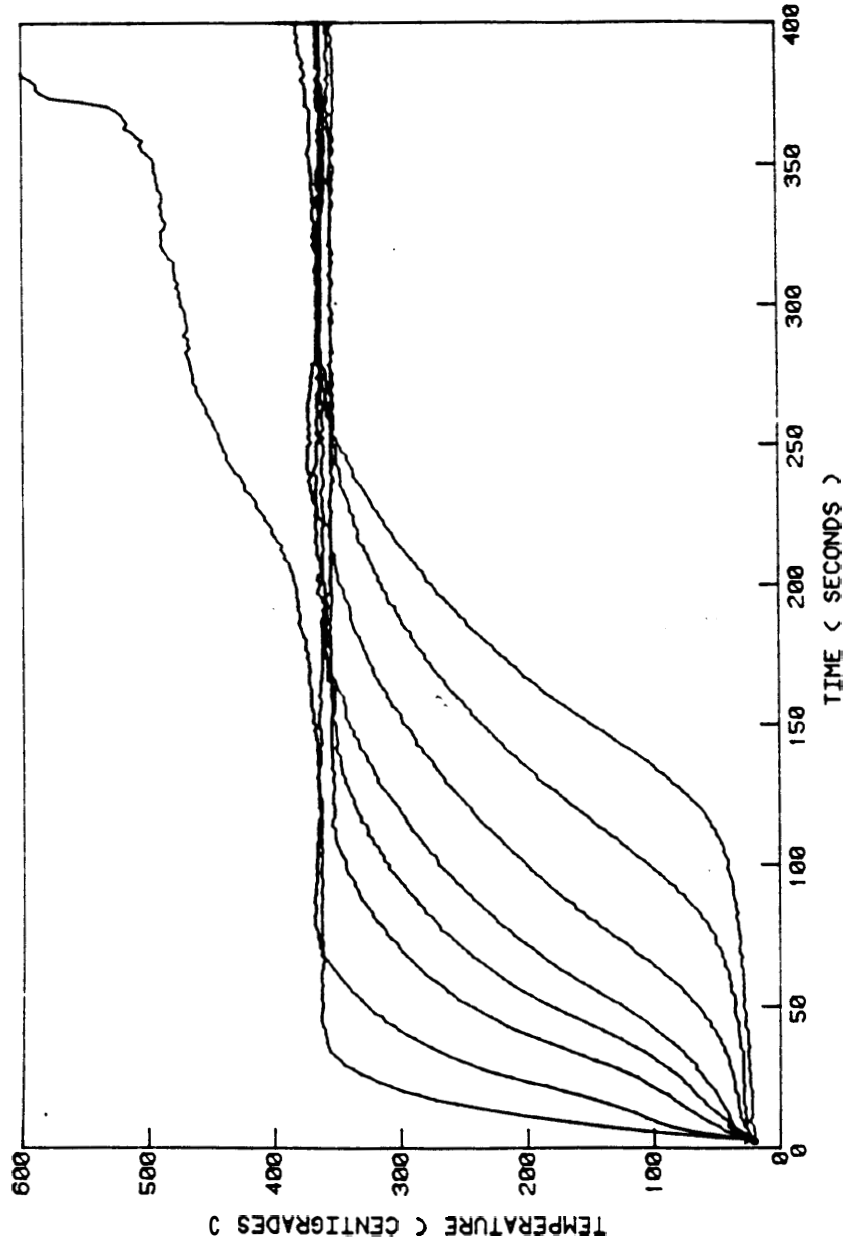
TEMPERATURE (CENTIGRADES)
600
500
400
300
200
100
0
0
50
100
150
200
250
300
350
400
TIME (SECONDS)

Fig. 2. 8

2.3.2 Results

The experimentally measured progress of the pyrolysis front over the PMMA surface is used to calculate the local rate of spread with the ratio of the increment of the pyrolysis distance to the time increment. Fig.2.9 shows a plot of the pyrolysis front histories at various flow velocities and fig.2.10 shows the effect of oxygen concentration on the pyrolysis length growing rate at $U_\infty =$ 1.5 m/s. Both plots shows that, within experimental error, there is a linear dependence on time of the distance from the upstream leading edge to the pyrolysis front (pyrolysis length X_p) at fixed U_∞ and $Y_{o\infty}$, therefore the rate of flame spread, which is the slope of the lines in the plot, is independent of time. It is also seen that from fig.2.9 and fig.2.10 that as either U_∞ or $Y_{o\infty}$ increases, the slope of the lines increase, which indicate the pyrolysis front velocity increases. The calculated rates of spread of the pyrolysis front, V_p, as a function of the concurrent forced. flow free stream velocity, U_∞, are presented in fig.2.11 for several oxygen mass fractions of the flow, $Y_{o\infty}$. Maximum standard deviation was found to be 5 %. The measurements were performed with the combustion tunnel in horizontal position, thus the data for gas velocities of less than 0.5 m/s are probably affected by normal buoyance.

From the results of fig.2.11 it is seen that for all oxygen concentrations there is a linear relationship between the rate of spread of the pyrolysis front and the flow velocity, with the constant of proportionality increasing as the oxygen concentration increases. For a fixed free stream velocity the flame spread rate increases with oxygen concentration following approximately a square power law relationship. It was found that for oxygen mass fractions of 0.2 or smaller, the initiation of the flame spread process becomes increasingly difficult and it appears that the flame do not spread for oxygen mass fractions below 0.18, at least within the current experimental conditions.

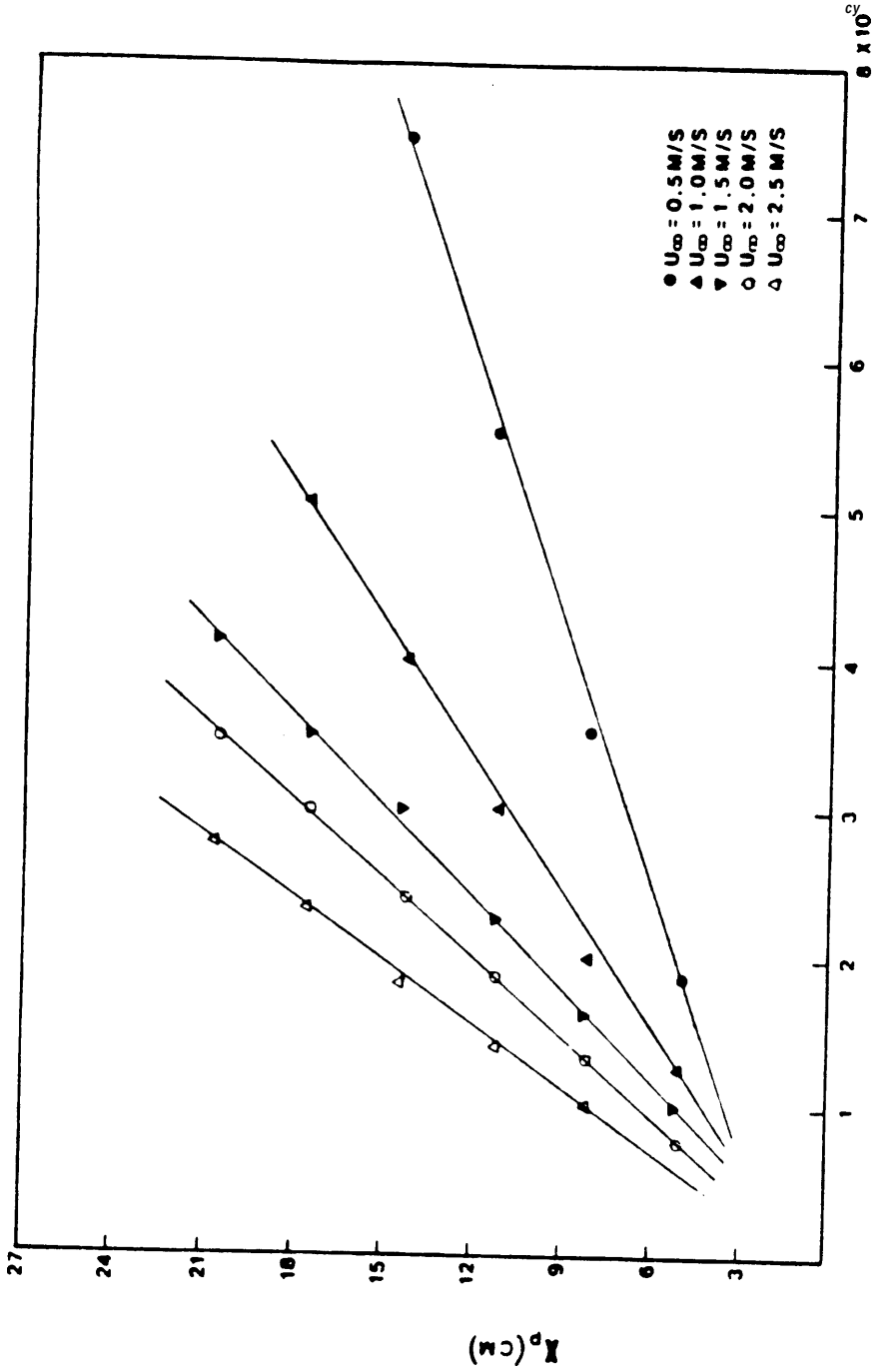
X_p(cm)
TIME (SECOND)
$\bullet$ U_∞ = 0.5 M/S
$\blacktriangle$ U_∞ = 1.0 M/S
$\blacktriangledown$ U_∞ = 1.5 M/S
$\circ$ U_∞ = 2.0 M/S
$\triangle$ U_∞ = 2.5 M/S
8 X 10^{-4}

Fig. 2. 9

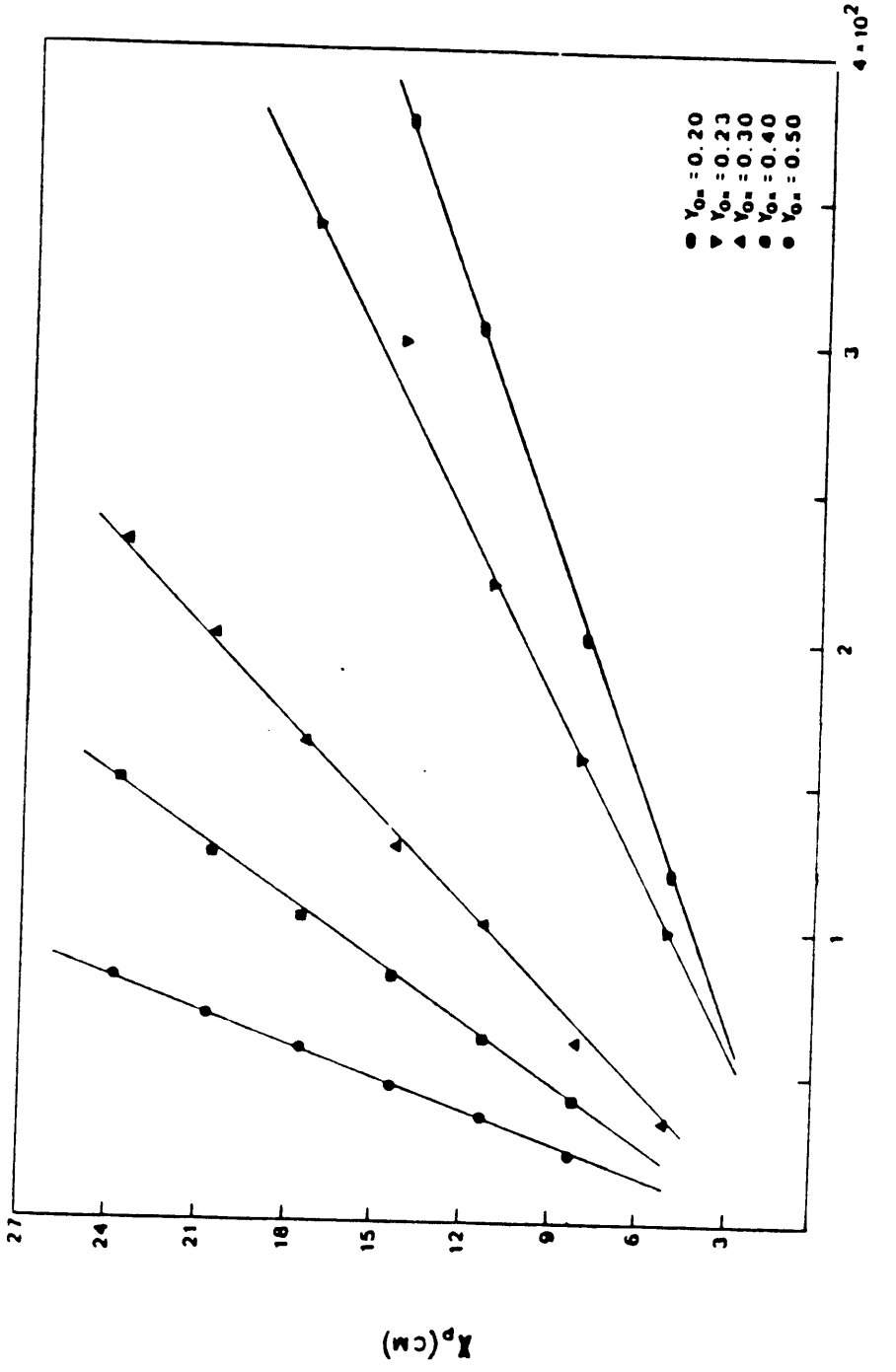
Y_{O_2} = 0.20
Y_{O_2} = 0.23
Y_{O_2} = 0.30
Y_{O_2} = 0.40
Y_{O_2} = 0.50
λ_p(cm)
TIME(SECOND)
4×10^2

Fig. 2. 10

The results of fig.2.11 for the dependence of the flame spread rate on the gas flow velocity and oxygen concentration can be readily explained in terms of the mechanisms that control the transfer of heat from the flame to the fuel. For the flame to spread over the combustible surface, sufficient heat must be transferred from the flame and/or an external source to the unburnt material to increase the combustible surface temperature to its pyrolysis temperature, and to sustain the vaporization of the fuel. The fuel vapors can then react with the oxidizer and sustain the spread of the flame. The rate at which heat is transferred from the flame zone to the combustible material will determine the rate of temperature increase and, consequently, the rate of spread of the pyrolysis region. From the schematic diagram of **fig.2.11** it is seen that the rate of heat transfer to the unburnt material depends on the magnitude of heat flux from the flame to the fuel and on the flame length. As the flow velocity is increased , the thickness of the boundary layer and the flame stand-off distance decrease. This results in the increase of the heat flux at the fuel surface. The increase of the heat flux at the burning surface causes the fuel vaporization rate to increase and as a result the lengthening of the flame. Both effects, the increase of the surface heat flux and of the flame length with the flow velocity, results in an increase of the unburnt fuel heating rate and consequently in a faster spread rate. As the oxygen concentration is increased, the flame temperature increases, the result is an increase of the local heat flux at the fuel surface and of the spread rate with the oxygen concentration. These trends are in agreement with the experimental results of **fig.2.11.**

The present results only provides information up to flow velocity of 4 m/s , however we feel that the data of fig.2.11 is representative of the characteristics of the flame spread process in a concurrent forced flow. Although for much larger flow velocities and/or lower oxygen concentrations, the linear relationship

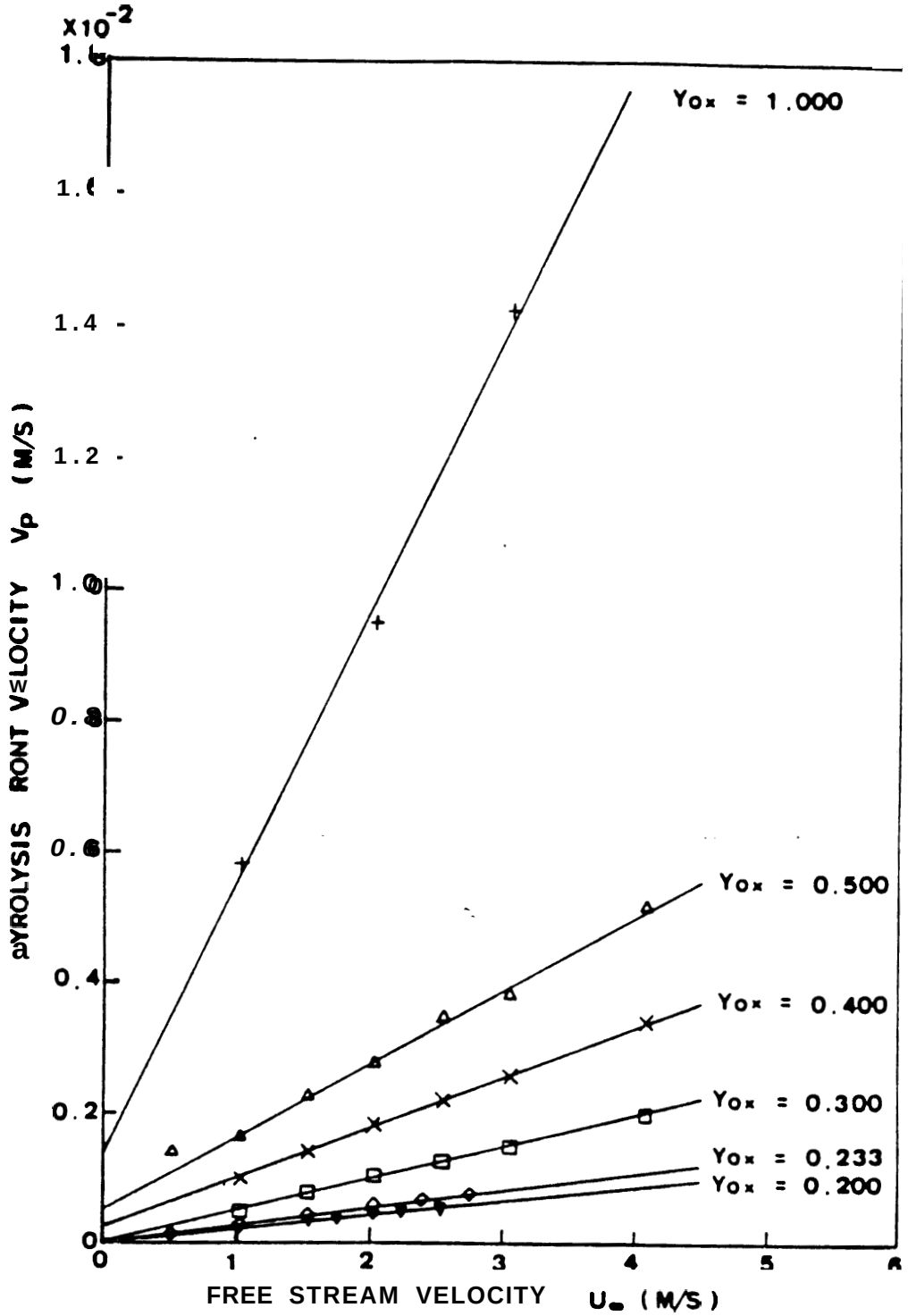
X10^-2
1.6
1.4
1.2
1.0
0.8
0.6
0.4
0.2
0
PYROLYSIS FRONT VELOCITY Vp (M/S)
Yox = 1.000
Yox = 0.500
Yox = 0.400
Yox = 0.300
Yox = 0.233
Yox = 0.200
0
1
2
3
4
5
FREE STREAM VELOCITY U∞ (M/S)

Fig. 2. 11

between the spread rate and time may not hold, this would be the result of phenomena related to the extinction of the flame at its upstream leading edge and not to the flow assisted flame spread process itself. Perturbations of the fuel burning process due to large gas velocities or low oxygen concentrations occur first at the upstream edge of the burning surface and not in the downstream region where the actual spread of the flame occurs. In experiments performed at low oxygen concentrations it was observed that even though a partial region of the burning surface near the upstream leading edge may extinguish, the flame continues to spread in the downstream region. However, since as the pyrolysis length decreases, due to extinction of the upstream region, the flame length will also decrease [15], it is expected that eventually this effect will cause the decrease of the spread rate and consequently the deviation from the characteristics deduced from fig.2.11. For the flame not to spread at all, it appears that the upstream flame must be extinguished to almost the location of the pyrolysis front. The environmental conditions for which this situation will occur can be derived from a steady state extinction analysis of a diffusion flame over a burning surface.

The results of fig.2.11 for the flame spread rate are in sharp contrast with those obtained for flames spreading in an opposed forced flow [12] where for low oxygen concentration the spread rate is found to decrease as the flow velocity increases, and for high oxygen concentrations the spread rate first increase, reaches a maximum, and then decreases as the flow velocity is increased. The dependence on oxygen concentration, although follows the same trend for both modes of flame spread, it is much stronger for the opposed flow mode of flame spread where a difference of three orders of magnitude is observed between the spread rates for pure oxygen and for an oxygen mass fraction of 0.21, while one order of magnitude was measured in the present case.

These differences in flame spread behavior emphasize and verify the earlier stated differences in the controlling mechanisms for both modes of flame spread [9]. While a balance between chemical kinetic and heat transfer mechanisms control the spread of flames in opposed flows, only heat transfer mechanisms appear to control the spread of flames in concurrent flows. The primary reason for this difference is the fact that in flat plate flows, as the flame spreads against the flow, its leading edge encounters higher velocity gradients and larger heat losses to the environment (the boundary layer is thinner), which make it more difficult for the flame to spread and can cause its extinction. In the concurrent mode of spread, however, the flames move toward regions of thick boundary layer, i.e. away from extinction. As a consequence chemical kinetic mechanisms play a lesser role unless the flow conditions are such that flame extinction occurs over most of the fuel burning surface.

2.3.3 Discussion

All of the theoretical models of the spread of flames in a concurrent forced flow published to date are heat transfer models [8,14,16,17]. The flame spread rate process is described as the spread of a pyrolysis or burning front, and the rate of spread depends on how fast the surface temperature of the solid combustible is raised to its pyrolysis temperature by heat transfer from the flame to the unburnt fuel. The flame chemical reaction is assumed to have an infinitely fast reaction rate, thus chemical kinetic effects are not considered. These theoretical models predict rate of flame spread that are linearly proportional to the free stream velocity of the concurrent flow and are, therefore, in qualitative agreement with the result of **fig.2.11.** The effect of the flow oxygen concentration appear in these models through the heat release during the combustion of the fuel (or equivalently the mass transfer number B) which in its turn effects the

heat **flux** at the fuel surface. The work of refs. [8,14] predict approximate square power **law** dependence between the spread rate and the mass transfer number.

The mathematical problem that describe this mode of flame spread basically consists of the solution of the solid phase energy equation with the heat flux at the interface **as** the primary boundary condition. Because the normal temperature gradients are much larger than the longitudinal ones, the one dimensional ,transient, form of the energy equation is sufficient to describe the solid phase process. Thus, the problem is reduced to the solution of the equation

$$\rho_s c_s \frac{\partial T_c}{\partial t} = \lambda_s \frac{\partial^2 T_c}{\partial y^2} \tag{2.4}$$

with the boundary condition that at the fuel surface $y = 0, \lambda_s (\frac{\partial T_c}{\partial y} = \dot{q}''$, and that for $y \rightarrow -\infty$ and at $X = X_f$, $T, = T_i$. Where T, is the solid temperature, T_i is its initial temperature, ρ_s its dnsity, **c,** its specific heat, λ_s its thermal conductivity, t is time, X_f is the flame length, and $\dot{q}''$ is the heat flux at the **gas** side of the interface. The coordinate system used in the above equation is indicated in the schematic diagram of fig.2.12.

The value of the surface heat flux $\dot{q}''$ is given by the solution of the gas phase conservation equations. **A** simple and qualitative approach to this problem is to negelect radiation and to assume that the heat flux at the surface is given by $\dot{q}'' = \lambda_g \frac{(T_f - T_v)}{\delta}$, where T_f is the flame temperature, T_v the fuel pyrolysis temperature and δ the flame stand-off distance. Following boundary layer theory, we can further assume that $\delta \sim \frac{X_p}{\mathrm{Re}^{1/2}}$, with the reynolds number defined **as** $\mathrm{Re} = \frac{U_\infty X_p \rho_g}{\mu_g}$, where U_∞ is the free stream gas velocity and X_p the pyrolysis length. Then the heat **flux** is given by

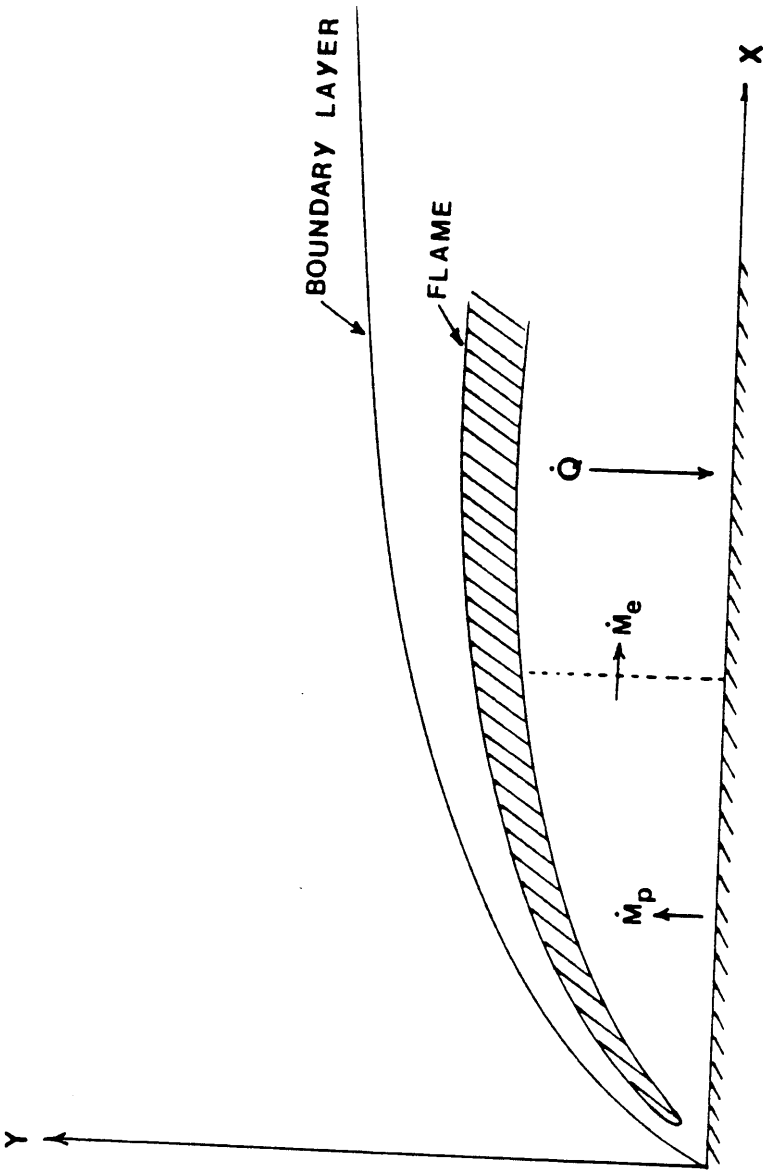

Fig. 2. 12

$\dot{q}'' = (\frac{\rho_g c_p \lambda_g U_\infty}{X_p P_r})^{1/2} (T_f - T_v)$, and by further assuming constant solid fuel properties it is possible to obtain an analytic solution for equation **(2.4)** [18]. Imposing the condition that at the pyrolysis front the surface temperature of the solid is equal to its vaporization temperature, the following expression is obtained for the rate of spread of the pyrolysis front

$$V_p = \frac{\rho_g c_p \lambda_g (T_f - T_v)^2}{\rho_s c_s \lambda_s (T_v - T_i)^2} U_\infty \qquad (2.5)$$

In **fig.2.13** a correlation is presented in terms of Equation **(2.5)** of the flame spread rate data of fig.2.10. The data used in the computation of the figure are: $\rho_s = 1.19 \times 10^3 Kg/m^3$, $c_s = 2.09 KJ/Kg$ **K**, $T_v = 663 K$, $T_i = 295 k$. The flame temperature T_f is calculated with the equation

$$T_f = T_v + \frac{Y_{o\infty}(Q - L)}{C_p \nu} - \frac{(T_v - T_i)}{1 + \frac{Y_{o\infty}}{\nu}} \qquad (2.6)$$

that corresponds to the adiabatic flame temperature for constant specific heat of the products of combustion, with' $L = 1.58 X 10^3 KJ/Kg$ of PMMA, $Q = 13.56 X 10^3 KJ/Kg$ of oxygen, $C_p = 1.25 KJ/Kg$ k, $\nu = 1.92$. The gas density ρ_g, specific heat C_g and thermal conductivity λ_g are taken as those of nitrogen at the PMMA pyrolysis temperature. From the results of **fig.2.13** it is seen that except at low flow velocities where buoyance effects becomes important, the expressions for the spread rate of equation **(2.5)** correlates quite well the flame spread data of **fig.2.11.** It should be pointed out that the value for the flame temperature given by the above equations are very high, particularly at high oxygen concentrations, however the use of more realistic flame temperatures as those given by the **NASA** equilibrium program [20] does not result in a good correlation of the experimental data. The fact that the nondimensional

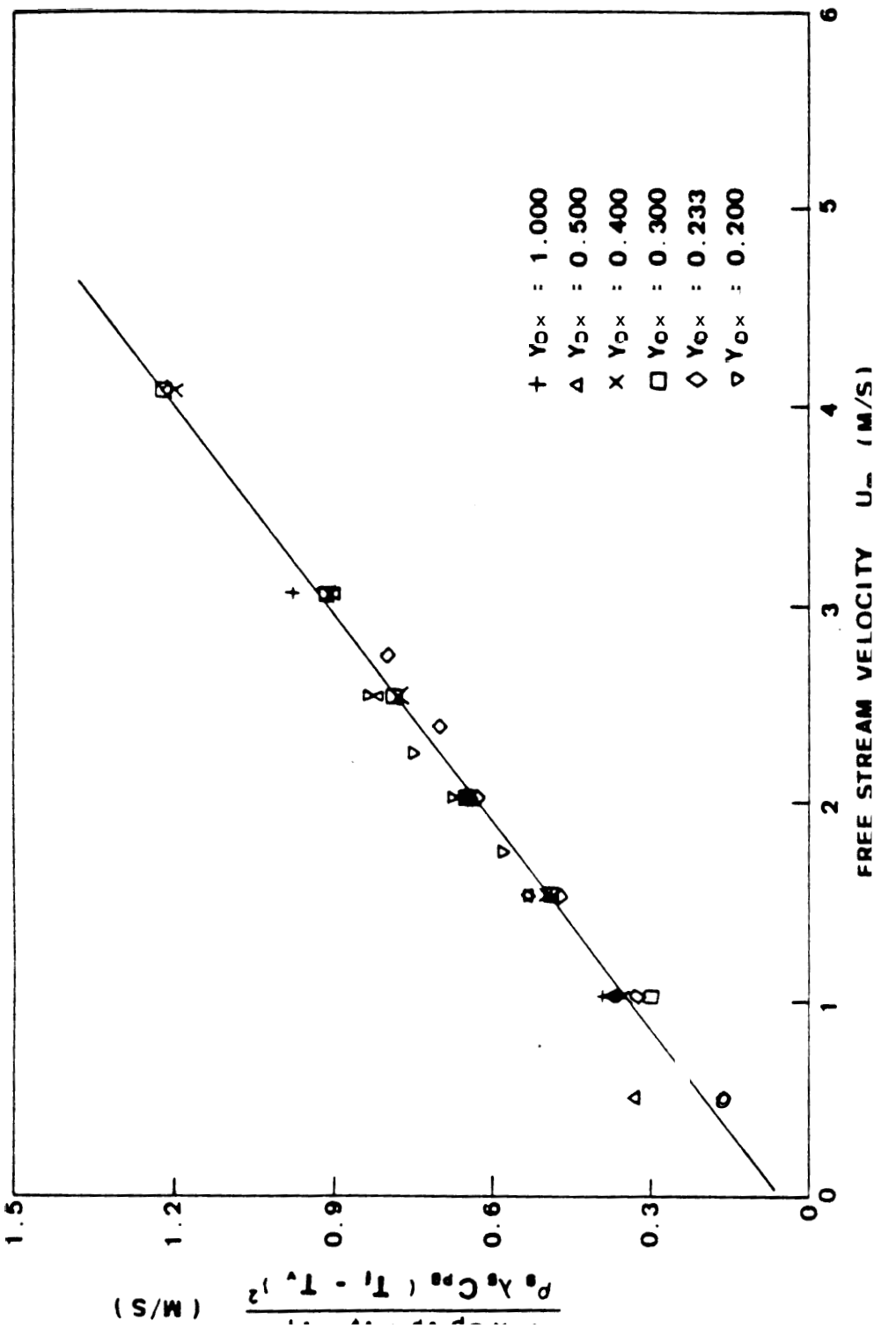
+ Y∞ = 1.000
△ Y∞ = 0.500
× Y∞ = 0.400
□ Y∞ = 0.300
◇ Y∞ = 0.233
▽ Y∞ = 0.200
FREE STREAM VELOCITY U∞ (M/S)
0
1
2
3
4
5
6
0.3
0.6
0.9
1.2
1.5
(M/S)

Fig. 2. 13

parameter used in the correlation is derived from an analysis [19] that assumes constant specific heat, provides justification for the use of such high temperature since they are obtained from an equation which is consistent with the analysis from which the correlation is deduced.

A correlation of the experimental results that also provides good results is one in terms of the mass transfer number B of the form $V_p \sim B^{1.8} U_\infty$, where

$$B = \frac{Y_{o\infty} Q - C_p (T_v - T_i) \nu M_o}{\nu M_o L} \tag{2.7}$$

The correlation of the data is practically identical to that presented in fig.2.13, thus it is not given here. The practically identical correlations that are obtained in terms of equation **(2.5)** or of the above B power law is understandable since comparison of equation **(2.6)** and **(2.7)** shows that both B and $T_f - T_i$ are almost linearly proportional to $Y_{o\infty}$ and to each other. The works of reference [8,14] predict power law dependence of V_p on B that are approximately square, and are consequently in qualitative agreement with the experimental results.

An important result, that is derived from the correlation of fig.2.13 is that, since no finite rate chemical kinetic parameters appear in the correlation, the flame spread process is only controlled by heat transfer mechanisms alone for the range of the present experimental conditions. Another interesting result is that the spread rate formula is, except for the constant of proportionality, identical to that given by the analysis of reference [19] for the spread of flames in an opposed forced flow when radiation heat transfer is not considered. This is at least at first glance surprising since the opposed and concurrent modes of flame spread appear quite different. However it should be noted that the analysis of reference [19] is a heat transfer model of flame spread that includes the same basic mechanisms as the ones controlling the spread of flames in a concurrent flow with the exception of the direction of the flow. Furthermore, the

authors of reference [21] have recently shown that in this type of analysis the rate of flame spread is controlled by an overall thermal balance between normal heat conduction from the flame and longitudinal convection through the gas and solid phases. A comparison of lump energy balances for the opposed and concurrent modes of flame sprad shows that the solid phase balances are identical, and that the gas phase balances also become identical because although the velocity in the convective terms have opposite sign, the temperature increments also have opposite sign, and both cancel each other. Thus, it is understandable that an analysis developed to describe the spread of flames in an opposed flow could also describe the concurrent mode of spread, at least in those aspects of the problem related to the heat transfer controlling mechanisms.

2.3.4 Conclusion

The experimental results for the rate of flame spread over thick PMMA sheets obtained in this work, and their successful correlation in terms of parameters deduced from heat transfer models of the flame spread process show that in the flow assisted mode of flame spread, heat transfer from the flame to the condensed fuel is the controlling mechanism. Although the correlation of the results is accomplished with analysis that consider laminar flow and do not includ radiation, it should be noted that the scale of the experiments is small enough for these conditions to prevail. I-Iowever, as the size of the fire increases, radiation aiid turbulent flow becomes of increased importance and it is expected that models that include these phenomena would be required to predict the corresponding experimental data. The basic information deduced in this work concerning the controlling mechanisms of the flame spread process should, however, apply to any fire scale. The extinction of the flame and the finite rate kinetic effects are limited priminarily to the upstream leading edge of the flame

and to the flame tip. These processes, however, cannot really be considered as part of the flame spread process in concurrent flows. They are more related to the mechanisms controlling the steady burning of fuel surfaces.

2.4 Thermally Thin Fuel Experiment

2.4.1 Experiment

A schematic diagram of the experimental installation is shown in **fig.2.14.** The experiments are carried out in the same test section. In order to generate a flat plate flow over both surfaces of the fuel sheets, the paper is positioned in the middle of the test section 10 cm from the exit of the convergent nozzle.

The gas flow in the wind tunnel is supplied either from a centralized compressed air installation or from bottles of compressed oxygen and nitrogen. The gas flows of the individual gases are metered with calibrated critical nozzles and mixed at the settling chamber of the tunnel. With the present installation, Oxygen or nitrogen mixtures with concentrations accurate to 1 % are obtainable.

In the flow assisted mode of flame spread it is very important to have a uniform and well defined initiation of the flame spread process to assure two dimensionality [4,24,10]. In the present tests, the simultaneous ignition of the filter paper along its entire lower leading edge is achieved by means of an electrically heated nichrome wire. A thin layer of Duco-Cement is applied to the paper where it touches the nichrome wire to favor the uniform ignition of the fuel. The cement burns very quickly and does not affect the subsequent flame spreading process. To favor the initiation of the flame spread process, the following steps are taken. With the fuel sheet positioned in the test section, the gas flow is established at the predetermined velocity arid oxygen concentration.

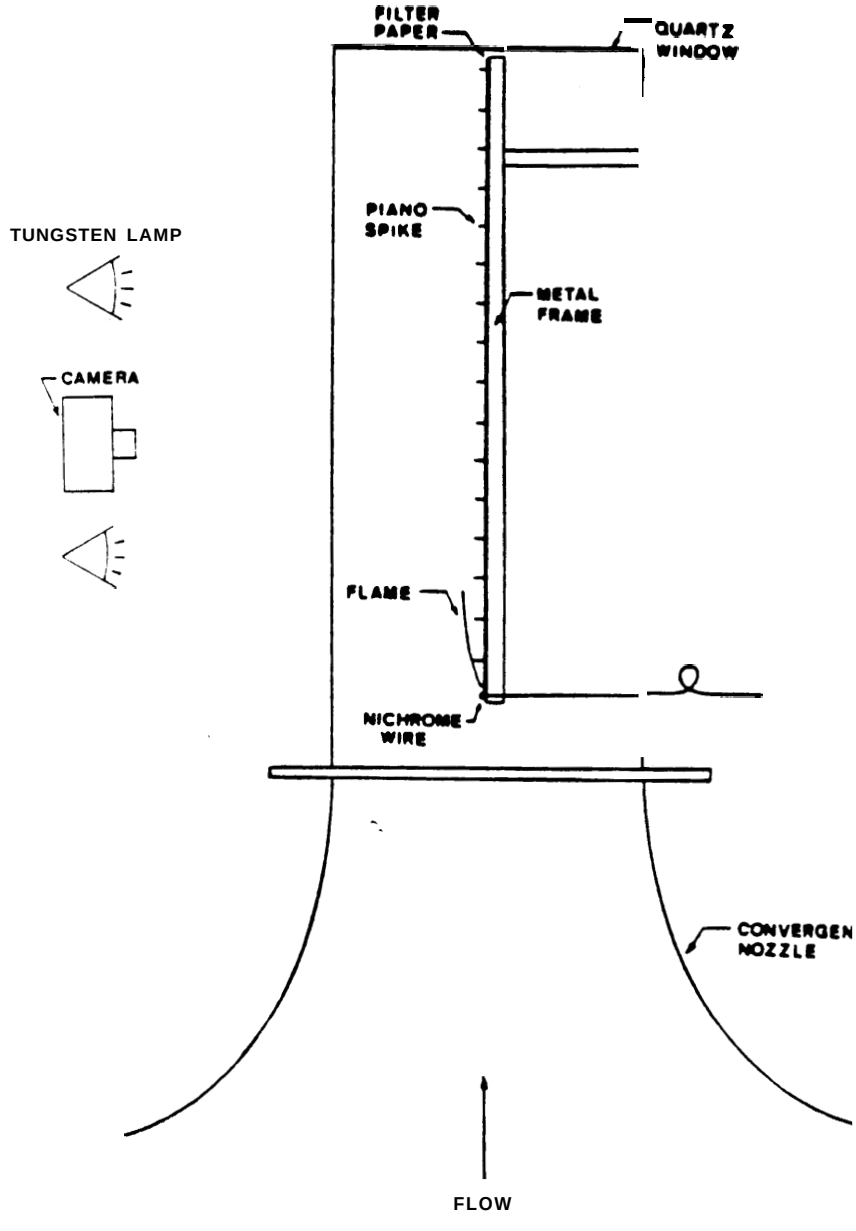
FILTER PAPER
QUARTZ WINDOW
TUNGSTEN LAMP
PIANO SPIKE
METAL FRAME
CAMERA
FLAME
NICHROME WIRE
CONVERGEN NOZZLE
FLOW

Fig. 2. 14

During the process of fuel ignition, the gas flow is by-passed to have a quiescent gas region near the leading edge of the fuel specimen and thus facilitate its ignition. On ignition, the heated nichrome wire pyrolyzes and ignites a thin region of the paper, initiating the flame spread process. As soon as ignition is observed, the bypass is closed and the data acquisition started.

The behavior of the flame is recorded with both direct photographs and thermocouple probling method. In the thermocouple probing method, the rate of flame spread is measured from the temperature histories of thermocouples placed at fixed 'distances along the fuel surface [6]. Eight Chromel-Alumel thermocouples 0.0762 mm in diameter are placed in grooves made on the filter paper sheets each at distances 5.715 cm apart. The output from the thermocouples is amplified and processed in a real time data acquisition system (PDP-11 minicomputer). The rate of spread of the pyrolysis front is obtained from the surface temperature histories by calculating the ratio of the distance between two consecutive thermocouples to elapsed time of pyrolysis arrival to the thermocouples. The arrival of the pyrolysis front at the thermocouple position is characterized by the leveling of the temperature profile when the pyrolysis temperature of the fuel reaches an approximately constant value. The burnout location of the upstream fuel is recorded by observing the sudden decrease or increase in temperature due to the disappearance of the fuel or the contact of the trailing edge of the flame with the thermocouple, respectively. Motion pictures, taken at about 18 frames per second of the fuel surface provide another means for quantitative measurement of the flame spreading process. The motion pictures are used to evaluate the locations of the pyrolysis and burn out fronts, and flame tip. Illumination of the paper surface with four 500W tungsten lamps, combined with the proper choice of exposure, yield well defined pyrolysis front locations. Photographically, this corresponds to the onset of the blacking

of the paper. The burn-out location is more difficult to determine because in the burning region the paper breaks and curls, making it difficult to establish the real location of the fuel's disappearance. To overcome the difficulty, the location of the fuel burn-out is first assumed to coincide with the position of the initiation of the paper break out. The tests are then repeated up to five times to obtain an average of this distance. The distance obtained with this method just after the initiation of the paper breaking is subsequently matched with the burn-out distance obtained prior to the onset of the paper break out. The resulting correction is then applied to the rest of the burn-out data. The accurate determination of the flame tip position is also difficult because of the fluctuations of the flame tip. The results presented here are average values of distance obtained from color photographs of repeated tests.

2.4.2 Results

The measurements of the distances of the pyrolysis front, X_p, the corresponding burn-out front, X_b, and the flame tip, X_f, to the location of the flame spread initiation for flames spreading over the surface of filter paper sheets, are presented in **fig.2.15** for several air flow velocities. The spread rates of each front can be deduced from these results by differentiating the corresponding distances with respect to time. The experiments are performed with the combustion tunnel in a vertical position to permit testing over the whole range of convective flow conditions (from free to forced flow). The pyrolysis front data is obtained using both the thermocouple and photographic methods. The data for the burn-out front and flame tip location are obtained primarily from the photographs, because this method seems to provide more reliable results. As explained above, because the method used to determine the locations of the burn-out front and the flame tip are not very accurate, the

burn-out and flame tip data presented here can only be considered as approximate. The velocity of 2 m/s is the maximum velocity for which the spread of the flame in air is observed. With thin fuels the length of the pyrolysis region remains relatively short due to the upstream consumption of the fuel, so the flame does not move into regions of larger boundary layer thickness. Consequently, extinction or non-flame propagation occurs at lower velocities than for the thick fuel sheets [23].

From the results presented in fig.2.15 it is seen that for air the flame spreading process is accelerative from ignition to approximately 15 to 20 cm downstream, becoming constant afterwards. This result follows the variation of the pyrolysis length $L_p = X_p - X_b$ and of the flame length $L_f = X_f - X_p$ with the distance from ignition. From fig.2.15 it is seen that both the pyrolysis and flame lengths increase rapidly during the initial period of the flame spread process until burn-out of the fuel starts. After that, the rate of increase of these lengths decrease as the burn-out front progresses until finally they becomes practically constant at approximately 15 cm from ignition. The results of fig.2.15 also show that, for low flow velocity (mixed convection), the pyrolysis and flame lengths decrease as the flow velocity increases. Both lengths approximately become constant for forced flow conditions ($U_\infty > 1\ m/s$). The flame spread rate follows the variations of these lengths, increasing with the flow velocity for fixed flow conditions and becoming practically constant for forced flow.

In Fig.2.16, a logarithmic plot of the spread rate data for the initial accelerative period is presented. It is seen that there is an approximate power law dependence between the pyrolysis distance and time of the form $X_p \sim t^n$. The value of the exponent varies from 1.6 for natural convection to 2 for forced flow. The only theoretical models of the flow assisted mode of flame spread over thermally thin fuels that have been published to date are those of refs.

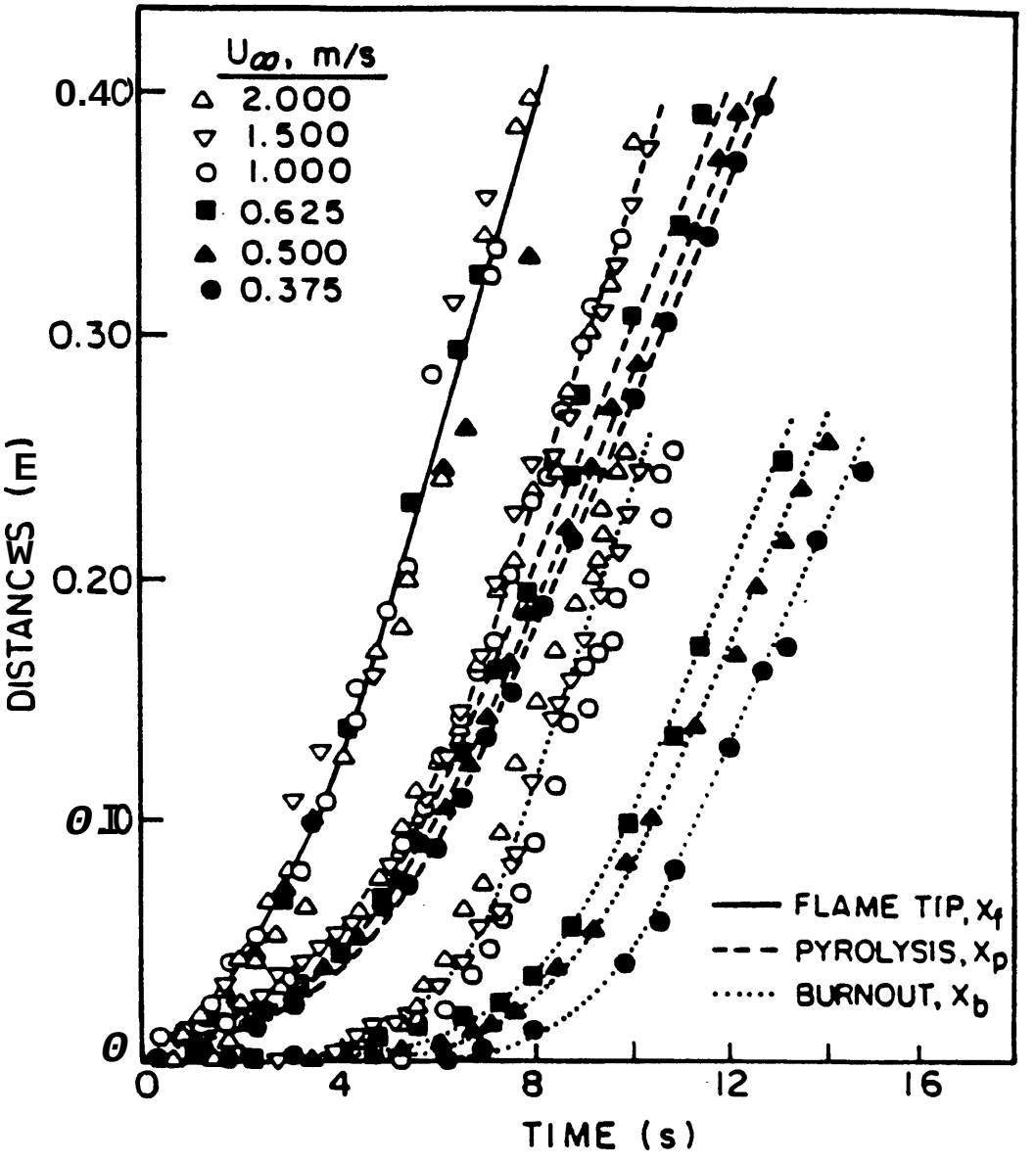
U_∞, m/s
2.000
1.500
1.000
0.625
0.500
0.375
0.40
0.30
0.20
0.10
0
DISTANCE (m)
0
4
8
12
16
TIME (s)
FLAME TIP, X_f
PYROLYSIS, X_p
BURNOUT, X_b

Fig. 2. 15

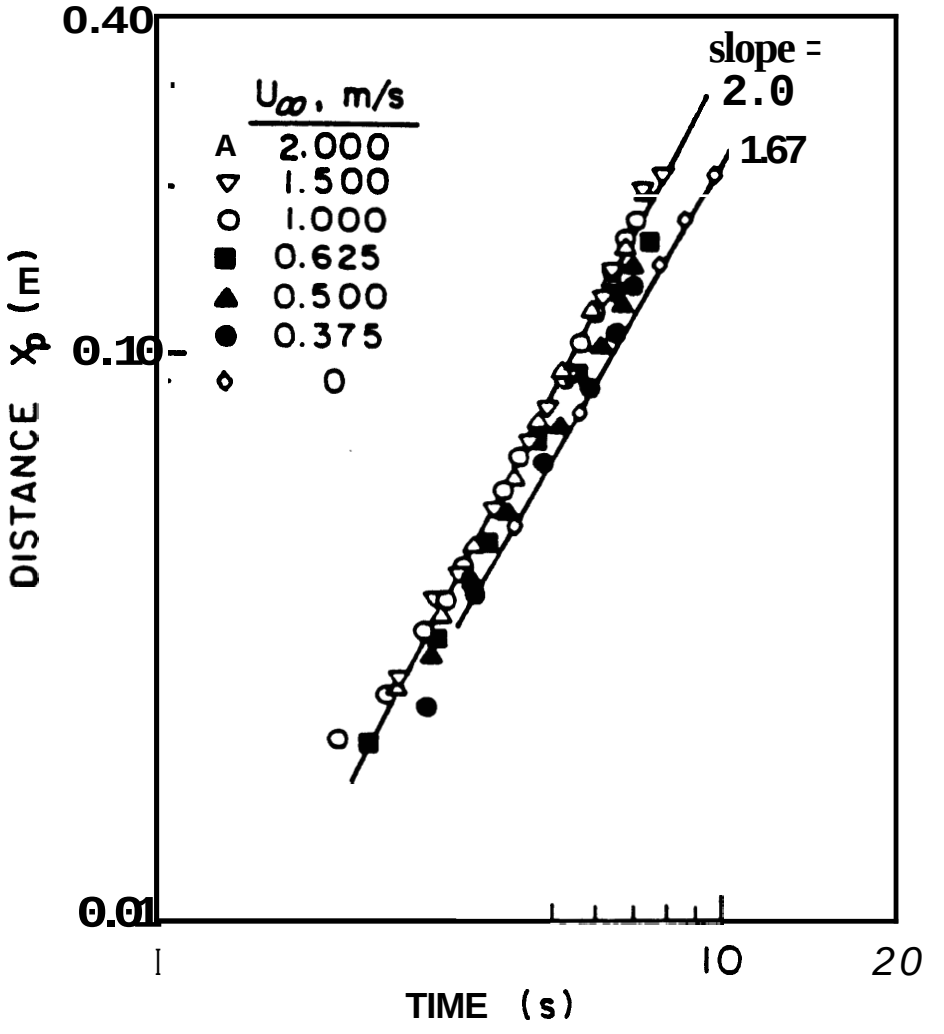
0.40
0.10
0.01
DISTANCE Xp (m)
U∞, m/s
A 2.000
1.500
1.000
0.625
0.500
0.375
0
slope = 2.0
1.67
10
20
TIME (s)

Fig. 2. 16

[1,2] and [25] for natural convection and ref. [9] for forced convection. An overview of these models is goven in ref. [26]. The analyses of refs. [1,2,23] are very similar and both predict a fourth power law dipndence between the pyrolysis distance and time. This is in disagreement with the results of Fig.2.16 for natural convection which gives a 1.6 power. On the other hand, the analysis of ref, [9] for forced convection predicts a square power dependence for the pyrolysis distance with time which is in agreement with the results of Fig.2.16. This last analysis, however, predicts a linear relationship between the pyrolysis distance and the free stream velocity. This prediction is in disagreement with the experimental results which show that the spread rate is practically independent of the flow velocity (Fig.2.16). These comparisons indicate that the present theoretical models of the flow assisted spread of flames over thin fuels are not capable of predicting the process accurately and that some improved versions of these models are needed.

In Fig.2.17 the rates of spread of the pyrolysis front, once the spread process has reached steady state, are presented as a function of the flow velocity for several oxygen concentrations. It is seen that for all oxygen concentrations the spread rate increases with the flow velocity for low flow velocities, and becomes practically independent of the gas velocity for forced flow conditions. Within the range of experimental conditions. the spread rate increases linearly with oxygen concentration.

2.4.3 Discussion

In order to explain the nature of the above results, it is convenient to develop a simple model of the flame spread process over a thermally thin fuel. Assuming that the primary controlling michanism of flame spread is lieat transfer from the flame to the non-burning material downstream from the

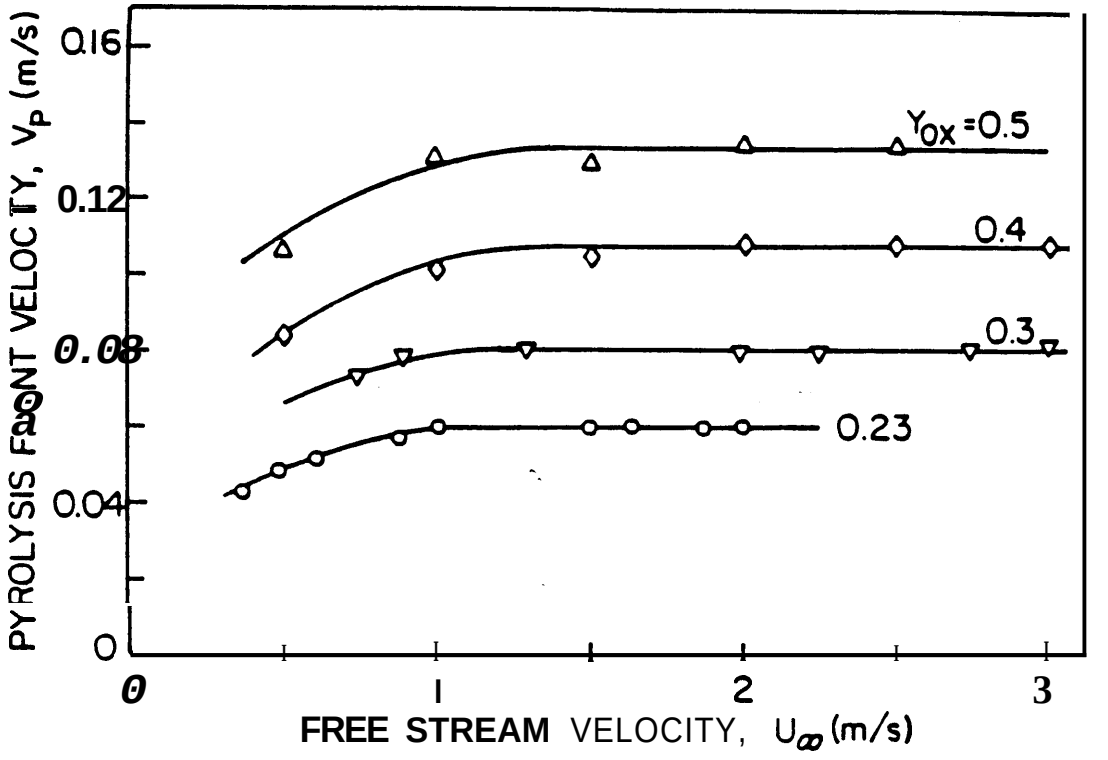
PYROLYSIS FRONT VELOCITY, V_p (m/s)
0.16
0.12
0.08
0.04
0
0
1
2
3
FREE STREAM VELOCITY, U_∞ (m/s)
Y_{Ox} =0.5
0.4
0.3
0.23

Fig. 2. 17

pyrolysis front, that the heat flux from the flame is constant over the flame length and zero afterward; that the temperature of the fuel is uniform along its thickness (thermally thin); and that the combustible does not vaporize until its temperature reaches a given value; and energy balance for a control volume in the solid downstream from the pyrolysis front gives

$$\rho\, C\, \tau\, V_p\, (\, T_v - T_i\,) = \dot{q}_f''\, L_f \qquad (2.8)$$

In the above equation, p, C, τ, T_v, and T_i are respectively the density, specific heat, thickness, pyrolysis and initial temperature of the fuel; V_p is the spread rate of the pyrolysis front; $\dot{q}_f$ the heat transfer from the flame to the fuel surface by radiation and convection; L_f is the flame length. The spread rate can also be expressed in terms of the pyrolysis length by replacing L_f in equation **(2.8)** by the relation $L_f = C\, L_p^n$ with $n \leq 1$, [4,25,26] ($n \approx$ **1.1** from the results of fig.2.20 and **fig.2.21).**

The heat **flux** at the surface, neglecting radiation, can be expressed in the form $\dot{q}_f'' \sim \lambda_g\, (\, T_f - T_v\,)/\delta$, where λ_g **is** the thermal conductivity, T_f is the flame temperature and δ is the flame stand-off distance. Substituting this relation in equation (1), the following expression is obtained for the rate of spread of the pyrolysis front,

$$V_p \approx \frac{\lambda_g\, (\, T_f - T_v\,)}{\rho c\, \tau (\, T_v - T_\infty\,)}\, (\, L_f\, /\delta\,) \qquad (2.9)$$

The variation of V_p with the pyrolysis front distance (or time) and with the flow velocity will depend on the respective variations of L_f and **6.** The variation of the former paramerer can be deduced [26] from the results of Fig.2.15 and of the latter from the results of **Fig.2.17.**

In **fig.2.18,** the surface heat **flux** calculated from surface temperature histories at different locations along the fuel surface is plotted as a function of the

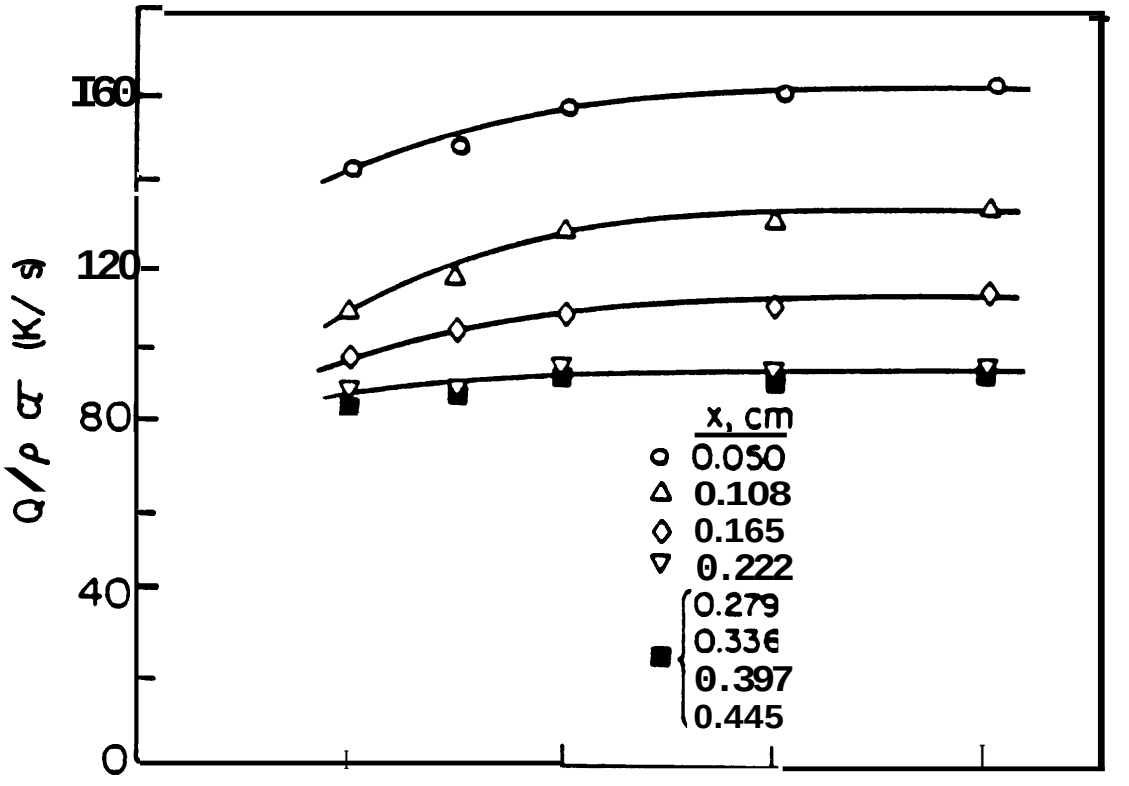
160
120
80
40
0
Q/ρ α (K/s)
x, cm
0.050
0.108
0.165
0.222
0.279
0.336
0.397
0.445

Fig. 2. 18

free stream velocity. It is seen that the heat flux decreases initially with the distance from the fuel ignition location and becomes approximately constant after a distance of approximately 15 cm. this trend is in qualitative agreement with the predictions of boundary layer analyses of burning surfaces where a scaling law for 6 of the form $6 \sim L_p^a U_\infty^b$ can be deduced [12]. The initial increase of the pyrolysis length (Fig.2.15) results in an increase of the flame stand-off distance and, consequently, in a decrease of heat flux. Once L_p becomes constant, so does δ and consequently $\dot{q}_f''$. From the dependence on U_∞, it is seen that the heat flux increases with the velocity for low velocities, but becomes practically constant for $U_\infty > 1$ m/s. This last result shows agreement of the above dependence of 6 on L_p but seems to disagree with the predicted dependence on U_∞. From the results of Fig.2.15 it is seen that, for low velocities, as U_∞ increases L_p decreases, which results in a decrease of the flame stand-off distance and consequently in an increase of the heat flux. For large flow velocities, however, the pyrolysis length is practically independent of the flow velocity. Since the heat flux is also very weakly dependent on L_p and not on U_∞. With regard to the apparent weak dependence of the heat flux on the flow velocity, it should be mentioned that the observed strong variation of the flame spread data with the flow velocity occurs during the transition from natural to forced convection, where markedly different flow patterns are expected. However, under forced flow conditions the variation of the flame spread parameters with the flow velocity is not very strong (1/2 power). Furthermore, because of the occurance of flame extinction the range of gas velocities tested (1 m/s to 2 m/s) is very small. This, in conjunction with the fact that the experimental data has considerable scatter, suggests that the apparent independency of the heat flux with the flow velocity may not be totally true and that indeed the heat flux is dependent on the flow velocity as expected from the

boundary layer analysis predictions.

The experimental results for the flame spread rate can be explained phenomenologically with the help of equation (2.8)(or equation **(2.9))** and the results of fig.2.15 and 18. The initial accelerative period of the flame spread rate (fig.2.15 and 2.16) is due to the increase of the pyrolysis length which in turn results in the increase of the flame length (fig.2.15) and consequently of the total heat flux at the fuel surface. The slight decrease of the local heat flux with the distance from ignition (fig.2.18) is counteracted by the increase of the flame length. Once the fuel starts to be depleted in the upstream region, the rate of increase of the pyrolysis length decreases and so does the spread rate. As the rate of spread of the burn-out front approaches that of the pyrolysis front, the pyrolysis length becomes constant. This results in a steady state flame spread process. Similarly, the increase of the spread rate with U_∞ for low flow velocities is due to the increase of the surface heat flux (fig.2.18) which counteracts the slight decrease of the flame length **(fig.2.15).** For larger flow velocities ($U_\infty > 1$ m/s), the pyrolysis and flame length and the surface heat flux become approximately constant, and consequently so does the rate of flame spread.

With regard to the independence of the flame spread rate on the gas velocity for forced flow conditions, it should be pointed out that the reasons given above for this result, i.e: the constancy of L_p , L_f and $\dot{q}_f''$ may not be totally accurate. As explained before, the present measurements have some scatter due to the experimeiital difficulties and the variation of the above paremeters with U_∞ is expected to be small due to the small range of velocities tested. Therefore, there is the possibility that the above parameters are not truly constant but vary with length and velocity according to the boundary layer predictions. Under these conditions the dependence of the flame spread rate on the flow velocity would be the result of the following mechanism. As the flow velocity

increases the thickness of the boundary layer and consequently the flame stand-off distance decrease, which results in an increase of the heat transferred from the flame to the fuel. This increase in heat transfer has a dual effect. While it increases the heat flux at the non-burning fuel surface, it also increases the gasification rate of the burning surface. **A** larger mass burning rate causes an increase in the rate of spread of the burn-out front that tends to decrease the length of the pyrolysis region and consequently of the flame length. As it is seen from equation **(2.8)** both effects -- the increase of the heat flux and the decrease of the pyrolysis length (or flame length) -- counteract each other, and, depending on their relative variation, the spread rate would either increase, remain constant, or even decrease. The results of **fig.2.15** and **16** seem to indicate that at large velocities (forced flow conditions) both effects would balance each other.

A correlation, using equation **(2.9)** of the flame spread rate data of **fig.2.17** with $\frac{L_f}{\delta}$ assumed constant for forced convection, is presented in fig.2.19. The properties used in the computation of the correlation are $\lambda_g = 0.046\ J/m\text{-}sec\ K$, $C_p = 1.06\ KJ/Kg\ K$, $\rho_s \tau = 18.5\ X\ 10^{-3}\ g/cm^2$. The flame temperature T_f is calculated with the equation

$$T_f = T_v + \frac{(T_\infty - T_v) + (\frac{Y_{o\infty}}{iC_p})(\Delta H_c - L)}{1 + \frac{Y_{o\infty}}{i}} \qquad (2.10)$$

that corresponds to the adiabatic flame temperature for constant specific heat of the product of combustion. The data used in calculating the flame temperature are: $i = 1.185$, $\Delta H_c = 1.674\ X\ 10^4\ KJ/Kg$ fuel, L=753 KJ/Kg, $T_\infty = 298\ k$, $T_v = 618\ k$ and $C_p = 1.06$ KJ/Kg k. From the resultsof **fig.2.18** it is seen that except at low flow velocities ($U_\infty < 1$ m/s), where buoyance effects become important, equation **(2.9)** correlates very closely the flame

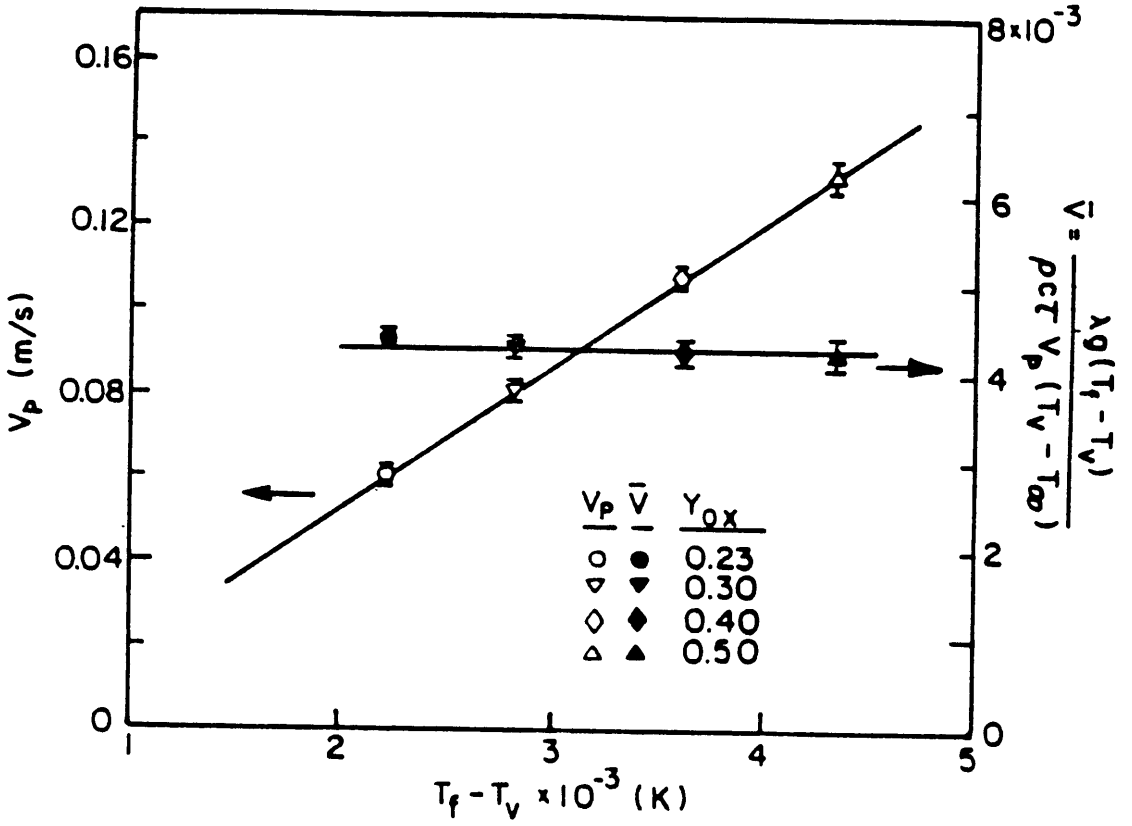
0.16
0.12
0.08
0.04
0
V_p (m/s)
8×10^{-3}
6
4
2
0
$\bar{V} = \frac{\lambda g(T_f - T_v)}{\rho c_T V_p (T_v - T_\infty)}$
1
2
3
4
5
$T_f - T_v \times 10^{-3}$ (K)
V_p $\bar{V}$ Y_{ox}
0.23
0.30
0.40
0.50

Fig. 2. 19

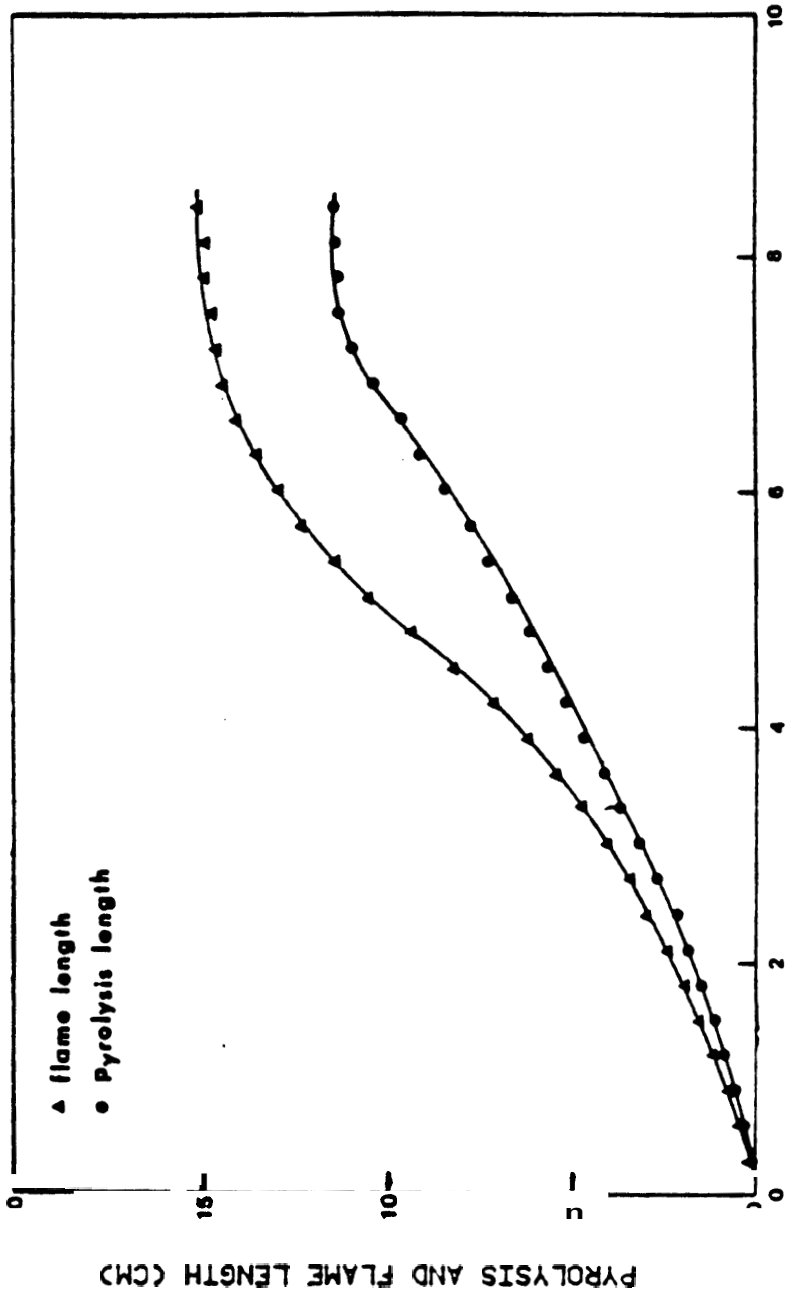
▲ flame length
● Pyrolysis length
PYROLYSIS AND FLAME LENGTH (CM)
TIME (SECONDS)
0
15
10
5
0
2
4
6
8
10

Fig. 2. 20

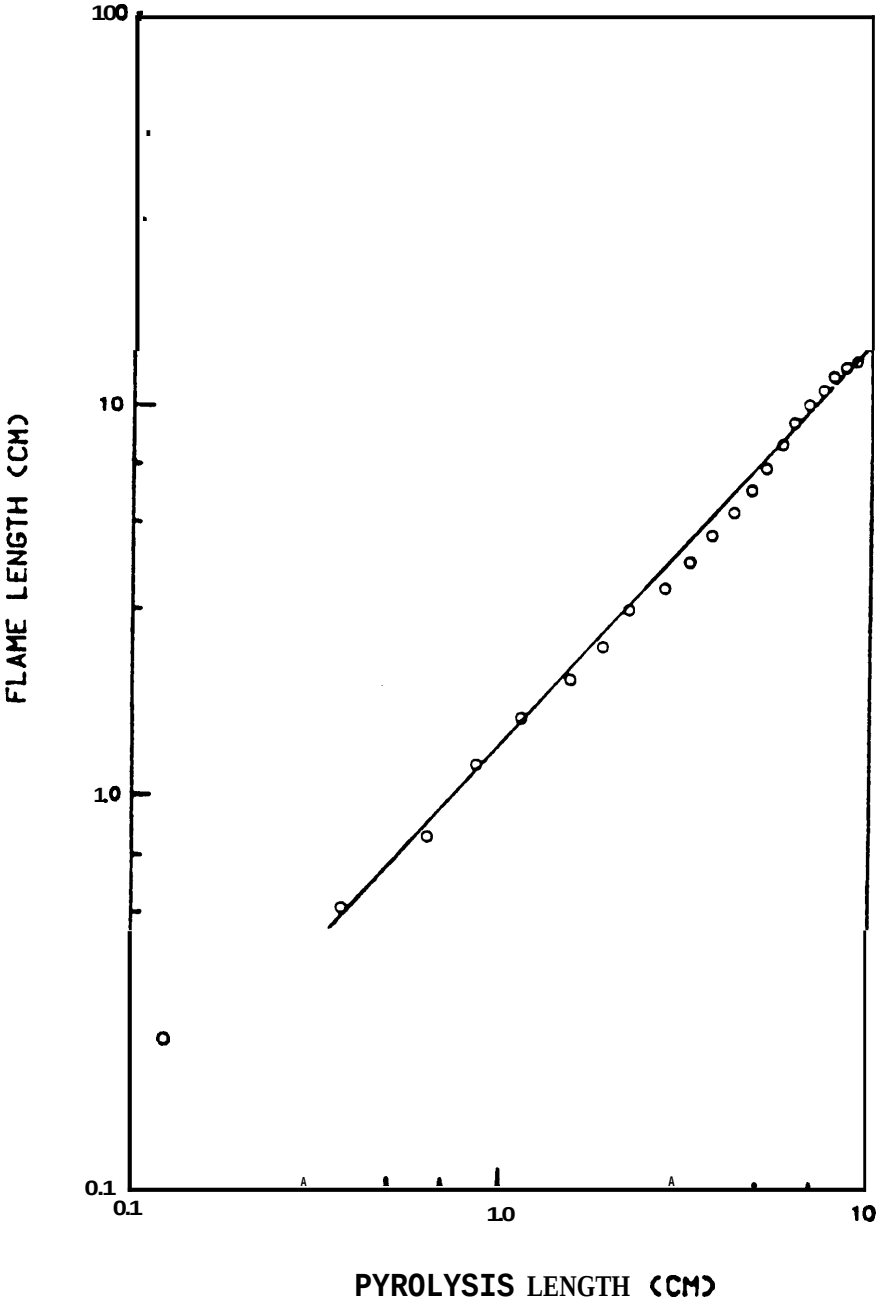

Fig. 2. 21

spread rate data of **fig.2.17.** It is interesting to note that the analysis of ref.[20] for the spread of a flame over a thin fuel in an opposed flow predicts a spread rate that is also given by an equation as in equation **(2.9)** and that is independent of the flow velocity. As it is explained in ref.[23] this is understandable. A lump energy balance of the gas phase for the opposed and concurrent modes of flame spread show that while the convective terms have opposite signs, the temperatures also have opposite signs, and both cancel each other. The result is a formula that is applicable to both models of heat transfer.

2.4.4 Conclusion

The measurement of the rates of flame spread over the surface of thin filter paper sheets and their comparison with currently available theoretical models show deficiencies in the predicative capabilities of the models. It appears that the major problem comes from the prediction of the variation with time and of the dependence on the flow velocities of the length of the pyrolysis region. This length determines in its turn the length of the flame and consequently the overall heat flux on the fuel surface. Thus an accurate prediction of the pyrolysis and flame lengths is imperative to predict accurately the rate of flame spread.

Chapter 3 Boundary Layer Model of Flame Spread

3.1 Introduction

In this section, a simplified mathematical model of concurrent mode of flame spread over a flat surface is presented. It makes use of a laminar, two-dimensional boundary layer and flame sheet approximation to describe the flow field and an ignition surface temperature to define the onset of fuel vaporization. It can only apply to small-scale fires or to the initial growing stages of a fire where the effect of radiation and turbulence are not important [41,52].

A schematic drawing of the simplified model is presented in Fig.3.1. A solid piece of fuel presented in a forced external oxidizing flow, then there will be a boundary layer generated near the fuel surface. Within this boundary layer adjacent to the fuel surface lies a diffusion flame due to the reaction of the fuel particles evaporated from the surface and the oxidizer from the main stream. The amount of heat that is generated in the flame zone then feeds back to the fuel surface through conduction, convection and radiation, which sustain the vaporization of fuel. However, the gaseous fuel evaporated from its surface is not completely consumed in the upstream flame, excess fuel [30] is driven ahead of the pyrolysis front by the external flow and continues to react with the oxidizer in the form of a diffusion flame until all the fuel has been consumed. The heat transfer from the diffusion flame generated in the downstream boundary layer produces a profile of elevated surface temperature along the fuel surface downstream from the pyrolysis front. The surface temperature of the solid will then increase from a value close to ambient temperature at the tip of the flame to its vaporization temperature at the pyrolysis front at which the fuel starts to vaporize vigorously.

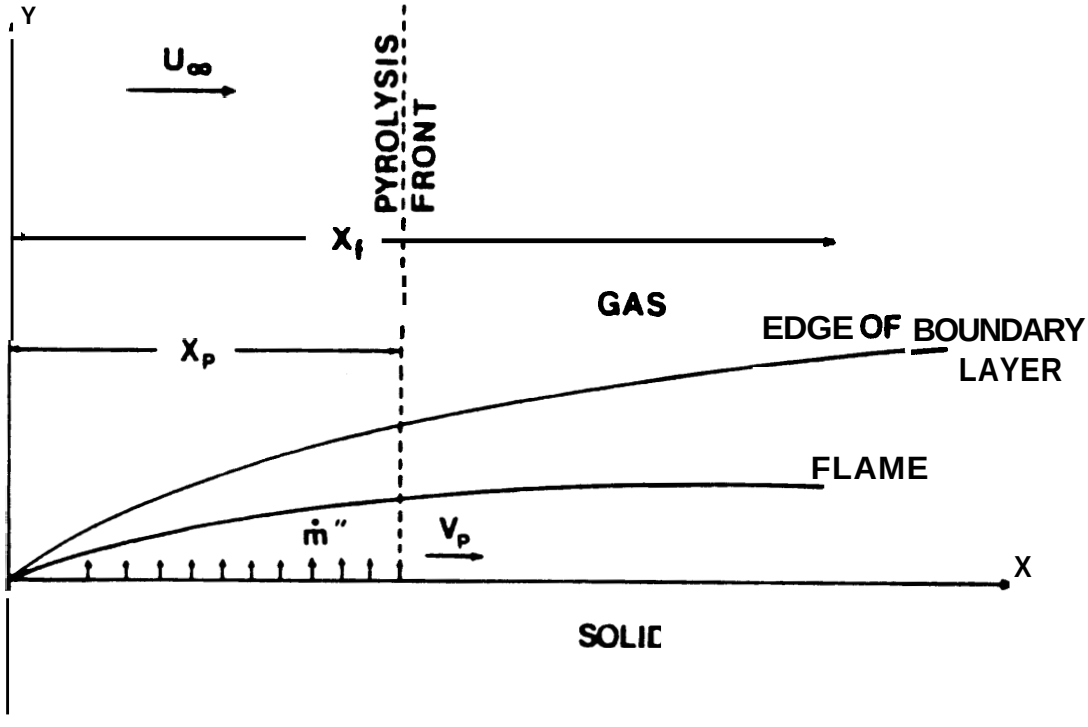
Y
U_∞
PYROLYSIS FRONT
X_f
GAS
EDGE OF BOUNDARY LAYER
X_p
FLAME
$\dot{m}''$
V_p
X
SOLID

Fig. 3. 1

It is seen that in this simplified model the pyrolysis front defines two distinct region characterized by the conditions at the solid-gas interface. Upstream from the pyrolysis front, the fuel surface is maintained at its vaporization temperature and pyrolyzes vigorously while downstream from the pyrolysis front, no fuel vaporization is assumed following the concept of an ignition temperature. Thus a discontinuous jump of the local surface mass flux across the pyrolysis front will exist from this split-type treatment of the problem.

Since the pyrolysis front is moving, this problem is basically a transient one and a complete solution would involve the simultaneous solution of both the gas phase and solid phase governing equations in their time-dependent form. However, because the characteristic transport time of the gas phase process is much shorter than the transport time for the solid phase process, a quasi-steady model is proposed here that assumes the transient terms in the gas phase equations have little effect on the flame spread process.

Following the steady state laminar boundary layer approximation, the equations that model the gas phase process are conversation of mass, momentum, energy and species [35,56]

$$\frac{\partial(\rho_g U)}{\partial x} + \frac{\partial(\rho_g V)}{\partial y} = 0 \tag{3.1}$$

$$\rho_g U \frac{\partial U}{\partial x} + \rho_g V \frac{\partial U}{\partial y} = \frac{\partial}{\partial y}\left(\mu_g \frac{\partial U}{\partial y}\right) \tag{3.2}$$

$$\rho_g U \frac{\partial h_g}{\partial x} + \rho_g V \frac{\partial h_g}{\partial y} = \frac{\partial}{\partial y}\left(\frac{\lambda_g}{C_p} \frac{\partial h_g}{\partial y}\right) + \dot{q}''' \tag{3.3}$$

$$\rho_g U \frac{\partial Y_i}{\partial x} + \rho_g V \frac{\partial Y_i}{\partial y} = \frac{\partial}{\partial y}\left(\rho_g D_g \frac{\partial Y_i}{\partial y}\right) + \dot{m}_i''' \tag{3.4}$$

where $h = \int_{T_\infty}^{T} C_p \, dT$ and the subscript i stand for fuel, oxidizer and product. $\dot{q}'''$ is the volumetric heat release rate due to combustion and $\dot{m}'''$ is the

species generation rate, which will be negative for fuel and oxidizer and positive for products.

As for the solid phase analysis, the fuel specimen is considered having a semi-infinite thickness in the normal direction and the temperature gradient in this direction is much lager than that in the longitudinal direction [49], i.e. $\frac{\partial T_c}{\partial y} >> \frac{\partial T_c}{\partial x}$. Hence the dominant mode of heat transfer in the solid phase is in its Y direction (fig.3.1) and the heat conduction equation of the solid phase can be simplified to give

$$\lambda_s \frac{\partial^2 T_c}{\partial y^2} - \rho_s C_s \frac{\partial T_c}{at} \tag{3.5}$$

Boundary conditions are also needed to completely specify the problem. Since the pyrolysis front defines two distinct regions along the fuel surface. a split-type boundary conditions at the solid-gas interface are needed. Upstream from the pyrolysis front, at the solid-gas interface ($y = 0, 0 \leq X \leq X_p$), the boundary conditions are

$$T_c = T_v \tag{3.6}$$

$$\lambda_g \left(\frac{\partial T_g}{\partial y}\right)_w = \dot{m}'' L_v \tag{3.7}$$

$$\dot{m}'' = (\rho_g V)_w = (\rho_g V Y_f)_w - \left(\rho_g D_g \frac{\partial Y_f}{\partial y}\right)_w \tag{3.8}$$

$$(\rho_g V Y_i)_w = \left(\rho_g D_g \frac{\partial Y_i}{\partial y}\right)_w \quad \text{for} \quad i \neq f \tag{3.9}$$

T_v is the fuel vaporization temperature, T_c the solid phase temperature and $\dot{m}''$ is the local mass **flux** at the interface. Downstream from the pyrolysis front ($y = 0, X > X_p$), the corresponding boundary conditions are :

$$\lambda_g \left(\frac{\partial T_g}{\partial y}\right)_w = \lambda_s \left(\frac{\partial T_c}{\partial y}\right)_w \tag{3.10}$$

$$\dot{m}''_w = (\rho_g V)_w = 0 \tag{3.11}$$

We also have the boundary conditions as $Y \to \infty$, both the temperature and species composition in the gas flow approach their free stream values

$$T_g = T_\infty \tag{3.12}$$

$$Y_o = Y_{o\infty} \tag{3.13}$$

$$Y_f = 0 \tag{3.14}$$

Boundary conditions for the solid phase are also needed to solve equation (3.5). It is observed from experiments that no significant increase of the fuel surface temperature prior to the arrival of flame tip, hence the heat transfer by the gas to the solid surface beyond its flame tip does not contribute significantly to the flame spread process. It is then assumed that at the flame tip location X_f, the surface temperature of the solid approach its ambient temperature

$$X \to X_f \qquad T \to T_\infty \tag{3.15}$$

$$Y \to -\infty \qquad T \to T_\infty \tag{3.16}$$

3.2 Upstream Region

3.2.1 Gas Phase Analysis

Assuming a one-step chemical reaction in the gas phase process

$$\nu_f F + \nu_o O \to \nu_p P + Q$$

the source terms $\dot{q}'''$ and $\dot{m}'''$ in equations (3.3) and (3.4) can be eliminated by defining the following Shvab-Zeldovich variables β and γ

$$\beta = \frac{C_p (T - T_\infty) + \dfrac{(Y_o - Y_{o\infty})Q}{M_o \nu_o}}{L_v} \tag{3.17}$$

$$\gamma = \frac{\dfrac{Y_f\, Q}{M_f\, \nu_f} - \dfrac{(Y_o - Y_{o\infty})Q}{M_o\, \nu_o}}{L_v} \tag{3.18}$$

since

$$\frac{\dot{q}'''}{Q\, \nu_p\, M_p} = -\frac{\dot{m}_f'''}{\nu_f\, M_f} = -\frac{\dot{m}_o'''}{\nu_o\, M_o}$$

A transformation from (x,y) coordinates to a new system (σ,η) are introduced to convert the boundary layer equations into incompressible form [36]

$$\sigma = \frac{X_p}{X} \tag{3.19}$$

$$\xi = \int_0^y \left(\frac{\rho_g}{\rho_{g\infty} X_p} \right) dy \tag{3.20}$$

$$\eta = \left(\frac{U_\infty \rho_{g\infty} X_p}{2\mu_{g\infty}} \right)^{1/2} \sigma^{1/2}\, \xi \tag{3.21}$$

Equation **(3.1)** is then identically satisfied by introducing a stream function of the form

$$\rho_g\, U = \mu_{g\infty} \frac{\partial \psi}{\partial y} \tag{3.22}$$

$$\rho_g\, V = -\mu_{g\infty} \frac{\partial \psi}{\partial x} \tag{3.23}$$

and the transformed new functions are taken to be

$$f = \left(\frac{\mu_{g\infty}}{2\rho_{g\infty} U_\infty X_p} \right)^{1/2} \psi \tag{3.24}$$

$$F = -\frac{\beta}{B} \tag{3.25}$$

$$G = -\frac{\gamma}{B} \tag{3.26}$$

where B is the mass transfer number, $B = \frac{Q_g Y_{o\infty}}{M_o \nu_o L_v} - \frac{h_v}{L_v}$, f, F, G are the normalized stream function, the energy-species function and the species-species function respectively.

Assuming constant of the quantities $\rho_g \mu_g$, C_p $\rho_g \lambda_g$ and $\rho_g^2 D_g$, equations (3.1) to(3.4) are expressed in terms of the new functions f, F and G to yield :

$$f_{\eta\eta\eta} + f f_{\eta\eta} = 0 \tag{3.27}$$

$$F_{\eta\eta} + P_r f F_\eta = 0 \tag{3.28}$$

$$G_{\eta\eta} + P_r f G_\eta = 0 \tag{3.29}$$

and the transformed boundary conditions become

$$f_\eta(0) = 0 \tag{3.30}$$

$$f_\eta(\infty) = 1 \tag{3.31}$$

$$F(0) = 1 \tag{3.32}$$

$$\frac{BF_\eta(0)}{P_r} = f(0) \tag{3.33}$$

Then the upstream gas phase solution becomes the same type as that solved by Emmons for the film combustion of liquid fuels [40]. The boundary layer equations provides a similar solution with η as the similarity variable. The solution of this problem provides the boundary conditions at the pyrolysis front needed for the solution in the downstream boundary layer.

3.2.2 Solid Phase Analysis

Since in the upstream region, the fuel surface is vaporizing vigorously and maintained at its ignition temperature. As long as the fuel surface regression rate can be considered small, the solid phase process is completely specified to

be a semi-infinite body with its bounding plane at a prescribed temperature T_v and decoupled from the gas phase, its solution, which is in the form of an error function, does not contribute to the solution of the gas phase process, therefore it is omitted here.

3.3 Downstream Region

3.3.1 Gas Phase Analysis

In this region, the fuel surface temperature varies smoothly from its vaporizing temperature at the pyrolysis front to approximately ambient temperature near the tip of the flame, a similarity variable η alone does not exist. The solution of this region requires the coupled solution of both the gas and solid phase equations and match the boundary conditions of equal temperature and heat flux at their interface.

Applying the pre-defined non-dimensional variable σ and η to equation (3.1) to (3.4), the gas phase governing equations are transformed to be

$$f_{\eta\eta\eta} + f f_{\eta\eta} = 0 \tag{3.34}$$

$$F_{\eta\eta} + P_r f F_\eta + 2P_r \sigma f_\eta F_\sigma = 0 \tag{3.35}$$

$$G_{\eta\eta} + P_r f G_\eta + 2P_r \sigma f_\eta G_\sigma = 0 \tag{3.36}$$

With the corresponding boundary conditions becomes

$$f_\eta(0) = 0 \tag{3.37}$$

$$f_\eta(\infty) = 1 \tag{3.38}$$

$$f(0) = 0 \tag{3.39}$$

$$F(\infty) = 0 \tag{3.40}$$

$$\lambda_{g\infty} \frac{L_{vB}}{C_p} \left(\frac{U_\infty \rho_{g\infty}}{2\mu_{g\infty} V_p}\right)^{1/2} F_\eta(\sigma,0) = \lambda_s \frac{\partial T_{c(0)}}{\partial s} \tag{3.41}$$

In the above expression, the last boundary condition comes from the heat flux condition at the solid-gas interface. T, is the downstream fuel surface temperature at its transformed location $(\sigma,0)$. This would come from the solution of the solid phase analysis and clearly indicates the coupling of the two domains.

3.3.2 Solid Phase Analysis

Since downstream from the pyrolysis front, both the gas phase and solid phase domain are coupled through the unknown surface temperature and heat flux distribution, simultaneous solution of both two phases are required to provide the information for the flame spread process. Assuming constant flame spread rate V_p and defining the following non-dimensional variables

$$\sigma = \frac{\cdot}{X} \tag{3.42}$$

$$S = - y \left(\frac{V_p}{X}\right)^{1/2} \tag{3.43}$$

The solid phase conduction equations becomes

$$\frac{\partial T_c}{\partial \sigma} = \alpha_s \frac{\partial^2 T_c}{\partial S^2} \tag{3.44}$$

With the boundary conditions

$$T_c (S \rightarrow \infty) = T_\infty \tag{3.45}$$

$$T_c (\sigma \rightarrow \frac{1}{\mathrm{A}}) = T_\infty \tag{3.46}$$

$$\lambda_s \frac{\partial T_c}{\partial S}(0) = \lambda_{g\infty} \frac{L_{vB}}{C_p} \left(\frac{U_\infty \rho_{g\infty}}{2\mu_{g\infty} V_p}\right)^{1/2} F_\eta(\sigma,0) \tag{3.47}$$

Where $\mathrm{A} = \frac{X_f}{X_p}$, which defines the ratio of flame length to pyrolysis length [41,44,45]. Thus, as $\sigma \rightarrow \frac{1}{\mathrm{A}}$ or $S \rightarrow \infty$,which imply at the flame tip, $X = X_f$

and at infinity, $y = -\infty$ the fuel remains at the ambient temperature.

3.4. Upstream Boundary Layer Solution

The fuel surface is vaporizing vigorously in this region and the surface temperature is assumed to be equal to its vaporizing temperature. The gas phase solution can be solved irrespective of the solid phase solution to yield the local rate of fuel gasification

$$\dot{m}'' = \left(\frac{\mu_{g\infty}\rho_{g\infty}U_\infty}{2X_p}\right)^{1/2} \sigma^{1/2} f(0) \tag{3.48}$$

with $f(0)$ comes from the solution of equation **(3.27)** to **(3.33)**, which determines the location at which the fuel has been gasified completely. A numerical solution of the f and F functions are presented in Fig.3.2 . The corresponding flow field behavior and temperature distribution in this upstream region can be reconstructed through the inverse transform from (σ,η) system to (x,y) coordinates.

3.5 Downstream Boundary Layer Solution

The solution in the downstream boundary layer becomes more involved because of the coupling of the solid and gas phase at their interface. The solid phase goverriing equation of **(3.44)** is first solved with its boundary conditions **(3.45)** to **(3.47).** This gives the downstream surface temperature distribution in (σ,η) coordinate in terms of the still to be determined function F [19]

$$T_c(\sigma,0) - T_\infty = -\lambda_{g\infty}\frac{L_v B}{C_p \lambda_s}\left(\frac{U_\infty \rho_{g\infty}\alpha_s}{2\pi V_p \mu_{g\infty}}\right)^{1/2} \int_{\frac{1}{\Lambda}}^{\sigma} \frac{F_\eta(\sigma-\tau,0)}{\tau^{1/2}}\, d\tau \tag{3.49}$$

With this expression, the surface temperature is then substitute back into the definition of the F function in equation **(3.17)** and **(3.25)** to yield

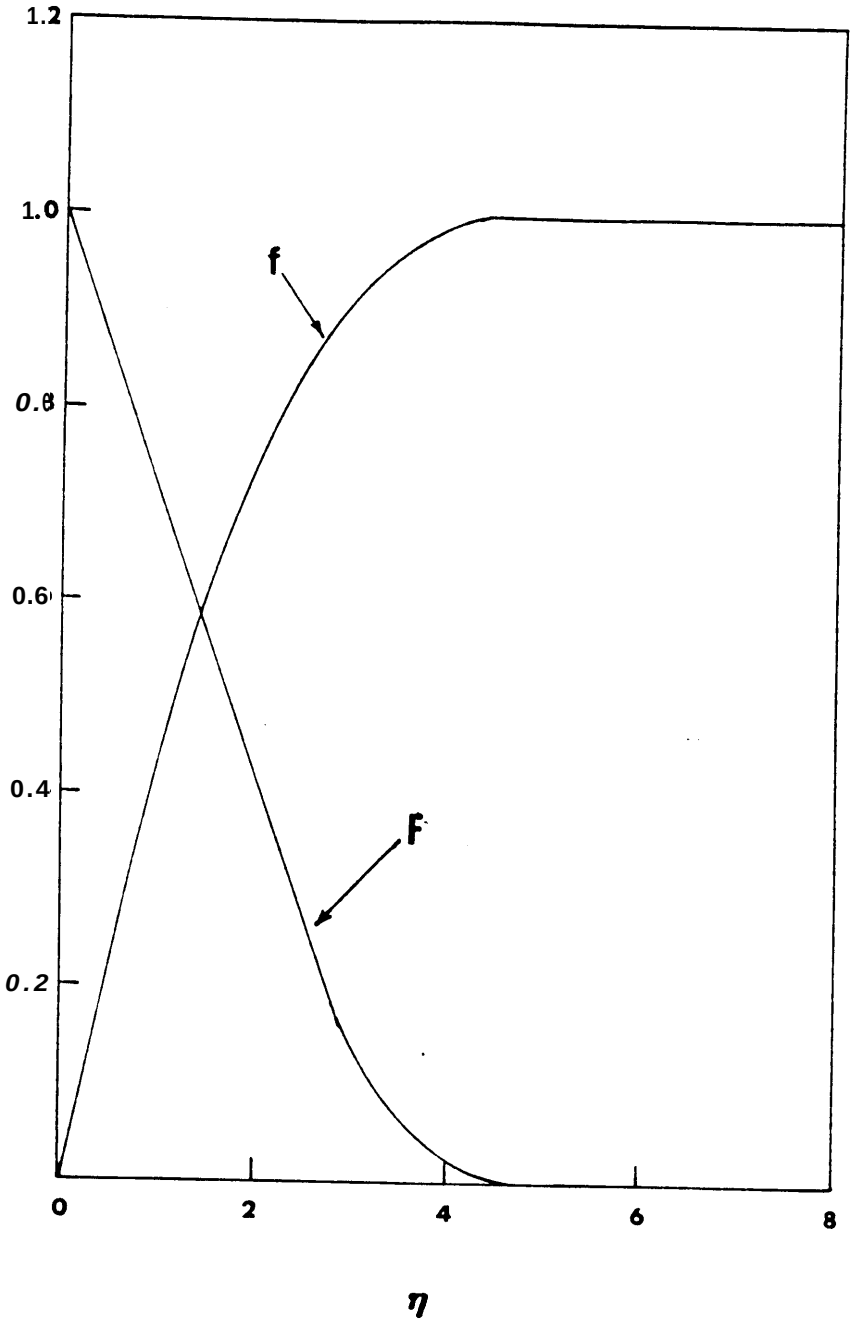

Fig. 3. 2

$$F(\sigma,0) = \frac{QY_{o\infty}}{BL_v\ M_o\ \nu_o} + \left(\frac{\rho_{g\infty}U_\infty\alpha_s}{2\pi\mu_{g\infty}V_p}\right)^{1/2}\frac{\lambda_{g\infty}}{\lambda_s}\int_{\frac{1}{\Lambda}}^{\sigma}\frac{F_\eta(\sigma-\tau,0)}{\tau^{1/2}}d\tau \quad (3.50)$$

This provides the unknown heat flux boundary condition for the gas phase equation of **(3.41).** Since $\sigma = \frac{r}{\Lambda r_p}$, in this region, $\sigma \leq 1$, the gas phase equations can be solved by using a power series expansion for the function F in terms of tlie parameter σ

$$F(\sigma,\eta) = F_0(\eta) + \sum_{m=1}^{m=\infty}\sigma^{\frac{m}{2}}F_m(\eta) \quad (3.51)$$

Substituting the expanded function F into the **gas** phase governing equations and its boundary conditions **(3.34)** to **(3.40)** and (3.50), we arrive at the following set of zeroth and first order equations

$$\sigma^0 \qquad F_{0\eta\eta} + P_r f F_{0\eta} = 0 \quad (3.52)$$

$$\sigma^{1/2} \qquad F_{1\eta\eta} + P_r f F_{1\eta} + P_r f_\eta F_1 = 0 \quad (3.53)$$

with their corresponding boundary conditions

$$F_0(\infty) = F_1(\infty) = 0 \quad (3.54)$$

$$F_0(0) = \left(\frac{\rho_{g\infty}U_\infty\alpha_s}{2\pi\mu_{g\infty}V_p}\right)^{1/2}\frac{\lambda_{g\infty}}{\lambda_s} + \frac{QY_{o\infty}}{BL,\ M_o\ \nu_o}\left(-2F_{0\eta}(0)\Lambda^{-\frac{2}{1}} + O(\Lambda^{-\frac{2}{3}})\right) \quad (3.55)$$

$$F_1(0) = 2\frac{QY_{o\infty}}{BL,\ M_o\ \nu_o}F_{0\eta}(0) - 2F_1(0)\Lambda^{-\frac{1}{2}} + O(\Lambda^{-\frac{3}{2}}) \quad (3.56)$$

Since **A** is usually a large number of order **10** or higher, higher order terms involving $\mathbf{A}^{-\frac{3}{2}}$ can be neglected. The above two equations can be solved to give

$$F_0(\eta) = \frac{(\frac{\rho_{g\infty} U_\infty \alpha_s}{2\pi\mu_{g\infty} V_p})^{1/2} \frac{\lambda_{g\infty}}{\lambda_s}}{1 - \frac{2\frac{QY_{o\infty}}{BL_v M_o \nu_o}\Lambda^{-\frac{1}{2}}}{\Omega}} (1 - \frac{1}{\Omega}\int_0^\eta e^{-\int P_r f d\eta} d\eta) \qquad (3.57)$$

$$F_1(\eta) = -\frac{2\frac{QY_{o\infty}}{BL_v M_o \nu_o}(\frac{\rho_{g\infty} U_\infty \alpha_s}{2\pi\mu_{g\infty} V_p})^{1/2} \frac{\lambda_{g\infty}}{\lambda_s}}{\Omega - 2\frac{QY_{o\infty}}{BL_v M_o \nu_o}\Lambda^{-\frac{1}{2}}} e^{-\int_0^\eta P_r f \, d\eta} \qquad (3.58)$$

$$where \quad \Omega = \int_\sigma^\infty e^{-\int_\sigma^\eta P_r f \, d\eta} d\eta$$

The rate of spread of the pyrolysis front is obtained from the solution of equation *(3.57)* and **(3.58)** by imposing the eigenvalue condition that at the pyrolysis front $T_c = T_v$, the surface temperature of the fuel equal to its vaporizing temperature. This results the pyrolysis front moving velocity to be

$$V_p = \frac{2\rho_{g\infty}\alpha_s}{\pi\mu_{g\infty}}(\frac{\lambda_{g\infty}}{\lambda_s})^2 (\frac{D_c - (D_c - 1)\Lambda^{-\frac{1}{2}}}{\Omega})^2 U_\infty \qquad (3.59)$$

where D_c is the non-dimensional heat of combustion, $D_c = \frac{QY_{o\infty}}{\nu_o M_o C_p (T_v - T_\infty)}$, and the rate of spread of the flame tip is given by

$$V_f = \Lambda V_p = \frac{2\Lambda\rho_{g\infty}\alpha_s}{\pi\mu_{g\infty}}(\frac{\lambda_{g\infty}}{\lambda_s})^2 (\frac{D_c - (D_c - 1)\Lambda^{-\frac{1}{2}}}{\Omega})^2 U_\infty \qquad (3.60)$$

further simplification of the expression can be deduced from the approximation of

following $\Lambda^{-\frac{1}{2}} < 1$ $\qquad D_c - (D_c - 1)\Lambda^{-\frac{1}{2}} \approx D_c$

then the pyrolysis front moving velocity becomes

$$V_p = \left(\frac{2\rho_{g\infty}\lambda_{g\infty}^2\alpha_s Q^2}{\pi\mu_{g\infty}\Omega^2\lambda_s^2 C_p^2(T_v - T_\infty)^2 M_o^2\nu_o^2} \right) U_\infty Y_{o\infty}^2 \qquad (3.61)$$

Although the flame tip travels faster than the pyrolysis front, which would results in an increase of the heated region downstream from the pyrolysis front, the flame also moves away from the fuel surface as the distance from the upstream leading edge increases, this reduces the heat flux from the flame to the fuel surface as the distance increases. These two effects counteract each other and resulted in a constant spread rate.

3.6 Conclusion

Present analysis provides an analytical prediction of the flame spread rate over a thermally thick fuel in a concurrent flow environment. The predicted dependence of the spread rate on U_∞ and $Y_{o\infty}$ can be explained as follows: For thermally thick fuel, the dominant direction of heat transfer in the solid phase is in the normal direction. This would results in a flame spread rate directly proportional to the heat flux square from a simple analysis of the heat conduction equation in an semi-infinite media. The thickness of the boundary layer (flame stand-off distances) is inversely proportional with U_∞ and the difference between the adiabatic flame temperature arid fuel vaporization temperature is directly proportional with oxygen concentration (equation (2.6)), this would result in a heat flux on the fuel surface as

$$\dot{q}'' \sim U_\infty^{1/2}(T_f - T_v) \sim U_\infty^{1/2} Y_{o\infty} \qquad (3.62)$$

Thus the spread rate is directly proportional with $U_\infty Y_{o\infty}^2$. **Fig.3.3** shows the predicted spread rate given by equation (3.61). It is seen that except at very low flow velocity ($U_\infty < 0.5$ m/s) where buoyancy effect is significant [32],

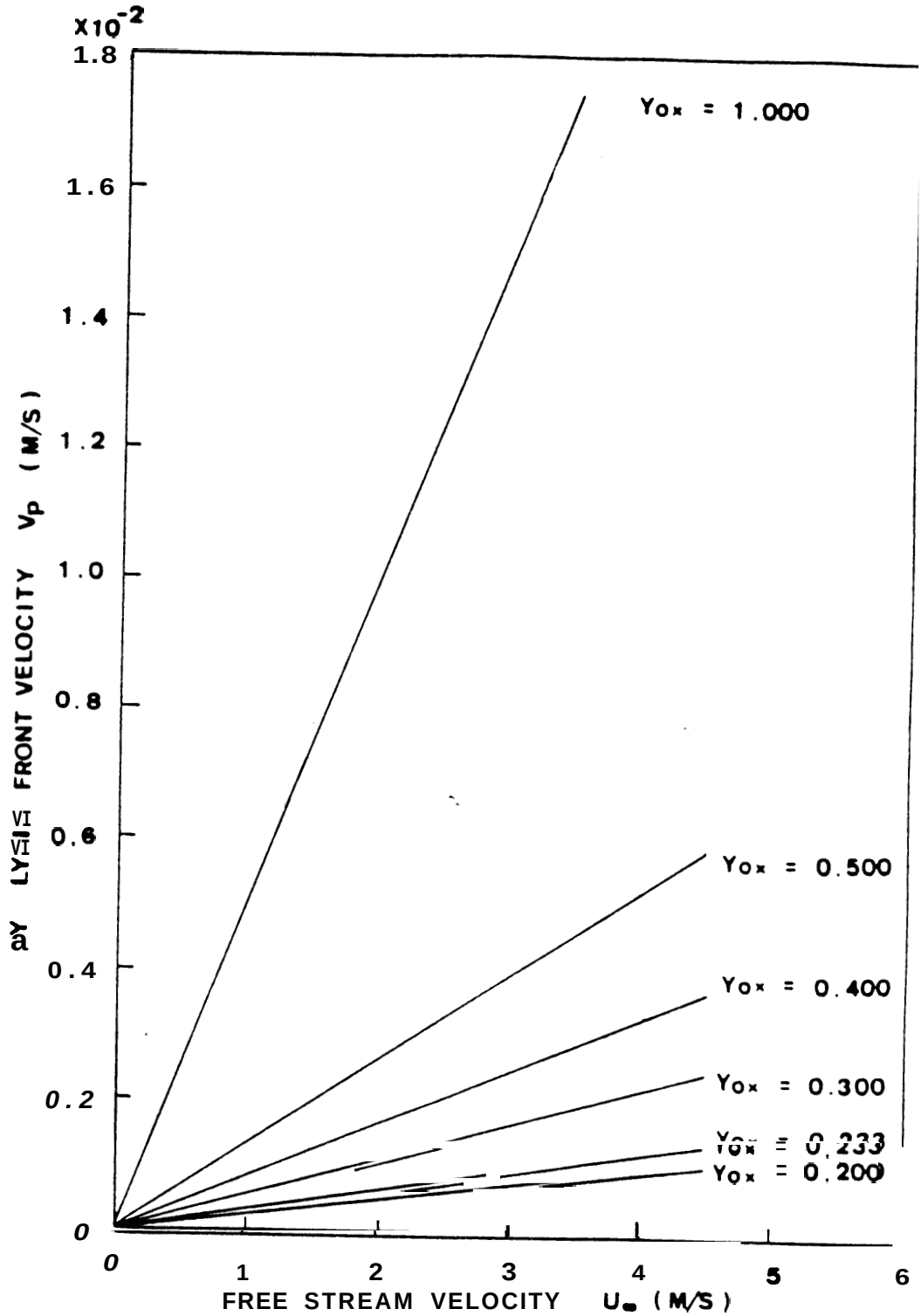
X10-2
1.8
1.6
1.4
1.2
1.0
0.8
0.6
0.4
0.2
0
0
1
2
3
4
5
6
FREE STREAM VELOCITY U∞ (M/S)
FRONT VELOCITY Vp (M/S)
Yox = 1.000
Yox = 0.500
Yox = 0.400
Yox = 0.300
Yox = 0.233
Yox = 0.200

Fig. 3. 3

there are good agreement between them over all the oxygen concentrations tested.

Chapter 4 Numerical Simulation of Flame Spread

4.1 Introduction

In many fire hazard problems, the vaporization and combustion of the fuel surface occurs in a convective environment. Heat transfer from the extended flame beyond the gasification region to the virgin fuel surface is responsible for the rapid flame spread rate. The heat flux transferred from this extended flame region to the fuel surface is dictated by three factors [1,2] : (1) The flame stand-off distance. **(2)** The extended flame length. **(3)** The local flame temperature. Which in their turn, ill change the aerodynamic structure of the flow field as well as the distributions of the various species compositions, Hence it is of interest to investigate the flow field behavior with the influence of a flame.

In this section, a numerical study of the burning of a laminar diffusion flame over a horizontal PMMA fuel surface is presented, it makes use of the GENMIX code with finite rate chemical reaction. The calculation domain is divided into two regions: (1) The upstream region where the fuel surface is vaporizing and the gas phase domain can be solved independent from the solid phase. (2)The downstream region where the solid and gas phase are coupled through their interfacial conditions and have to be solved simultaneously.

4.2 Model Formulation

A schematic diagram of the calculation domain is presented in Fig.4.1. The upstream region is a 5 cm long steady pyrolyzing PMMA surface and the downstream region is determined from the numerical computation marching along the fuel surface up to a location where the heat flux and fuel concentrations are within 1 % of their upstream value. Assuming an Arrhenius type of chemical reaction

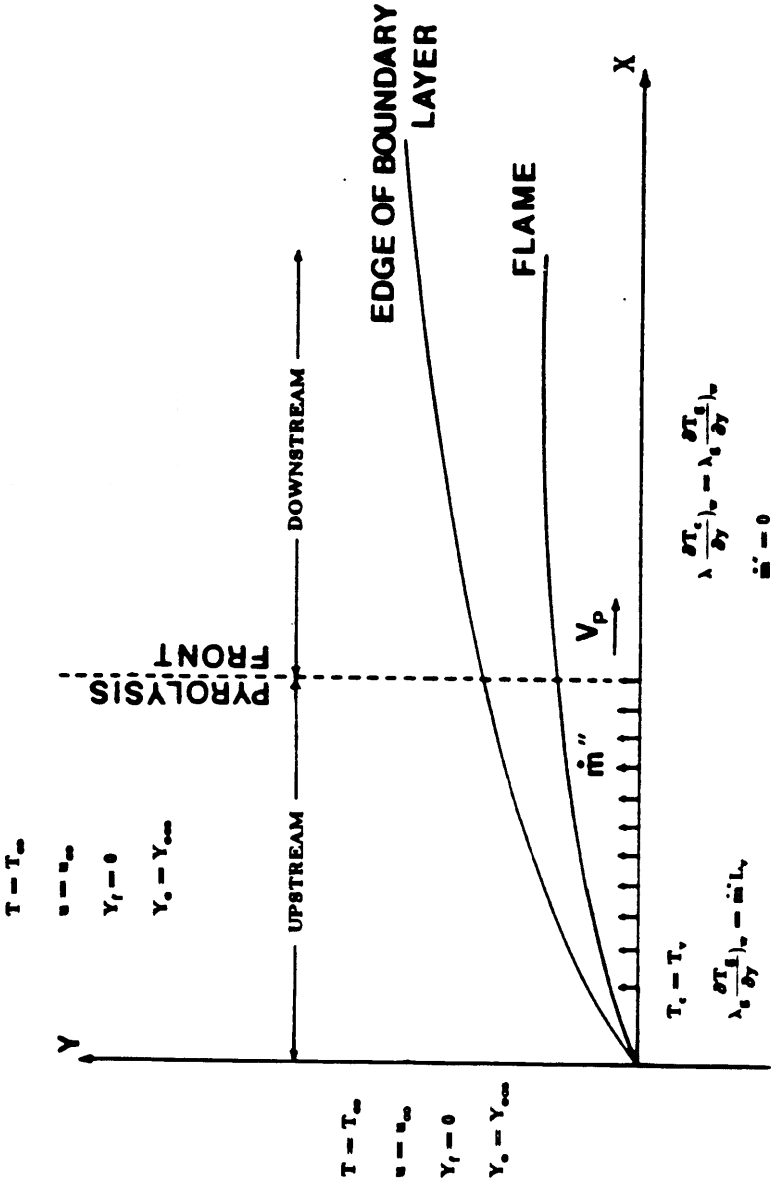
EDGE OF BOUNDARY LAYER
FLAME
PYROLYSIS FRONT
UPSTREAM
DOWNSTREAM
Y
X
V_p
$\dot{m}''$
$T - T_\infty$
$u - u_\infty$
$Y_f - 0$
$Y_o - Y_{o\infty}$
$T_s - T_v$
$\lambda_g \frac{\partial T_g}{\partial y}\Big|_w - \dot{m}'' L_v$
$\lambda \frac{\partial T_s}{\partial y}\Big|_w - \lambda_g \frac{\partial T_g}{\partial y}\Big|_w$
$\dot{m}'' = 0$
$\dot{m}'' = (\rho v)_w = (\rho v Y_{O_2})_w - (\rho D \frac{\partial Y_f}{\partial y})_w$
$(\rho v Y_f)_w = (\rho D \frac{\partial Y_f}{\partial y})_w$

Fig. 4. 1

$$\dot{q}''' = A Y_f \; Y_o \, \Delta H_R \, e^{-\frac{E}{RT}} \tag{4.1}$$

The set of equations to be solved becomes

$$\frac{\partial(\rho_g U)}{\partial x} + \frac{\partial(\rho_g V)}{\partial y} = 0 \tag{4.2}$$

$$\rho_g U \frac{\partial U}{\partial x} + \rho_g V \frac{\partial U}{\partial y} = \frac{\partial}{\partial y}\left(\mu_g \frac{\partial U}{\partial y}\right) \tag{4.3}$$

$$\rho_g U \frac{\partial h_g}{\partial x} + \rho_g V \frac{\partial h_g}{\partial y} = \frac{\partial}{\partial y}\left(\frac{\lambda_g}{c_p} \frac{\partial h_g}{\partial y}\right) + A Y_f \; Y_o \, \Delta H_R \, e^{-\frac{E}{RT}} \tag{4.4}$$

$$\rho_g U \frac{\partial Y_i}{\partial x} + \rho_g V \frac{\partial Y_i}{\partial y} = \frac{\partial}{\partial y}\left(\rho_g D_g \frac{\partial Y_i}{\partial n}\right) - A Y_f \; Y_o \, e^{-\frac{E}{RT}} \tag{4.5}$$

4.2.1 Upstream Region

The fuel surface is pyrolyzing in this region, there are three surface variables needed to solve the set of equations. Those are 'the fuel concentration at wall Y_{fw}, oxygen concentration at wall Y_{ow} and the blowing velocity at wall V_w [55]. To avoid the possible non-reacting solutions from the energy equation, the mass fraction of oxygen Y_o at wall is approximated to be zero, $Y_{ow} \approx 0$, the fuel concentration Y_{fw} at wall can be determined from energy and fuel balance at the wall :

$$\dot{m}'' L, = \frac{\lambda}{c_p} \frac{\partial h_g}{\partial y})_w = \rho_w V_w L, \tag{4.5}$$

$$\dot{m}'' = m'' Y_{fw} - \rho_g D_g \frac{\partial Y_f}{\partial y})_w \tag{4.6}$$

which yields

$$Y_{f1} = \frac{B - \frac{\nu_f M_f}{\nu_o M_o} Y_{o}}{1+B}$$

the blowing velocity V_w can be solved iteratively from the second and third terms of equation **(4.5).**

Other boundary conditions specified in this region are :

$$T(y = 0) = T_v \tag{4.7}$$

$$T(y = \infty) = T_\infty \tag{4.8}$$

$$Y_o(y = \infty) = Y_{o\infty} \tag{4.9}$$

$$Y_f(y = \infty) = 0 \tag{4.10}$$

The GENMIX code **was** adopted and extended to solve equations **(4.1)** to **(4.4)** along with the boundary conditions **(4.5)** to **(4.10)** in this region. Details relating to the finite difference formulation and numerical algorithms are provided in ref. [57], only a brief summary is given here. Numerical calculations are carried out in $X \sim w$ domain where X is the predominant flow direction and *w* is a normalized stream function with value between 0 and **1,** a set of non-uniform spacing of grids are specified which grows **as** the boundary layer grows at a preset rate. Calculations are repeated for several grid spacing to establish a grid-independent solution which was found to correspond to **93** grids across the boundary layer thickness (Y-direction). Once the coefficients for the finite difference equations have been evaluated for each node in the Y-direction, a tri-diagonal matrix algorithm **was** used to solve for U, T, Y_f , Y_o at each stream-wise location. To satisfy the energy balance at the wall, the blowing velocity V_w at the wall was first assumed and solved iteratively until equation **(4.5) was** satisfied, then the calculation proceeds to the next **x** location. In the compu-tation, physical and chemical properties used are the following [54,55] :

$L = 1.59 \times 10^6\ J/kg\ of\ monomer$, $T_v = 663\ k$, $C_p = 1210\ J/Kg\text{-}k$,

$\Delta H_R = 1.357 \times 10^7\ J/Kg\ of\ oxidizer$, $E = 1.05 \times 10^8\ J/Kg\text{-}mole$,

$A = 1.0 \times 10^{11}\ Kg/m\text{-}sec$ aiid $Q = 2.6 \times 10^6\ J/\nu_f\ mole\ of\ monomer$

When converged solutions are obtained for each grid location, an appropriate inverse transform was adopted to convert from $X \sim w$ domain to $X \sim Y$ coordinates.

4.2.2 Downstream Region

In this region, simultaneous solution of the gas and solid phase are required through their coupling at the interface. The solution procedure is the following :

(1) The gas phase equations are solved by assuming a temperature distribution along the non-pyrolyzing fuel surface.

(2) A sweep from upstream to downstream yields the corresponding heat flux distribution along the fuel surface downstream from the pyrolysis front.

(3) With the calculated heat flux on the wall, a temperature distribution

$$\frac{T(\sigma,0)-T_\infty}{T_v-T_\infty} = \frac{\int_{\frac{1}{\Lambda}}^{\sigma} (\sigma-\tau)^{1/2}\frac{1}{\tau}(q_\tau \tau^{1/2}-\frac{1}{2}q\,\tau^{-1/2})d\tau}{\int_{\frac{1}{\Lambda}}^{1} (1-\tau)^{1/2}\frac{1}{\tau}(q_\tau \tau^{1/2}-\frac{1}{2}q\,\tau^{-1/2})d\tau} \qquad (4.11)$$

along the fuel surface can be calculated from the solid phase analysis in (σ,η) domain, where q is the local heat flux on the fuel surface from the previous step gas phase solution and q_τ its derivative along the σ direction (τ being a dummy integration variable).

(4) Under-relax the updated temperature distribution

$$T_{new} = 0.5(\, T_{old} + T_{new} \,) \qquad (4.12)$$

return to step 2 until the relative change in the temperature values between consecutive iterations is less than 1 %. Then the pyrolyzing velocity can be calculated with the formula

$$V_p = \left(\frac{2\int_{\frac{1}{\Lambda}}^{1} (1-\tau)^{1/2}\frac{1}{\tau}(q_\tau \tau^{1/2}-\frac{1}{2}q\,\tau^{-1/2})d\tau}{T_v - T_\infty} \right)^2 \frac{\alpha_s X_p}{\pi \lambda_s^2} \qquad (4.13)$$

4.3 Numerical Results

4.3.1 Mass Flux Distribution

Fig.4.2 presents a comparison of the local mass flux distribution along its pyrolyzing surface from analytical solution, numerical solution and experiments with the experimental data taken from [52]. Because the flame sheet approximation was used in the model, an infinite fast chemical reaction rate results in the flame attaches the fuel bed at its leading edge, which produces an infinite amount of local mass flux there. While the finite rate chemical kinetic effect used in the numerical calculation produces a finite jump of mass flux at where the local gas phase temperature is high enough to have an appreciable amount of reaction. Both the numerical results and the model predicts a gradual decay of the local mass flux along the fuel surface following the boundary layer concept that the flame moves away from the wall as the boundary layer thickness grow along the X-axis.

4.3.2 Wall Temperature Distribution

A schematic diagram of the fuel surface temperature distribution beyond its pyrolyzing region is shown in Fig.4.3. Although our calculation proceeds to approximately $X = 5$ m downstream (where $X/X_p \sim 100$), it is seen that the temperature drops rapidly from its pyrolyzing temperature to around 400 K at $X \sim 40$ cm (where $X/X_p \sim 8$). The model predicts a temperature distribution decays faster than the experimental data shows while the numerical results agrees with the experimental data over most of the flame extended region and deviates near the tip of the flame.

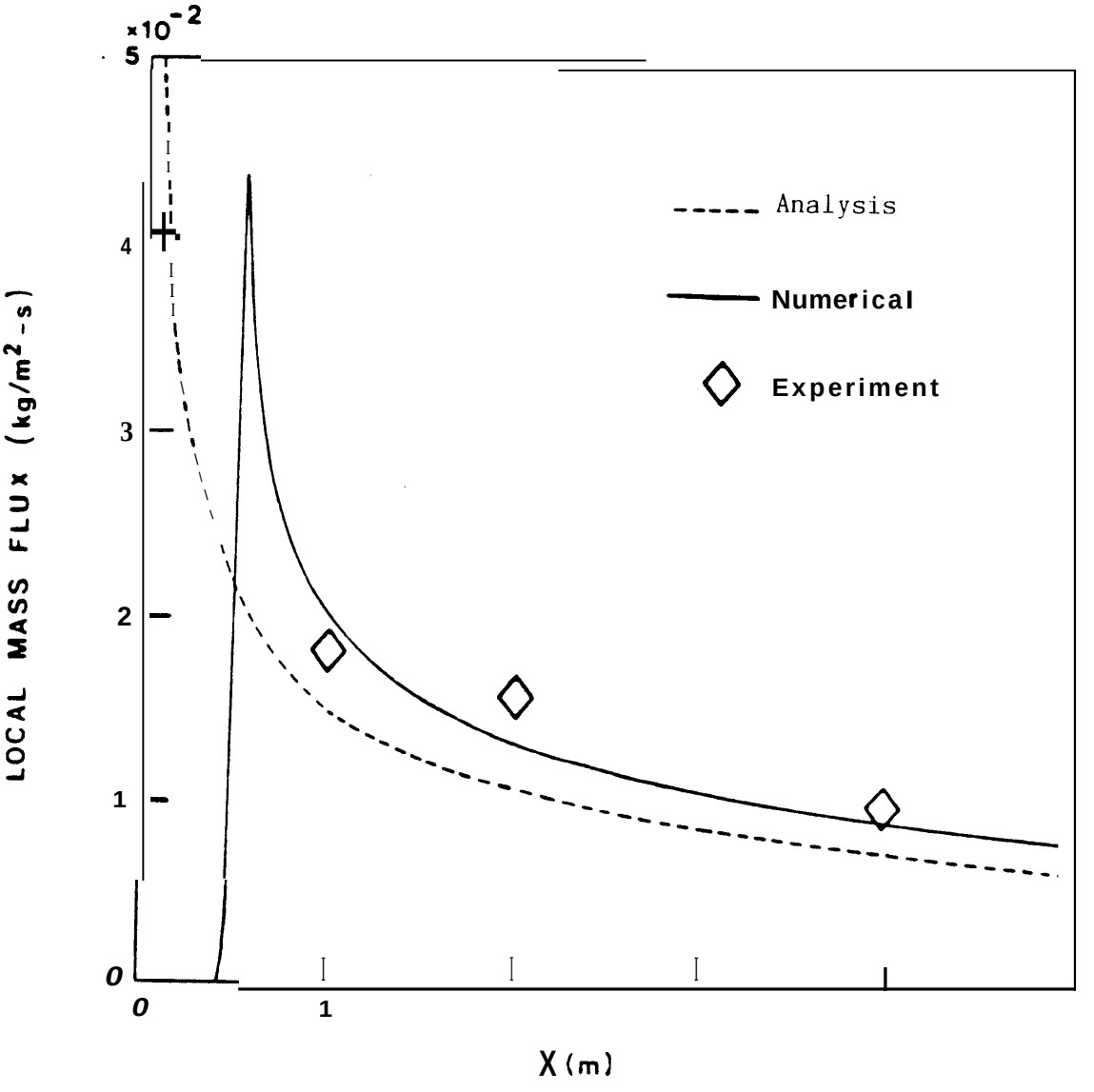
×10⁻²
5
4
3
2
1
0
0
1
LOCAL MASS FLUx (kg/m²-s)
X (m)
Analysis
Numerical
Experiment

Fig. 4. 2

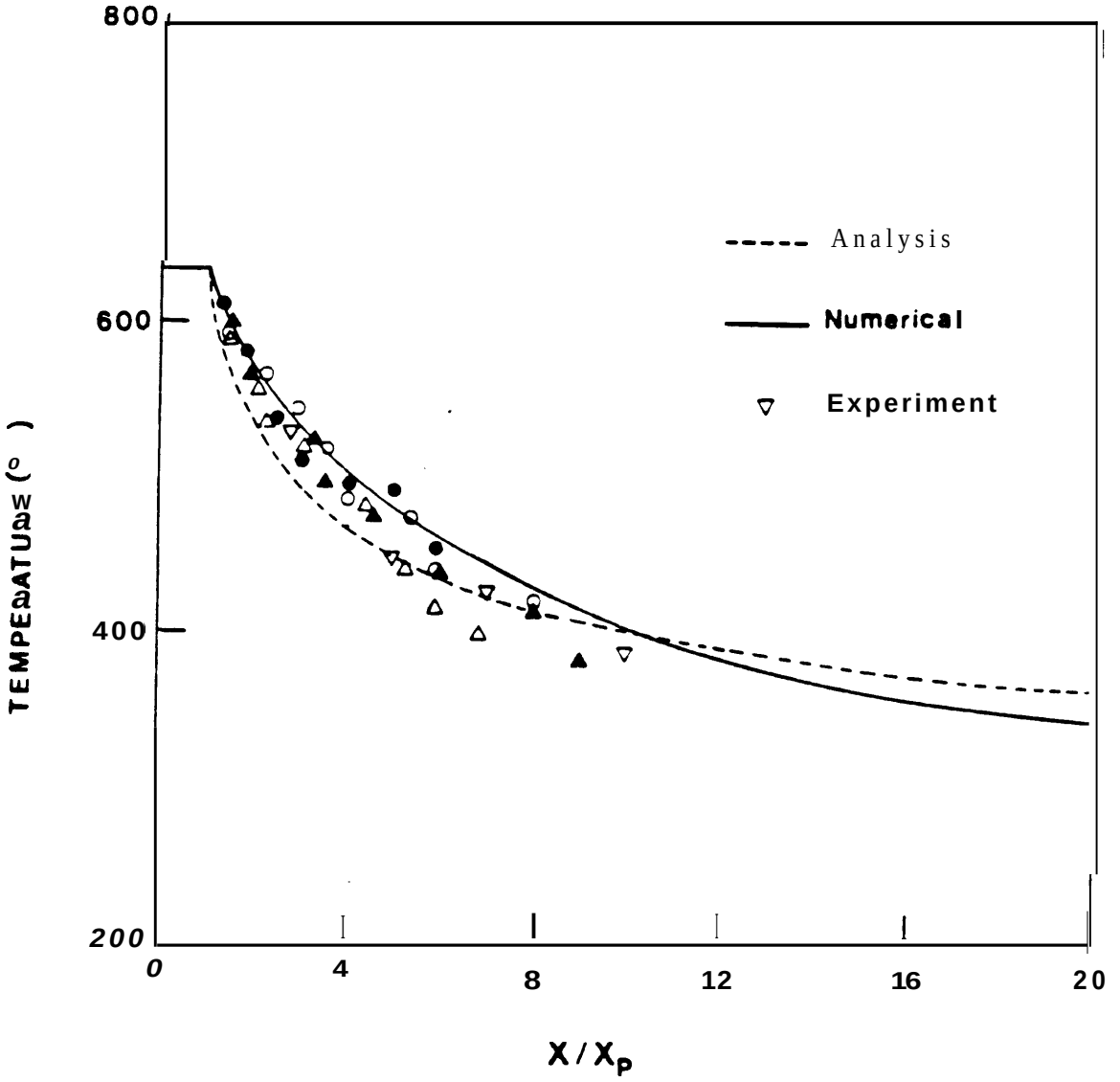
800
600
400
200
0
4
8
12
16
20
TEMPERATURE (°)
X / Xp
Analysis
Numerical
Experiment

Fig. 4. 3

4.3.3 Heat Flux Distribution

The predicted heat flux distribution along the downstream fuel surface is presented in fig.4.4. In the figure, the x coordinate is X_p/X to emphasize the larger amount of heat **flux** in the flame extended region that is responsible for the flame spread rate. It is seen that the heat **flux** first increase beyond the pyrolyzing region due to the decrease of surface temperature (hence larger temperature gradient), then remains at approximately a constant level over most of the flame covered region, finally rapidly decays to zero after the tip of the flame. As expected, the effect of oxygen concentration to local heat flux is approximately linearly proportional with $Y_{o\infty}$ since $T_f >> T_{local}$ and $(T_f - T_v) \tilde{} Y_{o\infty}$

4.3.4 Comparison of Flame Spread Rate

Fig.4.5 shows the comparison of the flame spread rate from experiment, model and numerical results over the oxygen concentration range from **20** % to 100 %. Good agreements among all three of them shows the validity of **quasi**-steady modeling and flame sheet approximation for the gas phase processes and the effect of radiation is insignificant in small scale fires.

4.4 Flow Field Behavior

4.4.1 Temperature Distribution

The predicted temperature distribution in the gas phase is shown in **fig. 4.6** and **4.7.** Fig.4.6 shows the temperature isotherms in the upstream pyrolyzing region and Fig.4.7 the downstream counterpart for $U_\infty = 1$ m/s and $Y_{o\infty} = 0.23$. In fig.4.6, the narrow spacing of the isotherms on the air side of the flame zone indicates that the temperature gradient there is sharper than on

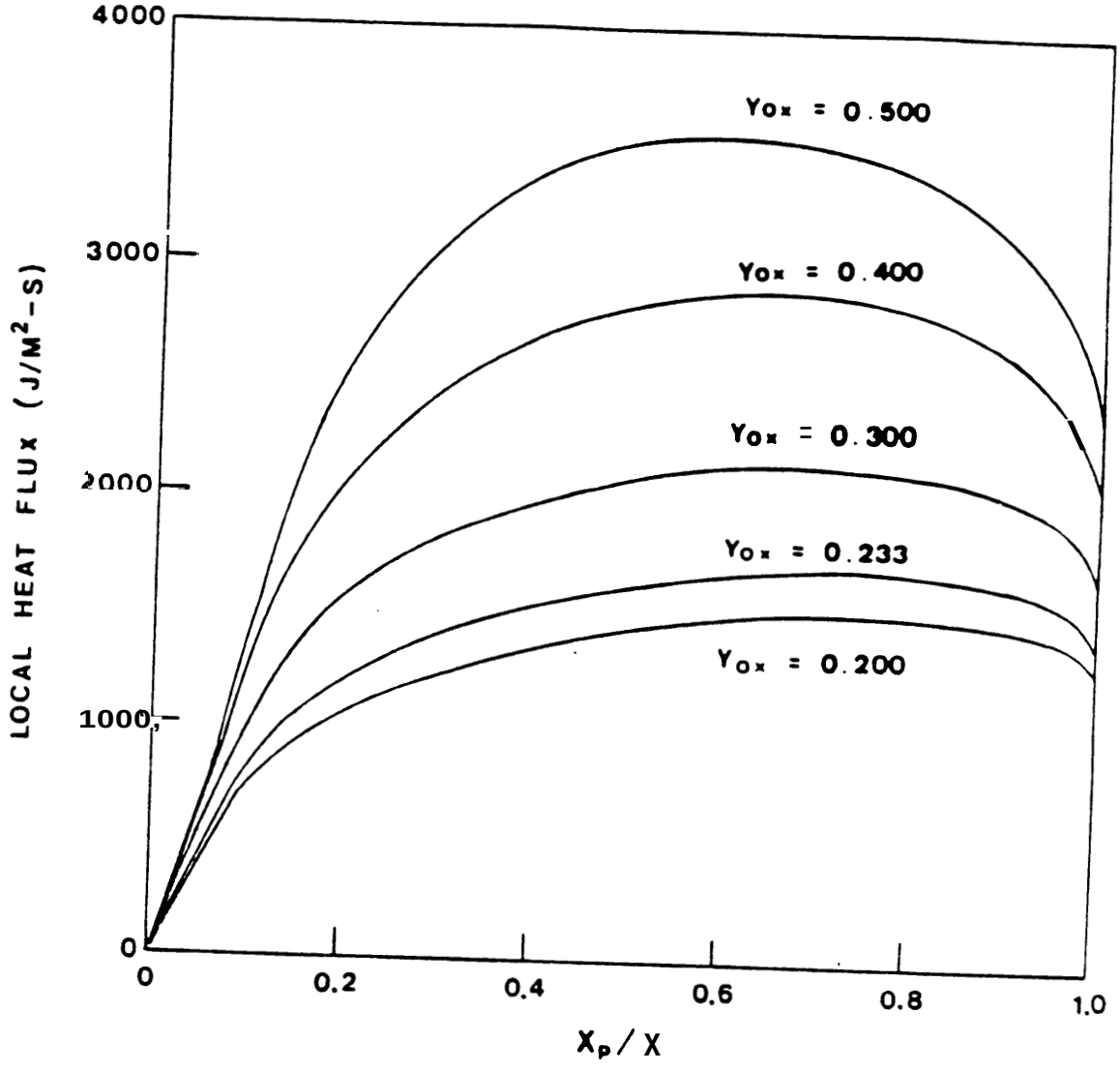
4000
3000
2000
1000
0
LOCAL HEAT FLUX (J/M²-S)
Yox = 0.500
Yox = 0.400
Yox = 0.300
Yox = 0.233
Yox = 0.200
0
0.2
0.4
0.6
0.8
1.0
Xp / X

Fig. 4. 4

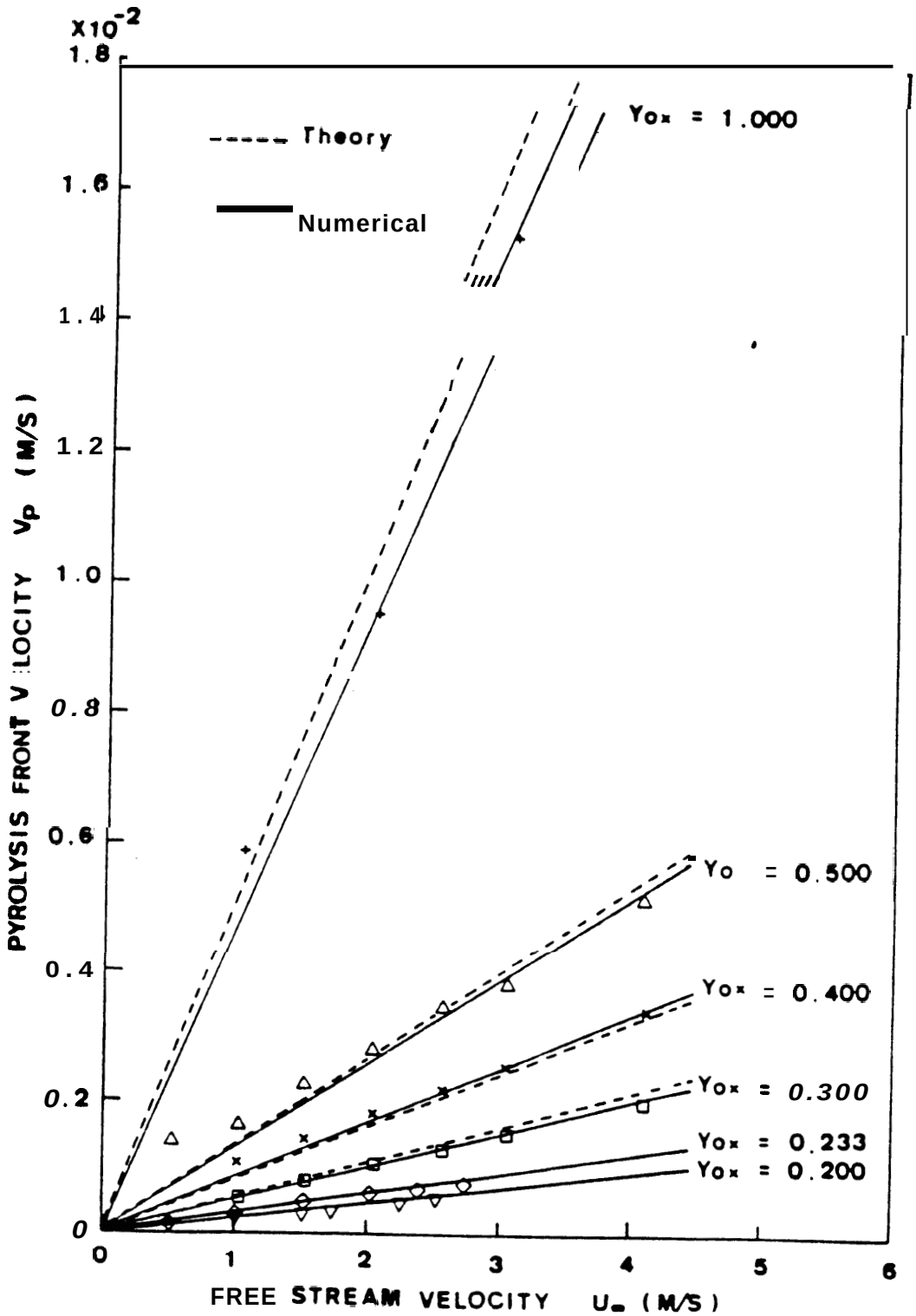
X10^-2
1.8
1.6
1.4
1.2
1.0
0.8
0.6
0.4
0.2
0
Theory
Numerical
Yox = 1.000
Yo = 0.500
Yox = 0.400
Yox = 0.300
Yox = 0.233
Yox = 0.200
PYROLYSIS FRONT VELOCITY Vp (M/S)
0
1
2
3
4
5
6
FREE STREAM VELOCITY U∞ (M/S)

Fig. 4. 5

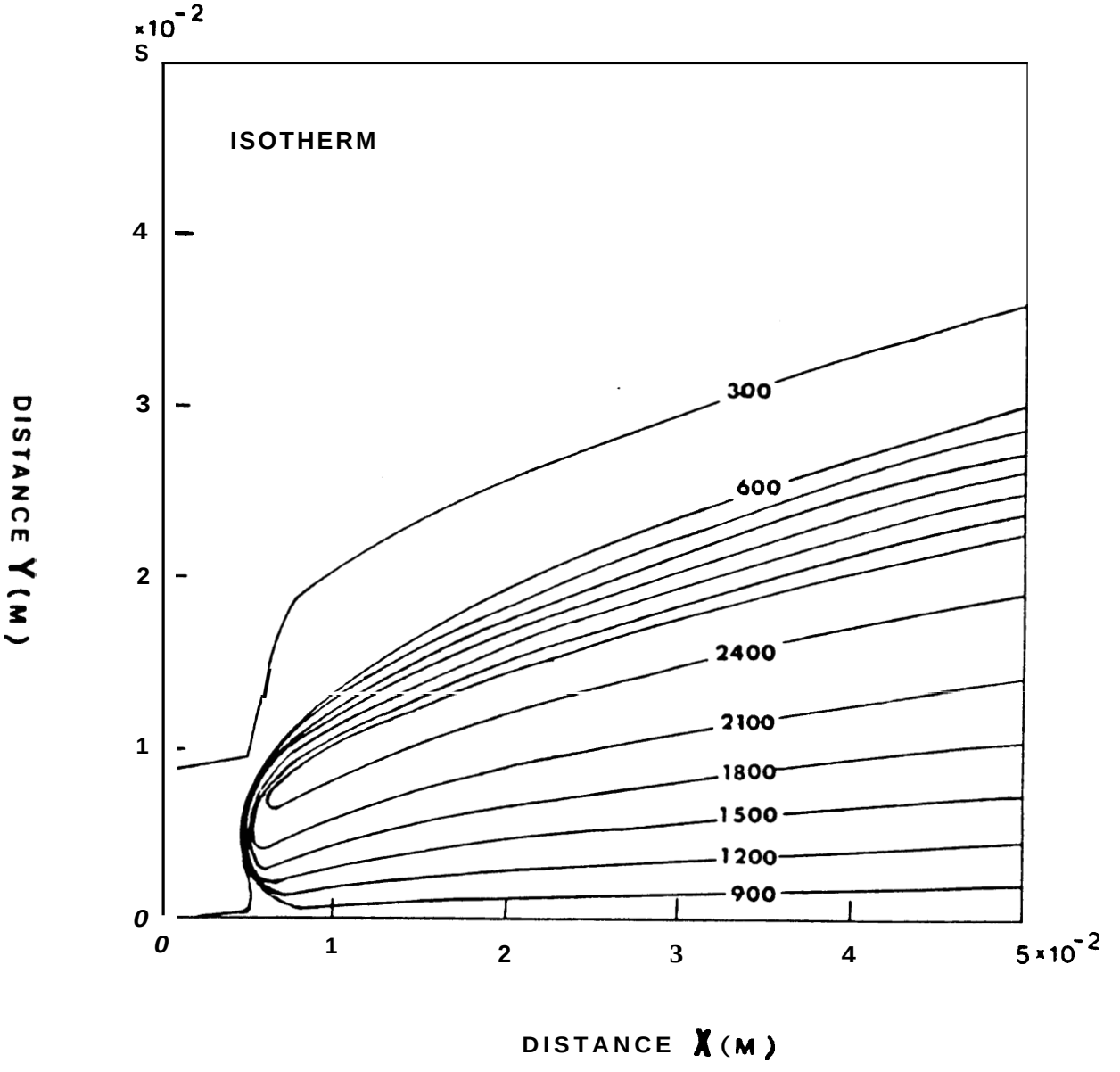
×10⁻²
S
ISOTHERM
4
3
2
1
0
0
1
2
3
4
5×10⁻²
300
600
2400
2100
1800
1500
1200
900
DISTANCE Y (M)
DISTANCE X (M)

Fig. 4. 6

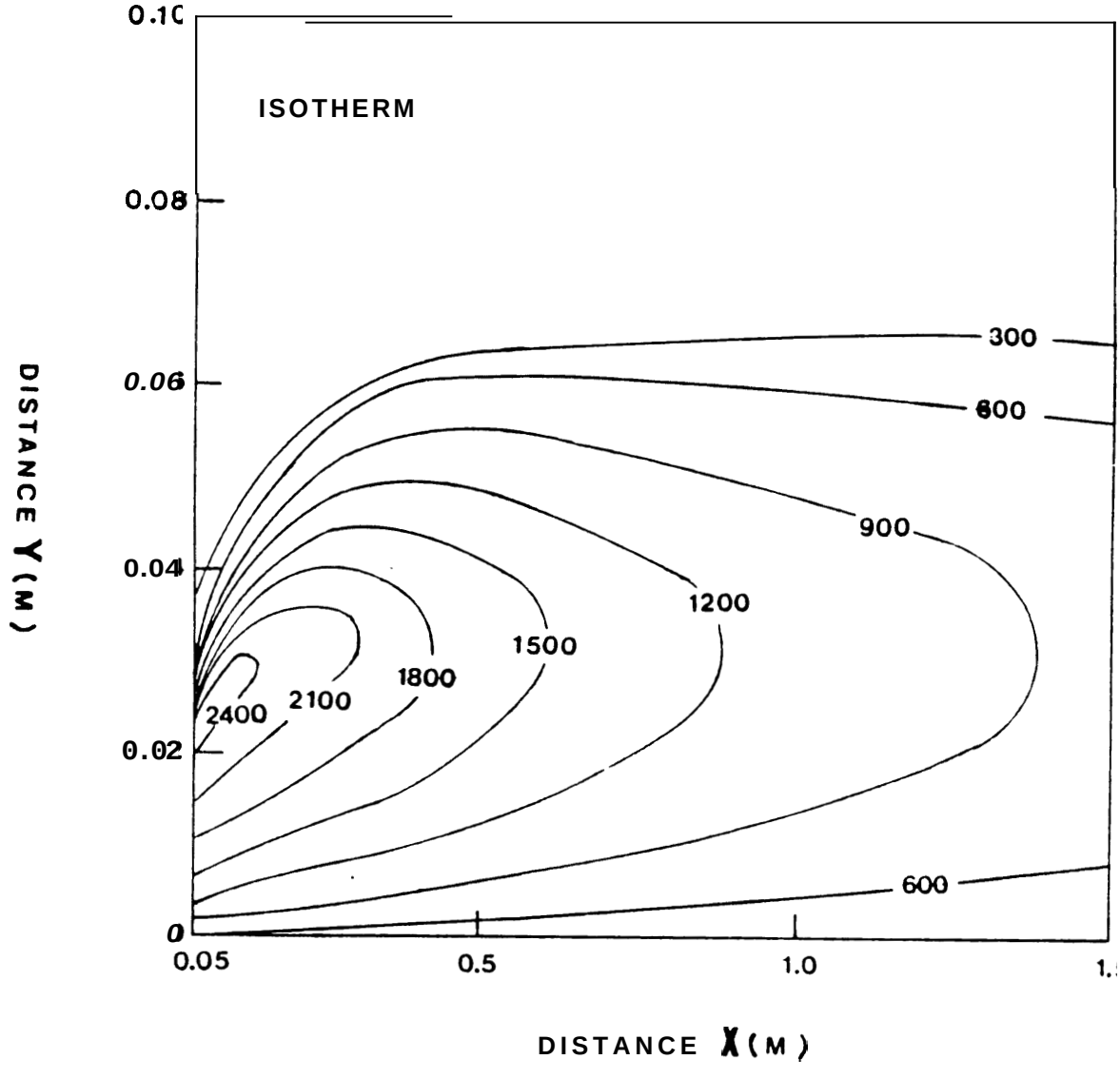
ISOTHERM
0.10
0.08
0.06
0.04
0.02
0
0.05
0.5
1.0
300
600
900
1200
1500
1800
2100
2400
600
DISTANCE Y (M)
DISTANCE X (M)

Fig. 4. 7

the fuel rich side and both grows as the boundary layer grows. With the presence of a flame around 2400 k, the boundary layer thickness expands at the leading edge of the flame due to the sudden presence of large temperature gradient and the increase of thermal diffusivity at high temperature. In the downstream isotherms of fig.4.7, it is seen that the peak temperature of the isotherms, which serves to indicate approximately the location of the flame, firstly move away from the wall due to the continuing growth of the boundary layer, then approach the fuel surface at further downstream because of the consumption of the excess fuel. The thermal boundary layer grows at a much slower rate than in the upstream because the lack of high temperature driving force.

4.4.2 Fuel Distribution

Fig.4.8 shows the predicted fuel mass fraction contours upstream and downstream from the pyrolysis front. In the upstream region, the constant fuel concentration lines follow the boundary layer growth and presents a finite jump at the leading edge of the flame, the presence of flame acts as a source to extract fuel evaporated from the surface. The large reaction rate existed at the flame prevents the penetration of fuel through the flame zone. Fig.4.9 shows the distribution of fuel in the downstream region. Because of the split type boundary condition imposed at the downstream region, there is no fuel evaporated from the surface, the excess pyrolysis was quickly consumed by the flame and the constant fuel concentration line approaches the fuel surface. Due to the boundary condition

$$\frac{\partial Y_{f-})_w}{\partial y} = 0 \qquad (4.14)$$

that each of the fuel contour is perpendicular to the fuel surface.

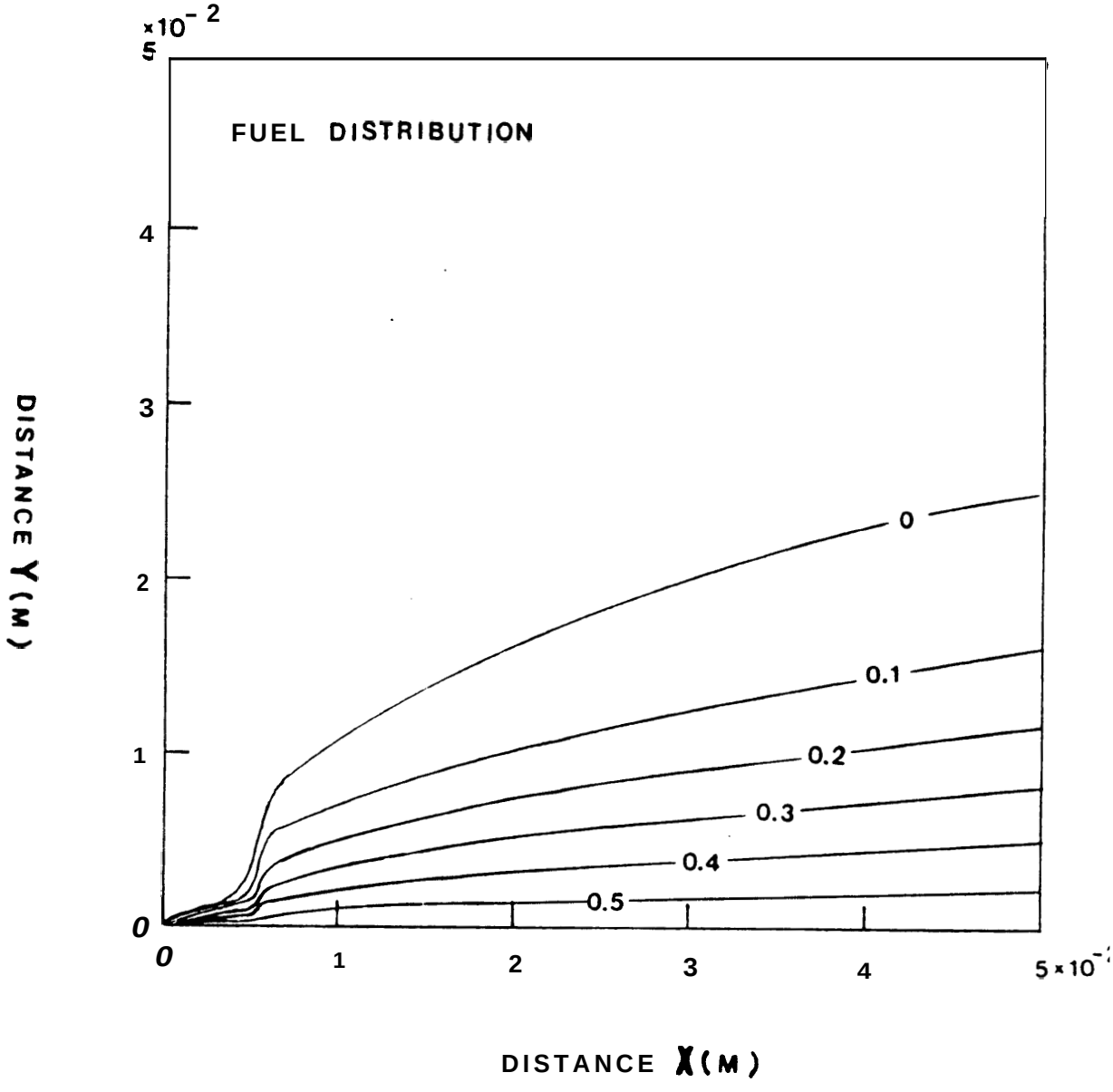
×10⁻²
FUEL DISTRIBUTION
DISTANCE Y(M)
DISTANCE X(M)
0
0.1
0.2
0.3
0.4
0.5
0
1
2
3
4
5

Fig. 4. 8

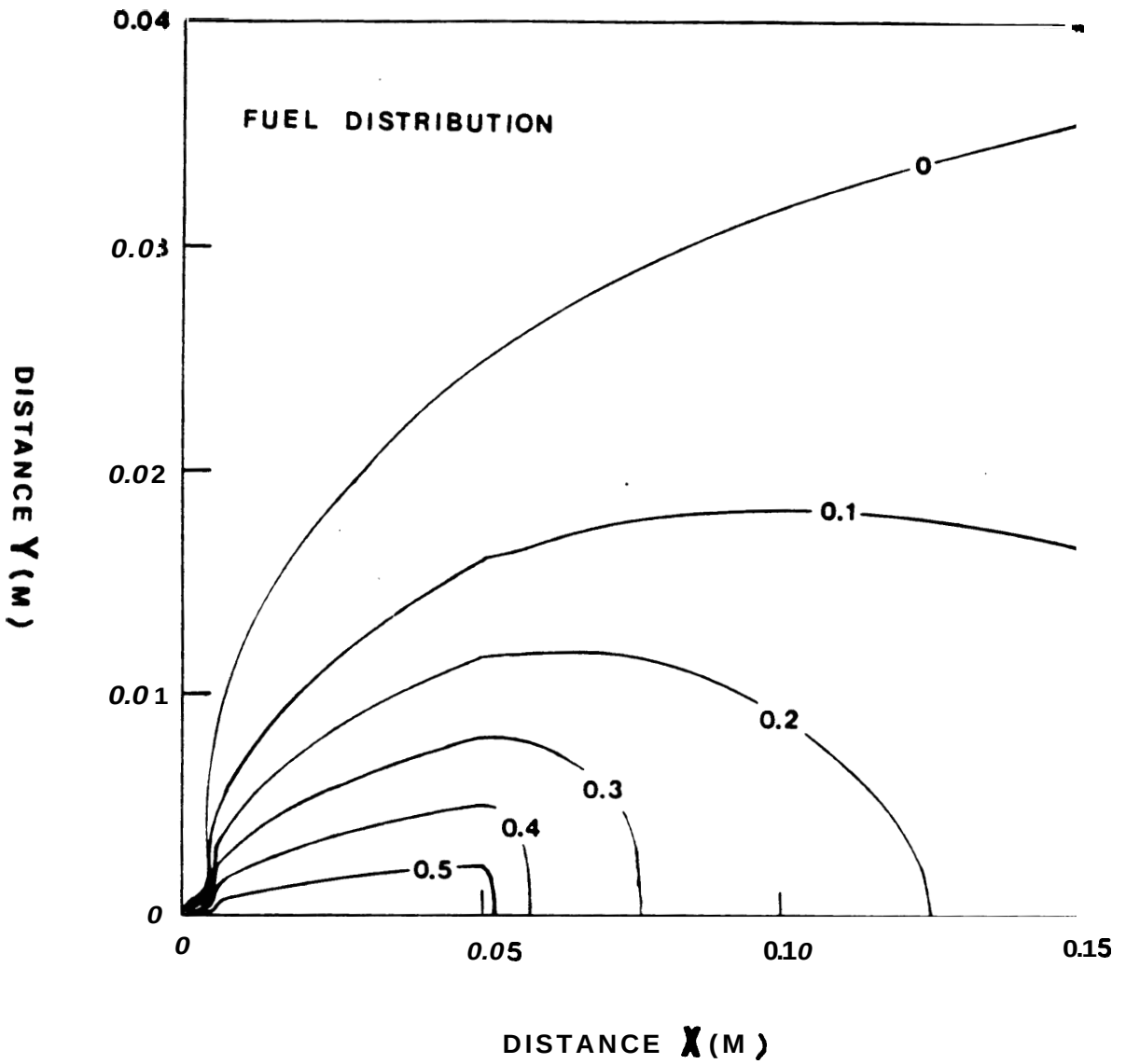
FUEL DISTRIBUTION
0.04
0.03
0.02
0.01
0
0
0.05
0.10
0.15
DISTANCE Y (M)
DISTANCE X (M)
0
0.1
0.2
0.3
0.4
0.5

Fig. 4. 9

4.4.3. Oxygen Distribution

The result of oxygen mass fraction distribution in the upstream and down stream region are presented in fig.4.10 and 4.11. The distribution of the oxygen mass fraction contours is quite similar to that of the fuel distribution except it positioned close to the external flow. Due to the large reaction in the flame zone, no oxygen presents within the flame. In the upstream region the oxygen contours are elevated at the flame leading edge due to its consumption at the flame, then slowly following the boundary layer growth as expected. In the downstream region, the oxygen lines approaches the fuel surface to compensate for the necessary reaction.

4.4.4 Stream Line Distribution

Fig.4.14 and 4.15 shows the distributions of stream lines in the upstream and downstream region. In the upstream region, the stream line moves away from the fuel surface along with the boundary layer. A sudden expansion in the flame leading edge is observed and the widening of the spacing between the lines shows the decrease of gas density at high temperature. Lines starts from the fuel surface indicates the trajectories of the fuel particles. In the downstream region, the lines approaches the fuel surface following the large amount of entrainmerit of fresh fluid from the edge of the boundary layer [48].

4.5 Conclusion

The flow structure of a two-dimensional laminar diffusion flame burning over a horizontal surface in an forced flow environment has been studied. The results of temperature, species concentration and stream line distribution provide important information in the gas phase heat and mass transfer processes. Although the validity of the numerical analysis at the leading edge of the flame

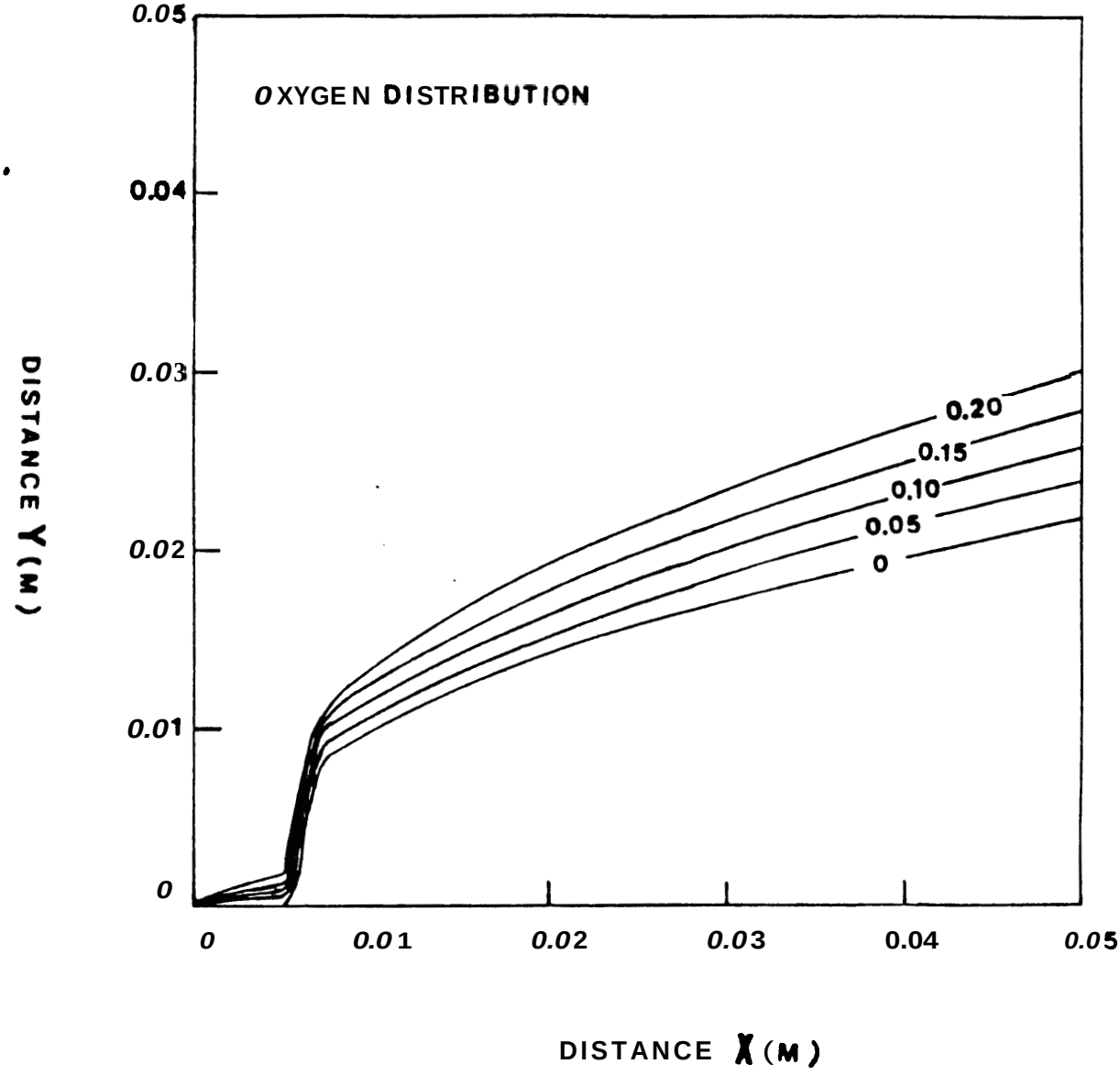
OXYGEN DISTRIBUTION
0.05
0.04
0.03
0.02
0.01
0
DISTANCE Y (M)
0.20
0.15
0.10
0.05
0
0
0.01
0.02
0.03
0.04
0.05
DISTANCE X (M)

Fig. 4. 10

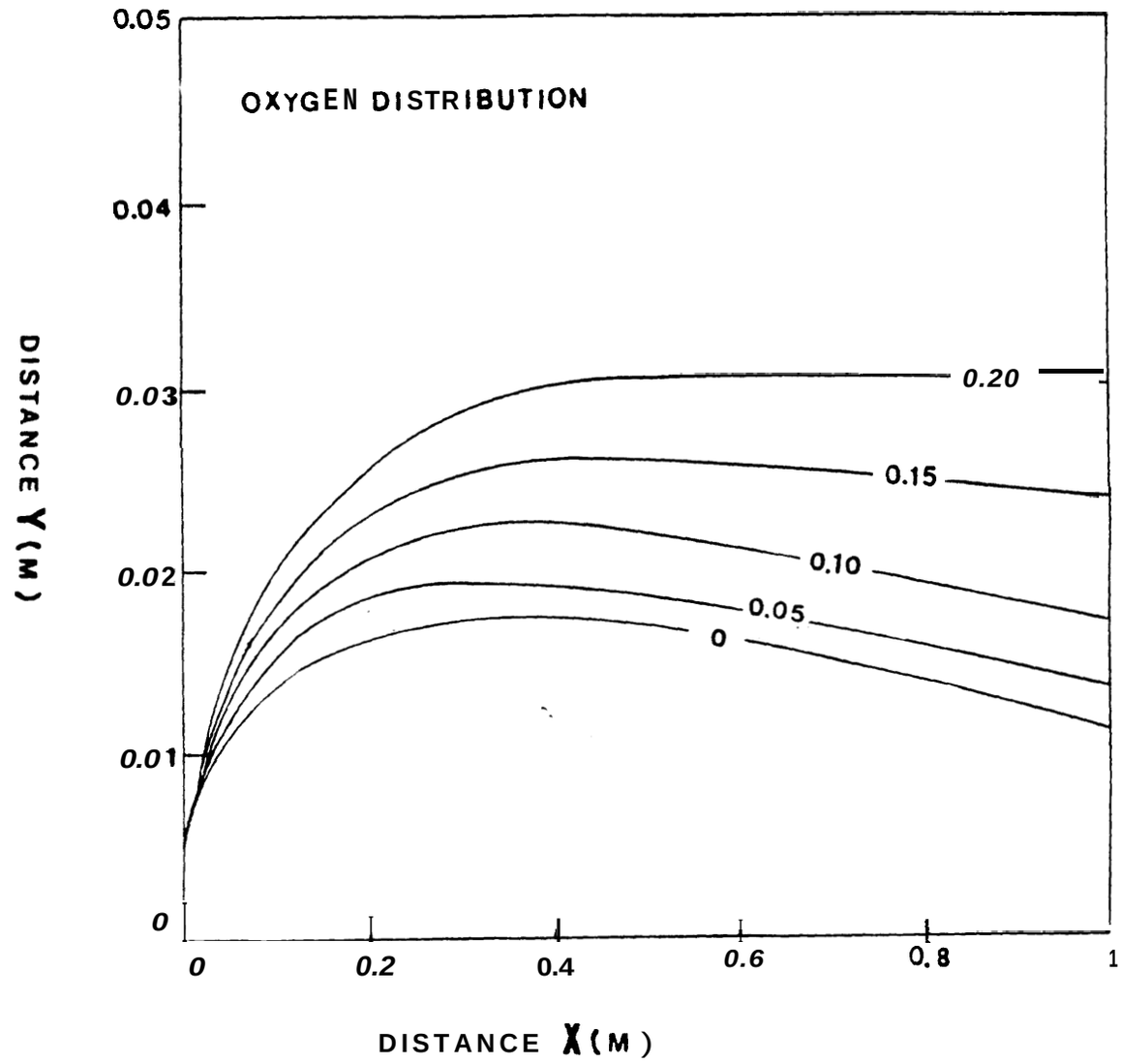
OXYGEN DISTRIBUTION
0.05
0.04
0.03
0.02
0.01
0
DISTANCE Y (M)
0.20
0.15
0.10
0.05
0
0
0.2
0.4
0.6
0.8
1
DISTANCE X (M)

Fig. 4. 11

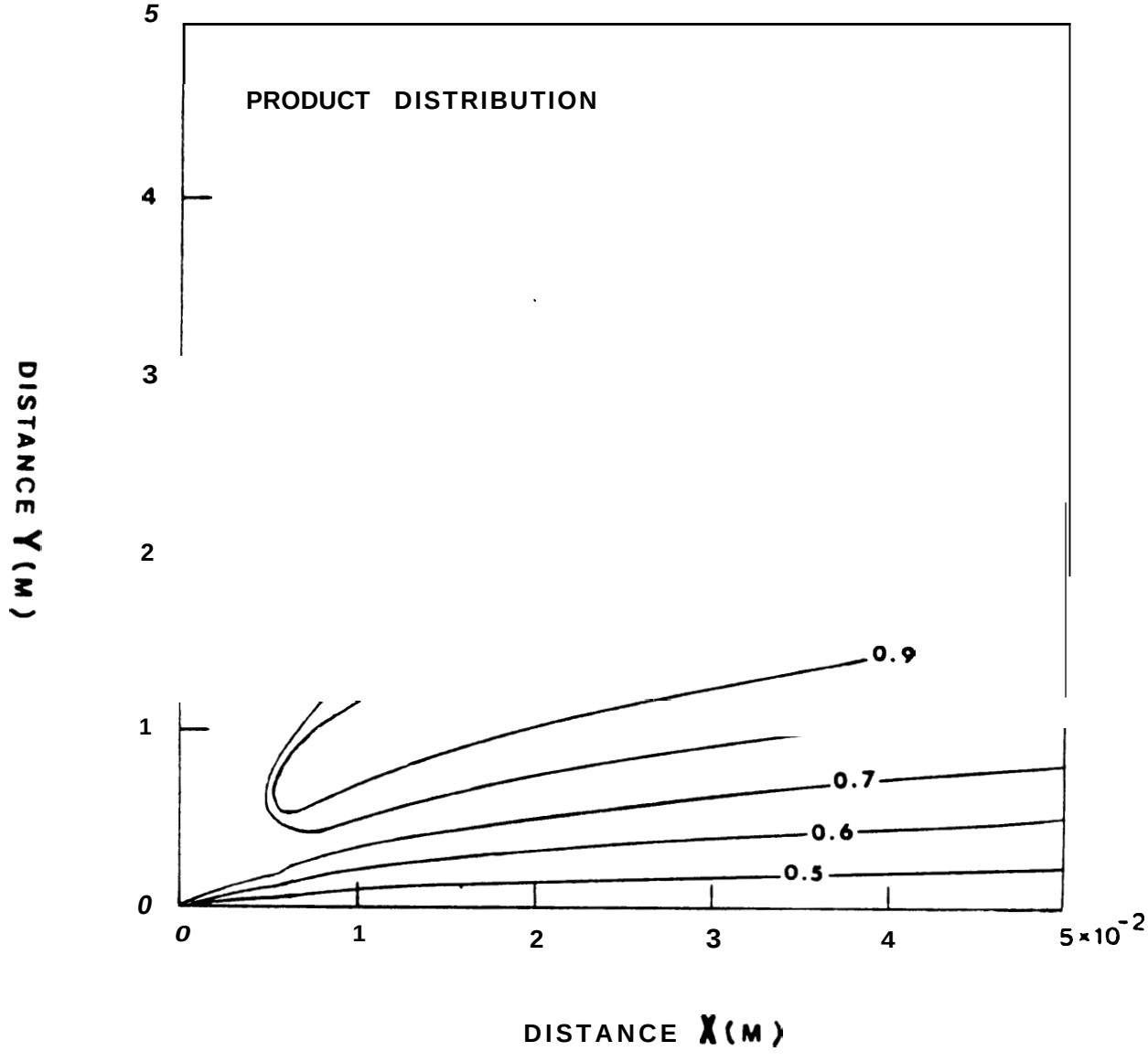
PRODUCT DISTRIBUTION
DISTANCE Y (M)
DISTANCE X (M)
0.9
0.7
0.6
0.5
0
1
2
3
4
5
0
1
2
3
4
5×10⁻²

Fig. 4. 12

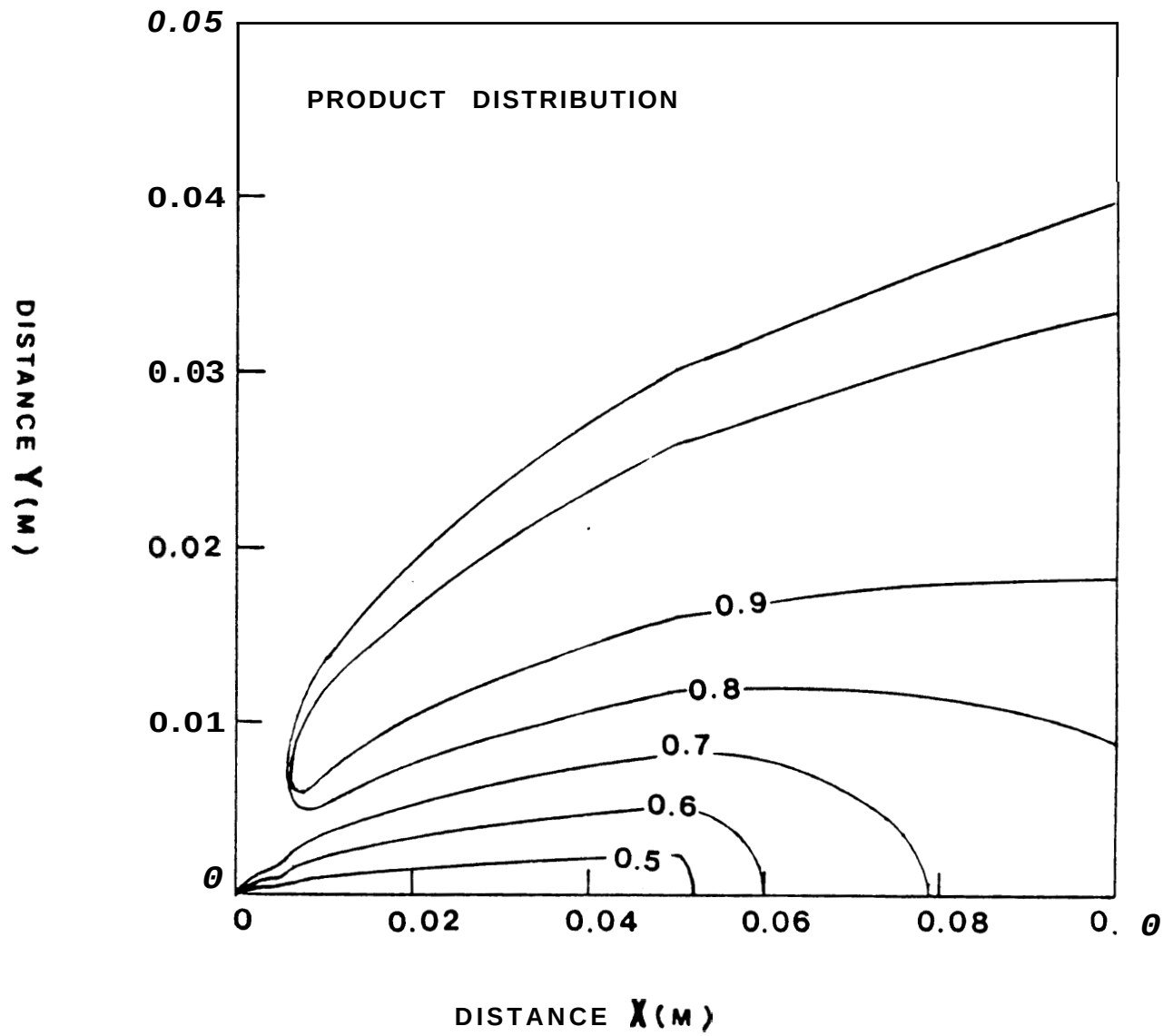
PRODUCT DISTRIBUTION
0.05
0.04
0.03
0.02
0.01
0
DISTANCE Y(M)
0.9
0.8
0.7
0.6
0.5
0
0.02
0.04
0.06
0.08
0.0
DISTANCE X(M)

Fig. 4. 13

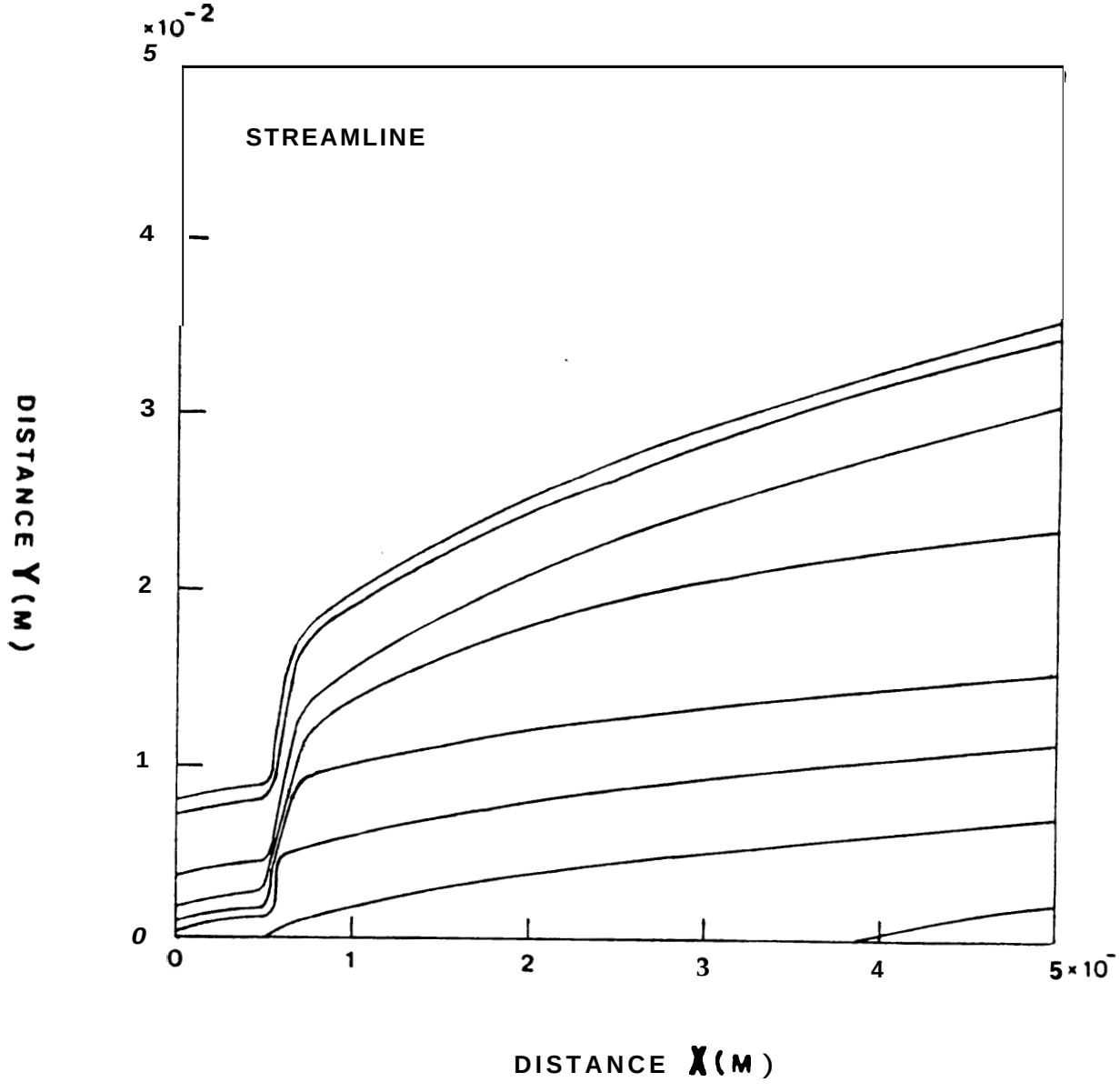

Fig. 4. 14

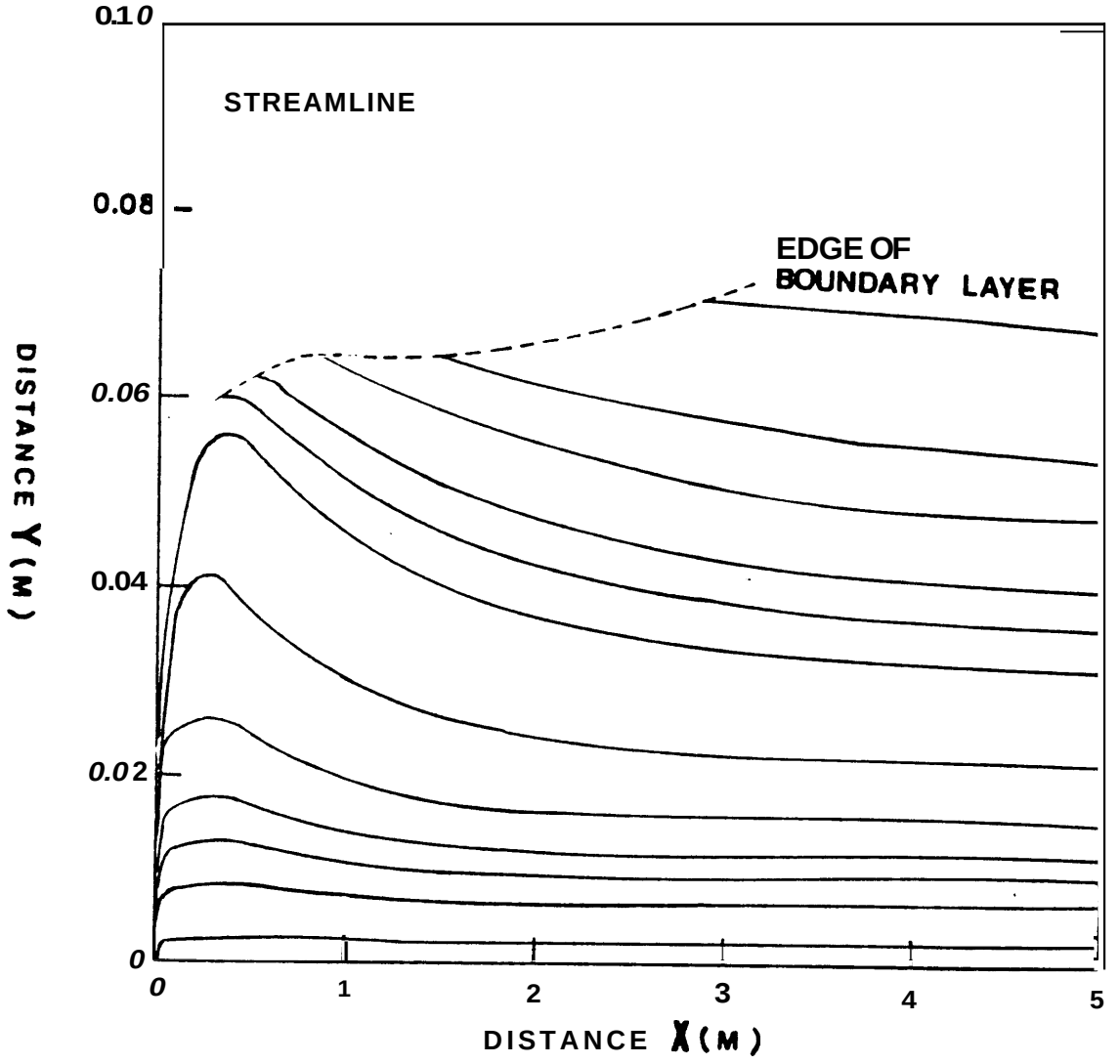
0.10
STREAMLINE
0.08
EDGE OF
BOUNDARY LAYER
0.06
0.04
0.02
0
DISTANCE Y (M)
0
1
2
3
4
5
DISTANCE X (M)

Fig. 4. 15

is questionable due to the parabolic nature of the boundary layer simplification. At farther downstream, a boundary layer type analysis is adequate due to the larger gradients of the field properties in the cross-stream direction than that in the stream-wise direction. To study in detail the behavior of the flame and of the flow structure in its leading edge would require a solution of the equations **(4.1)** to (4.4) including their longitudinal diffusion terms.

Chapter 5 Conclusion and Future Work

5.1 Summary of Results

An experimental study of the flame spread rate over both thermally thick and thin fuels in a forced flow environment was conducted. The detailed mechanisms of the flame spreading process are, however, not well understood. A simple correlation of equation (2.5) and (2.9) reveals that the flame spread process can be explained from a heat transfer point of view and that chemical kinetic effect is of secondary importance. In the experiments, a thermocouple probing technique is used to measure the flame spread rate over PMMA surface by recording the temperature histories and a photographic method is used to record the spread rate on thin filter paper sheets. The different behavior of their pyrolysis growing rate indicates their different heat transfer path in the solid phase and the influence of the burn-out process. For the thermally thick fuel study, the dominant heat transfer path is in the normal direction and the major conclusions can be summarized as follows :

(1) Equation (2.5) correlate closely all our experimental data under forced flow conditions for $U_\infty < 4$ m/s and $20\ \% < Y_{o,\infty} < 100\ \%$. The fact that there is no chemical kinetic effect in the correlation suggests that the flame spread rate is controlled primarily by heat transfer mechanisms alone.

(2) A simplified analysis using a quasi-steady model and flame sheet approximation results in a flame spread rate linearly proportional with $U_\infty Y_{o,\infty}^2$. The linear dependence of V_p on U_∞ is due to the decrease of the boundary layer thickness (or flame stand-off distance) as the flow velocity increases. While the dependence of V_p on the oxygen concentration is due to the increase of the flame temperature as the oxygen concentration increases. Being simple, the model identifies the controlling parameters in the flame

spread process.

(3) A numerical study using finite rate kinetics indicates the influence of the flame on the boundary layer growth rate and its aerodynamic structure. The primary effect of the finite rate kinetics occurs at the leading edge of the flame and subsequent behavior of the flow structure is then controlled by the diffusion process of the fuel and the oxidizer in their cross-stream direction.

(4) That the heat flux distribution is almost constant over the fuel surface as predicted in ref [15] has been verified through our numerical results.

For a thermally thin fuel, because the fuel thickness is thin enough that the temperature gradient across the thickness of the fuel can be neglected and the following conclusions can be drawn from our investigation :

(1) In the early developing stages of the flame spread process, the flame spread rate is accelerative from flame initiation to approximately **15** to **20** cm downstream and the spread rate is linearly proportional with time, $V_p \sim t$.

(2) During the flame spreading process, the flame length L_f is linearly proportional with its pyrolysis length L_p at all times.

(3) Flame spread rate V_p reaches a steady state value at approximately **15** to 20 cm from flame initiation and independent of the flow velocity under forced flow conditions.

(4) A correlation of equation **(2.0)** shows that the steady state flame spread rate is direct proportional with oxygen concentration.

5.2 Future Work

Temperature measurements by thermocouple and velocity measurement by laser doppler anemometry are planed to give a more detailed structure of the flow field behavior in the combusting boundary layer. Temperature measurement will determine the location of flame upstream and downstream from the pyrolysis front and its distributions in the gas phase domain. Detailed velocity measurement could determines the streamline distributions in the flow field.

Since our experiments was performed with small scale fuel sample of 3 inch by 12 inch and the flow velocity between 0 to 4 m/s. A valuable information would be to study the flame spread rate at larger velocities and the effect of radiation on the flame spread process.

Although several theories has been proposed in modeling flame spread over thermally thin fuel, none of them seems to predict correctly the behavior of its transition from an initial accelerating stage proportional to time to finally reach a steady state spread rate independent of flow velocity. A more detailed study of the flow structure as well as ingenuity to model the process would be of fundamental interests.

Reference

1 Markstein, G.H. and de Ris, J.N.: Fourteenth Symposium (International) on Combustion, p. **1085,** The Combustion Institute, **1973.**

2 Markstein, G.H. and de Ris, J.N.:"Dynamics of Textile Fires-A Study of the Mechanisms-Theory and Experiments" Factory Mutual Research Corporation Report no. 20588, **1972.**

3 Hansen, A. and Sibulkin, M.:"Flame Spreading from a Point Source of Ignition on a Vertical Fuel Surface" Combustion Science and Technology, **9,** p. **173, 1974.**

4 Orloff, L., de Ris, J.N. and Markstein, G.H.:"Upward Turbulent Fire Spread and Burning of Fuel Surfaces" Fifteenth Symposium (International) on Combustion, p. **183,** The Combustion Institute, **1975.**

5 Hirano, T. and Sato, K.:"Effects of Radiation and Convection on Gas Velocity and Temperature Profiles of Flame Spreading Over Paper" Fifteenth Symposium (International) on Combustion, p. **233,** The Combustion Institute, **1975.**

6 Fernandez-Pello, A.C.:"Upward Laminar Flame Spread Under the Influence of Externally Applied Radiation" Combustion Science and Technology, **17,** p. **87, 1977.**

7 Annamalai, K. and Sibulkin, M.:J. Fire and Flammability, **9,** p. **445, 1978.**

8 Alpert, R.L.: ASME-AICHE National Heat Transfer Conference, **ASME** publication no. 79-MT-28, **1979.**

9 Fernendez-Pello, A.C.:"Flame Spread in a Forward Forced Flow" Combustion and Flame, **36, p. 63, 1979.**

10 Fernandez-Pello, A.C. and Hirano, T.:"Controlling Mechanisms of Flame Spread" Combustion Science and Technology, **32, p.** 1, **1983.**

11 Fernandez-Pello, A.C.:"Flame Spread Modeling".Combustion Science and Technology, **1983.**

12 Altenkirch, R.A., Eichhorn, R. and Shang, P.C.:"Buoyancy Effects on Flames Spreading Down Thermally Thin Fuels" Combustion and Flame, **37,** p. **71,** 1980.

13 Fernandez-Pello, A.C., Ray, S.R. and Glassman, I.:"Flame Spread in an Opposed Forced Flow - The Effect of Ambient Oxygen Concentration" Eighteenth Symposium on Combustion, p. **579,** The Combustion Institute, **1981.**

14 Altenkirch, **R.A.,** Eichhorn, R. and Rizvi, A.R.:Combustion Science and Technology, **32,** p. **49, 1983.**

15 Annamalai, K. and Sibulkin, M.:"Flame Spread over Combustible Surfaces for Laminar Flow Systems" Combustion Science and Technology, **19,** p. **183, 1979.**

16 Pagni, P.J.:"Diffusion Flame Analysis" Fire Safety Journal, **3, 2-4, 273, 1981.**

17 Carrier, G.F., Fendell, F.E. and Feldman, P.S.: Combustion Science and Technology, **23, p. 41, 1980.**

18 Carrier, G.F., Fendell, F.E. and Fink, S.: Combustion Science and Technology, **32,** p. **161, 1983.**

19 Carslaw, H.S. and Jaeger, J.C.:"Conduction of Heat in Solids", Oxford at the Clarendon Press, p. **75, 1973.**

20 de Ris, J.N.:"Spread of a Laminar Diffusion Flame" Twelfth Symposium on Combustion, **p. 241,** The Combustion Institute, **1969.**

21 Gordon, S. and Mcbrige, B.J.:"Computer Program for Calculation of Complex Chemical Equilibrium Compositions, Rocket Performance, Incident

and Reflected Shocks and Chapman-Jouguet Detonations" NASA Scientific and Technical Publication **SP-273, 1971.**

22 Wichman, I.S. and Williams, F.A.: Combustion Science and Technology, **32,** p. **9, 1983.**

23 Loh, H.T. and Fernandez-Pello, A.C.: "A study of the Controlling Mechanisms of Flow Assisted Flame Spread." The Twentieth (International) Symposium on Combustion, the Combustion Institute, **1984.**

24 Hirano, T., Noreikis, S.E. and Waterman, T.E.:"Measured Velocity and Temperature Profiles Near Flames Spreading Over a Thin Combustible Solid" Combustion and Flame, **23, p. 83, 1974.**

25 Fernandez-Pello, A.C.:"A Theoretical Model for the Upward Laminar Spread of Flames over Vertical Fuel Surfaces" Combustion and Flame, **31, p. 135, 1978.**

26 Fernandez-Pello, A.C.: Combustion Science and Technology, **39,** p. 119, **1984.**

27 Sohrab, S.H., Williams, F.A.:"Extinction of Diffusion Flames Adjacent to Flat Surfaces of Burnong Polymers" Journal of Polymer Science, 19, p. **2955- 2976, 1981.**

28 Tewarson, **A.,** Pion, R.F.:"Flammability of Plastics" Combustion and Flame,'**26, p. 85-103, 1976.**

29 Sohrab, S.H., Linan, A., Williams, F.A.:"Asymptotic Theory of Diffusion Flame Extinction with Radiation Loss from the Flame Zone" Combustion Science and Technology, **27,** p. **143-154, 1982.**

30 Pagni, P.J., Shih, T.M.:"Excess Pyrolyzate", Combustion and Falrne, **p. 1329- 1343.**

31 Orloff, L., Modak, A.T. and Alpert, R.L.:"Burning of Large Scale Vertical Surfaces" Fire and Explosion Research, p. 1345- 1354.

32 Lavid M., Berlad, A.L.:"Gravitational Effects on Chemically Reacting Laminar Boundary Layer Flows Over a Horizontal Flat Plate" Sixteenth Symposium on Combustion, p. 1557, The Combustion Institute, 1976.

33 Liu, C.N., Shih, T.M.:"Laminar, Mixed-Convection, Boundary Layer, Nongray-Radiative, Diffusion Flames" Transactions of ASME, 102, p. 724, 1980.

34 Fernandez-Pello, A., Williams, F.A.:"Laminar Flame Spread Over PMMA Surfaces" Fire and Explosion Research, p. 217.

35 Shih, T.M., Pagni, P.J.:"Laminar Mixed-Mode, Forced and Free, Diffusion Flames" Journal of Heat Transfer, 100, p. 253, 1978.

36 Fernandez-Pello, A.C., Mao, C.P.:"A Unified Analysis of Concurrent Modes of Flame Spread" Combustion Science and Technology, 26, p. 147 , 1981.

37 Hirano, T.:"A Further Study on Effects of External Thermal Radiation on Flame Spread over Paper" Combustion and Flame, 32, p. 95, 1978.

38 Hirano, T., Sato, K., Tazawa, K.:"Instability of Downward Flame Spread Over Paper in an Air Stream" Combustion and Flame, 26, p. 191, 1976.

39 Fernandez-Pello, A.C.:"Downward Flame Spread Under the Influence of Externally Applied Thermal Radiation" Combustion Science and Technology, 17, p. 1, 1977.

40 Emmons, H. W.,:"The Film Combustion of Liquid Fuel" Z. angew. Math. Mech., 36, p. 60-71, 1956.

41 Kinoshita, C. M. and Pagni, P. J.:"Laminar Wake Flame Heights" ASME J. of Heat Transfer, 102, p. 104-109, 1980.

42 Kosden, F. J., Williams, F. A. and Buman, C.:"Combustion of Vertical Cellulous Cylinders in Air" Twelfth Symposium (International) on Combustion, **p.253,** the Combustion Institute, **1969.**

43 Kim, J. S., de Ris, J. and Kroesser, F. W.:"Laminar Free-Convective Burning of Fuel Surfaces" Thirteenth Symposium (International) on Combustion, **p.949,** The Combustion Institute, **1971.**

44 Ahmad, T. and Faeth, G. M.:"An Investigation of the Laminar Overfire Region Along Upright Surfaces" ASME J. of Heat Transfer, **100, p. 112, 1978.**

45 Groff, E. G. and Faeth G. M.:"Laminar Combustion of Vertical Free-Standing Fuel Surfaces" Combustion and Flame, **32,** p. **139, 1978.**

46 Sparrow, E. M. and Yu, H. S.:"Local Nonsimilarity Thermal Boundary Layer Solutions'' J. of Heat Transfer, **93,** p. **328, 1971.**

47 Sibulkin, M., Kulkarni, A. K. and Annamalai, K. "Burning on a Vertical Fuel Surface with Finite Chemical Reaction Rate" Combustion and Flame, **44,** p. **187, 1982.**

48 Hirano, T. and Kanno, Y.:"Aerodynamic and Thermal Structure of the Laminar Boundary Layer over a Flate Plate with a Diffusion Flame" Fourteenth Symposium (International) on Combustion, The Combustion Institute, p. **391, 1972.**

49 Fernandez-Pello, A. C. and Santoro, R. J.:"On the Dominant Mode of Heat Transfer in Downward Flame Spread" Seventeenth Symposium (International) on combustion, The Combustion Institute, **p. 1201, 1979.**

50 Fernandez-Pello, A. C. and Williams, F. A.:"Experimental Techniques in the Study of Laminar Flame Spread Over Solid Combustibles" Combustion Science and Technology, **14, p. 155, 1976.**

51 Ray, S. R. and Glassman, I.:"The Detailed Processes Involved in Flame Spread over Solid Fuels" Combustion Science and Technology, **1983.**

52 Beier, R. **A.** "Radiation in Laminar Combusting Boundary Layer" Ph.D. Thesis, University of California, Berkeley, **1981.**

53 Fernandez-Pello, **A.** C. **"A** Theoretical Model for the Upward Laminar Spread of Flames over Vertical Fuel Surfaces" Combustion and Flame, **31, p. 135, 1978.**

54 Orloff, L., de Ris, J. and Tewarson, **A.** "Thermal Properties of PMMA at Elevated Temperatures" Factory Mutual Research Corporation, Technical Report **22355-2, 1974.**

57 Spalding, D. B.:"A General Computer Program for Two-Dimensional Boundary Layer Probolems" Sep., **1973.**

55 Mao, C. P.:"A Study of the Burning of a Solid Fuel Surface in Partial Enclosures" Ph.D. Thesis, University of California, Berkeley, **1983,**

56 Williams, F. **A.:** Combustion Theory, Addison-Wesley, **1985.**

Appendix A

Calculation of Flow Velocity and Oxygen Concentration

The flow velocity and oxygen concentration in the flow as used in equation **(2.2)** and **(2.3)** are derived here. The mass flow rate passing through the choked orifice in each of the sonic nozzle is given as :

$$\dot{m} = \left(\frac{k \left(\frac{2}{k+1}\right)^{\frac{k+1}{k-1}}}{\frac{R}{M}} \right)^{1/2} \frac{P^o}{\sqrt{T^o}} \frac{\pi}{4} D^2 C$$

$$= 0.02624 \frac{P^o}{\sqrt{T^o}} M^{1/2} D^2 \qquad \text{(A-1)}$$

where **k** : *Ratio of specific heats* $\frac{C_p}{C_v}$

m : *Mass flow rate through sonic nozzle*

R : *Universal gas constant*

M : *Molecular weight of gas*

P^o : *Stagnation pressure*

T^o : *Stagnation temperature*

D : *Orifice diameter of sonic nozzle*

C : *Sonic nozzle calibration constant*

The flow rate of oxygen and nitrogen passing each nozzle can be calculated from equation (A-1), which in their turn are used to calculate the mixture flow velocity and oxygen concentration in the test section according to :

$$\rho_{mix} = \frac{m_{total}}{V_{total}} = \frac{m_{total}}{V_{o_2} + V_{n_2}} = \frac{m_{o_2} + m_{n_2}}{\frac{\dot{m}_{o_2}}{\rho_{o_2}} + \frac{\dot{m}_{n_2}}{\rho_{n_2}}}$$

$$= \frac{1}{\frac{1}{\rho_{o_2}}\left(\frac{\dot{m}_{o_2}}{\dot{m}_{total}}\right)+\frac{1}{\rho_{n_2}}\left(\frac{\dot{m}_{n_2}}{\dot{m}_{total}}\right)} = \frac{1}{\frac{Y_{o_2}}{\rho_{o_2}}+\frac{1-Y_{o_2}}{\rho_{n_2}}} \qquad \text{(A-2)}$$

$$Y_{o_2} = \frac{m_{o_2}}{\dot{m}_{o_2}+\dot{m}_{n_2}} = \frac{D_{o_2}^2 P_{o_2}^o}{D_{o_2}^2 P_{o_2}^o + D_{n_2}^2 P_{n_2}^o \left(\frac{M_{n_2}}{M_{o_2}}\right)^{1/2}} \qquad \textbf{(A-3)}$$

$$U = \frac{\dot{m}_{total}}{\rho_{mix}\ A_{tunnel}} = \frac{\dot{m}_{total}}{A_{tunnel}}\left(\frac{Y_{o_2}}{\rho_{o_2}}+\frac{1-Y_{o_2}}{\rho_{n_2}}\right) \qquad \textbf{(A-4)}$$

Equation **(A-3)** and **(A-4)** can be solved to find the setting pressure and orifice diameter to achieve the desired flow velocity and oxygen concentration in the test section.

APPENDIX B

Program GENMIX

```
      program main
c**********************G E N M I X 4A **********************
            D .B . Spalding, Imperial College, 1972---c
c-----version of the appendix B program of S.V.patankar    c
c       and D.B.Spalding'heat and mass transfer in boundary c
c       layers',intertext,london,2nd.  c       edition,1970. c
        this version comprises one standard case (kase=1,    c
c       combustion of methane and air in a divergent duct    c
c       exhausting into the atmosphere) togather with a      c
c       number of lessons and other kases. The former are    c
c       intended to aid self-instruction in the use of the   c
c       program, the latter are special versions likely to be
c       of interest to potential users.
c       ------------------------------------------
chapter0000000000000000  preliminaries 0000000000000000000
c       ----------- dimensions and common blocks ----------
      dimension title(24),out(93),temp(93),psi(93),ddd(93)
      dimension outu(93),outt(93),outf(93),outo(93)
      dimension xplot(93),yplot(10,93),yaxes(10),symbol(10)
      dimension flux(5),dfi(5),dfe(5),ajid(5),ajed(5)
      character*10 yaxes(10),symbol(10),xaxis,lab
      character*24 title(24)
      common/coma/a(93),aje(5),aji(5),b(93),c(93),csalfa,
     1 d(93),dpdx(93),dx,emu(93),f(5,93),fs(5,93),iax,iend,
     2 ifin,inde(5),indi(5),iout,istep,itest,iutrap,js,jsw,
     3 jv,jy,kex,kin,krad,n,nd2,nf,novel,np1,np2,np3,
     4 om(93),omd(93),p(93),pei,pr(5),pref(5,93),psie,psii,
     5 r(93),rho(93),rme,rmi,ru(93),sd(5,93),su(5,93),taue,
     6 taui,u(93),xd,xu,y(93),ye,yi,emau(93),us(93)
      common/comb/ak,almg,arrcon,ewall,fr,h,hfu,inert,masstr,
     1 model,oxdfu,preexp,press,ubar,ufac
      common/comc/omi,bpi,ome,bpe,r25,rn15,yn15,thlp,gd4,hlp,
     1 ttp,pd4,rmid2,fra
      common/comd/gi(5),ge(5),fdifi(5),fdife(5)
      common/come/tex,sigma,epw,skappa,qro,twall,ji
      common/comf/hf(10000),tsn(10000),tso(10000),csi(10000),
     1 du(10000),ipyrol,nend,xpyrol,error,sumt,tlim,it,itmax,
     2 itchose
      dimension ssu(93),sus(2,93),sds(2,93),sf(3,93),
     1 fuel(10000),sssu(93),ssf(3,93),ssus(2,93),ssds(2,93)
      dimension tsnt(10000),fuelt(10000),dut(10000)
      common/comg/ftemp(6,93),peit,psit,np3t,ifinal(6),yt(93),
     1 tt,ff,oo,pp,vv,ss
c     write(6,*) " enter the title name "
      write(6,*)'select the temperature interval, tt ,'
      write(6,*)'          fuel       , ff ,'
      write(6,*)'          oxygen     , oo ,'
      write(6,*)'          product    , PP ,'
      write(6,*)'          velocity   , vv ,'
      write(6,*)'          stream fn  , ss ,'
```

```
      read(5,*) tt,ff,oo,pp,vv,ss
      write(6,*)'tt=',tt,'ff=',ff,'oo=',oo,'pp=',pp,
     1'vv=',vv,'ss=',ss
      ifinal(1)=0
      ifinal(2)=0
      ifinal(3)=0
      ifinal(4)=0
      ifinal(5)=0
      ifinal(6)=0
c
c     read(5,*) tittle
c     write(6,*) ' title =  ',tittle
c    1format (12a6)
      read(5,*) nstat,nprof,nplot
      write(6,*) ' nstat = ',nstat,' nprof = ',nprof,' nplot
     1 = ',nplot
c
c     ---------------------------------------------
chapter1111111111 parameters and control indices 1111111111
      lesson=0
      kase=1
c     -------- nstat= no.of steps between output of single
c     variables.
c     --------- nprof= no.of steps between output of array
c     variables.
c     nstat=20
c     nprof=40
c     --------- nplot= no.of steps between output of plot.
c     in this example, plot is called at the end of
c     integration only.
c     nplot=10000
      nend=10000
      lind=0
c      ------ itest.ne.0 gives extra test output.
c      ------ iutrap.gt.O is active for negative u's, see
c      stride(3).
      itest=0
      iutrap= 2
c
c     ---------------------------------------------
chapter222222222222222 grid and geometry  222322223222222222
      read(5,*) n,xulast,lastep,xout,xpyrol,xend
      write(6,*)' n = ',n,' xulast = ',xulast,' lastep = ',
     1lastep,' xout = ',xout,'xpyrol=',xpyrol,'xend=',xend
c     n=19
c     xulast=2.
c     lastep=500
c     xout=1.
c     xend=9.9
c     fra=0.05
      read(5,*)fra
      write(6,*) 'fra=',fra
c     fra=0.01
      ulim=0.025
```

```
cl    tan=0.01
      tan=0.
      peilim=0.02
      afac=0.2
      aexdlm=0.02
cl    krad=1
      krad=0
      read(5,*) fluxlim,tlim,fuellim
      write(6,*)'fluxlim=',fluxlim,'tlim=',tlim,'fuellim=',
     1fuellim
      csalfa=1.
c     xpyrol=5.
      ipyrol=10000
c     ---------- r(1) adjustment made just before call
c     stride(1).
c     -----stride(4)-------stride(4)-------stride(4)-----
      call stride(4)
      kex=2
      if (xend.eq.0.0) iend=0
      if (xout.eq.0.0) iout=0
      iout=0
c     ---------- change iend, iax and iout, if necessary.
c     power=1.0
c     power=2.0
      read(5,*) power
      write(6,*) 'power=',power
      do 20 i=2,np2
   20 om(i)=(float(i-2)/float(n))**power
c
c ..................................................
chapter33333333333 dependant variables selection 33333333333
c     u(i)=velocity
c     f(1,i)=concentration of enthalpy
c     f(2,i)=concentration of fuel
c     f(3,i)=concentration of oxidant-oxdfu*f(2,i)=phi
c     fs(1,i)=concentration of oxidant
c     fs(2,i)=temperature
c     fs(3,i)=concentration of product
c
c -------- masstr=0=uniform composition, otherwise masstr=1
      masstr=1
c -------- novel= 1=no velocity, otherwise novel=2
      novel=2
c
      neq=4
      if (masstr.eq.0) neq=2
      nf=neq-1
c
c ..................................................
chapter444444444444444 material constant 4444444444444444444
c
cl    gascon=8300.
      gascon=8314.34
c     cfu=1100.
```

```
c     cox=1100.
c     cpr—1100.
c     cmix=1100.
      read(5,*) cfu,cox,cpr,cmix
      write(6,*)'cfu=',cfu,'cox=',cox,'cpr=',cpr,'cmix=',
     1 cmix
c     wfu=16.
      wfu=100.
      wox=32.
      wpr=28.
      wmix=29.
      wmix=30.
      gamma=cmix/(cmix-gascon/wmix)
      if (masstr.ne.0) go to 41
      wpr=wfu
      wox=wfu
      wmix=wfu
      wdgson=wmix/gascon
   41 read(5,*)visfu,visox,vispr,vismix
      write(6,*)'visfu=',visfu,'visox=',visox,'vispr=',
     1 vispr,'vismix=',vismix
      read(5,*) hfu
      write(6,*) 'hfu=',hfu
c ------- arrcon is activation energy divided by universal
c ------- gas constant
c     arrcon=18.e3
c     arrcon=12.63e3
      read(5,*) arrcon,preexp
      write(6,*)'arrcon=',arrcon,'preexp=',preexp
c     preexp=1.0
c     preexp=10.0
c     oxdfu= 4.0
      oxdfu= 1.92
c
c ------- model=1=laminar, =2=turbulent.
c -------- inert=1= inert fluid, otherwise inert=:!
c     model=2
      read(5,*) model
      write(6,*) 'model=',model
      inert=:!
c
      do 40 j=1,nf
c     pr(j)=0.7
      read(5,*) pr(j)
      pref(j,1)=0.86
   40 if(model.eq.1)pref(j,1)=pr(j)
      h=0.9
      ak=0.435
      almg=0.09
      fr=0.033
      ufac=0.01
c
c ..........................................
chapter5555555555555555 iniotial conditions 555555555555555
```

```
c1    ua=100.0
      read(5,*) ua,ub,uc,ud
      write(6,*)'ua=',ua,'ub=',ub,'uc=',uc,'ud=',ud
c     ua=10.
c1    ub=100.0
c     ub=10.
c1    uc=50.0
c     uc=10.
c1    ud=0.0
c     ud=10.
c1    ta=2000.0
c     ta=300.
c     tb=300.0
c     tc=tb
c1    td=300.0
c     td=300.0
c1    twall=299.0
c     twall=668.0
c     tex=300.0
      read(5,*)ta,tb,tc,td,twall,tex
      write(6,*)'ta=',ta,'tb=',tb,'tc=',tc,'td=',td,
     1'twall=',twall,'tex= ',tex
      read(5,*)ji,kk,mm,iinput,ki,iwrite
      write(6,*)'ji=',ji,'kk=',kk,'mm=',mm,'iinput=',iinput,
     1'ki=',ki,'iwrite=',iwrite
c ---------- r's are inner radii of streams.
c1    ra=0.0
      ya=0.
c1    rb=0.02
      yb=0.
c1    rc=0.03
c     rc=0.025
c     yc=0.1
c     yc=0.002
c1    rd=0.05
c     yd=0.1
c     yd=0.002
      read(5,*) yc,yd
      write(6,*)'yc=',yc,'yd=',yd
      if (masstr.eq.0) go to 54
      f2a=0.0
c1    f2b=1.0
      f2b=0.
      f2c=0.0
      f2d=0.0
      read(5,*) oxa,oxb,oxc,oxd
      write(6,*) 'oxa=',oxa,'oxb=',oxb,'oxc=',oxc,'oxd=',
     1oxd
c     oxa=0.0
c     oxb=0.0
c     oxb=0.232
c     oxc=0.232
c     oxd=0.232
c
```

```
      f1a= ta*(cfu*f2a+cox*oxa+cpr*(1.-f2a-oxa))+
     1 .5*ua**2+hfu*f2a
      f1b=tb*(cfu*f2b+cox*oxb+cpr*(1.-f2b-oxb))+
     1 .5*ub**2+hfu*f2b
      f1c=tc*(cfu*f2c+cox*oxc+cpr*(1.-f2c-oxc))+
     1 .5*uc**2+hfu*f2c
      f1d=td*(cfu*f2d+cox*oxd+cpr*(1.-f2d-oxd))+
     1 .5*ud**2+hfu*f2d
      f3a=oxa-f2a*oxdfu
      f3b=oxb-f2b*oxdfu
      f3c=oxc-f2c*oxdfu
      f3d=oxd-f2d*oxdfu
      go to 55
   54 f1a=ta*cmix+.5*ua*ua
      f1b=tb*cmix+.5*ub*ub
      f1c=tc*cmix+.5*uc*uc
      f1d=td*cmix+.5*ud*ud
      f2b=0.0
      f2c=0.
      f3b=0.
      f3c=0.
   55 continue
c
c     bb=1.7
      bb=(hfu*oxd/1.92-cmix*(twall-tex))/1.59e6
      yfw=(bb-oxc/oxdfu)/(1.+bb)
c     yfw=0.59
c     al=1.6e6
      read(5,*) al
      write(6,*)'al=',al
      press=1.e5
      dpddx=0.0
c1    r(1)=rb
c1    rout=rd
c1    roa=press*wpr/ta/gascon
c     rob=press*wfu/tb/gascon
      rob=press*wmix/tb/gascon
c1    roc=press* wpr/tc/gascon
c1    floa=roa*ua*.5*rb**2
      floa=0.
c1    flob=rob*ub*.5*(rc**2-rb**2)
      flob=rob*ub*yc
c1    floc=roc*uc*.5*(rd**2-rc**2)
      floc=rob* ub*(yd-yc)
c
      omdiv=flob/(flob+floc)
c ------ sequence to put cell boundary at omdiv --------
      if (omdiv.eq.0..or.omdiv.eq.1.) go to 53
      do 52 i=3,np2
      if (om(i).le.omdiv) go to 52
      dif=omdiv-.5*(om(i)+om(i-1))
      om(i-1)=amax1(om(i-1)+dif,om(i-2)+1.e-7)
      om(i)=amin1(om(i)+dif,om(i+1)-1.e-7)
      go to 53
```

```
 52   continue
 53   continue
c
c ------------ initial profils are uniform ----------
      do 50 i=1,np3
      if(om(i).gt.omdiv) go to 51
c     u(i)=uc
c     f(1,i)= f1c
c     f(2,i)=f2c
c     f(3,i)=f3c
      u(i)=ub
      f(1,i)=f1b
      f(2,i)=f2b
      f(3,i)=f3b
      go to 50
 51   u(i)=ud
      f(1,i)=f1d
      f(2,i)=f2d
      f(3,i)=f3d
 50   continue
c     f(1,1)=cmix*twall+.5*uc*uc
      psii=floa
      pei=flob+floc
      psie=psii+pei
c1    flotot=pei
      sigma=5.6693e-8
      read(5,*) epw,skappa
      write(6,*)'epw=',epw,'skappa=',skappa
c     epw=1.0
c     skappa=0.034
      ll=0
      nend=100000
      it=0
      hinfi= cmix*tex
      hwall=cmix*twall+hfu*yfw
      rmi=0.0
      rmin=0.0
      kkk=0
      itrmi=0
      href=1.0e20
      rmirat=0.01
c  59 continue
c     if(iinput.eq.1) kkk=1
c     if(iinput.eq.1) then
c     open(3)
c     do58 i=np3
c  58  read(3,*)u(i),f(1,i),su(2,i),sd(2,i),f(2,i),f(3,i)
c      read(3,*)istep,pei,bpi,bpe,xu,taui,psii,psie,gi(1),
c     1fdifi(1)
c      close(3)
c      endif
c ---------------------------------------------------
chapter6666666666666 thermodynamic properities 666666666666
c ******************** start of main loop ******************
```

```
      itno—0
      itrmi—0
      ipp=0
c     emuinfi=1.568e-5
      read(5,*)rmibound,itmax
      write(6,*)rmibound,itmax
      iprint=0
      open(unit—1,file='proft',status='unknown')
      open(unit=2,file='proff',status='unknown')
      open(unit=3,file= 'profo',status='unknown')
      open(unit=4,file= 'profp',status='unknown')
      open(unit—7,file= 'profv',status='unknown')
      open(unit=9,file='profs',status='unknown')
c     open(unit= 10,file='mass',status='unknown')
      read(5,*)fraa,frab,xlim,iiprint
      read(5,*)xutest1,xutest2
      read(5,*)xuprint,xinc,xtry
      read(5,*)itchose,finter,lprint
      read(5,*)lstep1,lstep2,xadvance
      read(5,*)xu1,xu2,frad,llprint,lstep3
      write(6,*)'fraa=',fraa,'frab=',frab,'xlim=',xlim,
     1'iiprint=',iiprint,'xutest1=',xutest1,'xutest2=',
     2xutest2,'xuprint=',xuprint,'xinc=',xinc,'xtry=',
     3xtry,'itchose=',itchose,'finter=',finter,'lprint=',
     4lprint,'lstep1=',lstep1,'lstep2=',lstep2,
     5'xadvance=',xadvance,'xu1=',xu1,'xu2=',xu2,'frad=',
     1frad,'llprint=',llprint
      lplot=0
   60 continue
      jjj=0
 6001 continue
      if(istep.eq.ipyrol.and.ll.ne.1.and.kkk.eq.1)then
c     open(unit= 3,file= 'save',type='unknown ')
      do 15 i=1,np3
      ssu(i)=u(i)
      sf(1,i)=f(I,i)
      sus(2,i)=su(2,i)
      sds(2,i)=sd(2,i)
      sf(2,i)=f(2,i)
      sf(3,i)=f(3,i)
c     write(3,*)ssu(i),sf(1,i),sus(2,i),sds(2,i),sf(2,i),
     1 sf(3,i)
   15 continue
      isistep=ipyrol
      spei=pei
      sbpi=bpi
      sbpe=bpe
      sxu=xpyrol
      staui=taui
      spsii=psii
      spsie=psie
      sgi=gi(1)
      sfdifi=fdifi(1)
c     close(3)
```

```
      endif
C
c ---------------------------------- test 1
      if(itest) 602,601,602
 602  lab=6htest 1
      write(6,100) lab,r(1),press,dx,psii,psie,pei,fra,
     1 ulim,peilim,afac,aexdlm
      lab=1hu
      write(6,100) lab,(u(i),i=1,np3)
      lab=6hf(1,i)
      write(6,100) lab,(f(1,i),i=1,np3)
      lab=6hf(2,i)
      write(6,100) lab,(f(2,i),i=1,np3)
      lab=6hf(3,i)
      write(6,100) lab,(f(3,i),i=1,np3)
 601  continue
C
      press=press+dpddx*dx
      pdgson=press/gascon
      if(masstr.ne.0) go to 64
      do 65 i=1,np3
      fs(2,i)=amax1(1.,(f(1,i)-.5*u(i)**2)/cmix)
 65   rho(i)=pdgson/fs(2,i)*wmix
      go to 66
 64   do 61 i=1,np3
      go to (606,605),inert
C
c ------ correction of effects of excessive reaction -----
 605  if((i-1)*(i-np3)*istep) 69,62,69
 69   ddd(i)=su(2,i)+sd(2,i)*f(2,i)
      if(ddd(i))62,62,68
c69   if(su(2,i)+sd(2,i)*f(2,i)) 62,62,68
 68   if(su(2,i)) 67,63,67
 67   f(2,i)=-f(3,i)/oxdfu
      go to 62
 63   f(2,i)=0.0
C
 62   fs(1,i)=amin1(amax1(f(3,i)+oxdfu*f(2,i),0.),oxd)
 606  fs(3,i)=1.-f(2,i)-fs(1,i)
      cmix=cfu*f(2,i)+cox*fs(1,i)+cpr*fs(3,i)
      enth=f(1,i)-.5*u(i)*u(i)-hfu*f(2,i)
      fs(2,i)=amax1(enth/cmix,100.0)
      rhocon=pdgson/fs(2,i)
      vmix=f(2,i)/wfu+fs(1,i)/wox+fs(3,i)/wpr
 61   rho(i)=rhocon/vmix
 66   continue
      if(istep.ge.ipyrol.and.lprint.eq.1) then
      do 567 k=1,np3
      if(fs(1,k).eq.0.0) kind=k
  567 continue
      do 568 j=1,kind
      fs(1,j)=0.0
  568 continue
      do 569 i=1,np3
```

```
      fs(3,i)=1.-f(2,i)-fs(1,i)
      cmix=cfu*f(2,i)+cox*fs(1,i)+cpr*fs(3,i)
      enth=f(1,i)-.5*u(i)*u(i)-hfu*f(2,i)
      fs(2,i)=amax1(enth/cmix,100.0)
      rhocon=pdgson/fs(2,i)
      vmix=f(2,i)/wfu+fs(1,i)/wox+fs(3,i)/wpr
  569 rho(i)=rhocon/vmix
      ddd(1)=0.
      ddd(np3)=0.
      endif
      rho(2)=rho(1)
      rho(np2)=rho(np3)
      if(istep.gt.ipyrol.or.ll.eq.1) go to 6002
      if(istep.le.lstep3) go to 6002
c     if(istep.le.ipyrol) go to 6002
      if(istep.le.ipyrol.and.jjj.eq.1) go to 6002
      rmin=-gi(1)*(cmix*(fs(2,1)-0.5*(fs(2,2)+fs(2,3)))-
     1 fdifi(1))/al
      if(rmin.le.0.0) rmin=0.0
      rmilim=abs(rmi)*rmirat+10e-30
      if(rmilim.le.rmibound) rmilim=rmibound
      if(istep.le.ipyrol.and.abs(rmi-rmin).le.rmilim) then
c     write(10,*) xu,rmi
c     if(istep.eq.ipyrol) go to 120
      lplot=1
      if(istep.le.ipyrol.and.iiprint.eq.4) then
      write(6,*)'rmi=',rmi,'istep=',istep,'xu=',xu
      endif
      if(istep.eq.ipyrol.and.iiprint.eq.4) go to 120
      if(istep.eq.ipyrol) kkk=1
      if(istep.eq.ipyrol) fuel(istep+1-ipyrol)=yfw
      do 2 i=1,np3
      sssu(i)=u(i)
      ssf(1,i)=f(1,i)
      ssus(2,i)=su(2,i)
      ssds(2,i)=sd(2,i)
      ssf(2,i)=f(2,i)
    2 ssf(3,i)=f(3,i)
      issistep=is tep
      sspei=pei
      ssbpi=bpi
      ssbpe=bpe
      ssxu=xu
      sstaui—taui
      sspsie=psie
      sspsii=psii
      mm=3
      itrmi=0
      endif
      if(istep.le.ipyrol) then
      if(ipp.eq.0) then
      read(5,*)irepeat
      write(6,*)'irepeat=',irepeat
      ipp=1
```

```
      endif
      if(itrmi.gt.irepeat) go to 120
      itrmi=itrmi+1
      do 10 i=1,np3
      u(i)=sssu(i)
      f(1,i)=ssf(1,i)
      su(2,i)=ssus(2,i)
      sd(2,i)=ssds(2,i)
      f(2,i)=ssf(2,i)
   10 f(3,i)=ssf(3,i)
      istep=issistep
      pei=sspei
      bpi=ssbpi
      bpe=ssbpe
      xu=ssxu
      taui=sstaui
      psii=sspsii
      psie=sspsie
      jjj=1
      endif
      if(istep.le.ipyrol) go to 6001
 6002 if(istep.ge.ipyrol.and.kkk.eq.1)then
      if(iwrite.eq.1)then
      do 6100 i=1,np3
      ftemp(1,i)=fs(2,i)
      ftemp(2,i)=f(2,i)
      ftemp(3,i)=fs(1,i)
      ftemp(4,i)=fs(3,i)
      ftemp(5,i)=u(i)
      ftemp(6,i)=psi(i)
 6100 continue
      peit=pei
      psit=psii
      np3t=np3
      endif
      hflux=-gi(1)*(cmix*(fs(2,1)-0.5*(fs(2,2)+fs(2,3)))-
     1fdifi(1))
c     if(hflux.le.0.0) then
c     if(istep.le.ipyrol+150) then
      if(it.eq.itmax-1)then
      if(iiprint.eq.llprint)then
      write(6,*)'hflux=',hflux,'xu=',xu,'istep=',istep,
     1'gi(1)=',gi(1),'fs(2,1)=',fs(2,1),'fs(2,2)=',fs(2,2),
     2'fs(2,3)=',fs(2,3),'rme=',rme,'yi=',yi,'pei=',pei
      endif
      endif
c     endif
c     endif
      if(hflux.le.0.0) hflux=0.0
      hf(istep+1-ipyrol)=hflux
      if(istep.eq.ipyrol)href=hflux
      csi(istep+1-ipyrol)=xpyrol/xu
      stemp=tsn(istep+1-ipyrol)
      tsn(istep+1-ipyrol)=fs(2,1)
```

```
      if(lind.eq.1)tsn(istep+1-ipyrol)=tex
      sfuel=fuel(istep+1-ipyrol)
      if(it.eq.itmax-1)then
      if(iiprint.eq.llprint)then
      fueldif=sfuel-f(2,1)
      tempdif=stemp-fs(2,1)
      write(6,*)'fueldif=',fueldif,'tempdif=',tempdif
      endif
      endif
      fuel(istep+1-ipyrol)=amax1((f(2,1)+sfuel)*finter,0.0)
      du(istep+1-ipyrol)=xu
      if(istep.eq.lastep-1) then
      write(6,*)'****** INTERRUPT ******'
      write(6,*)'xu=',xu,'hflux=',hflux,'fs(2,1)=',fs(2,1),
     1 'f(2,1)=',f(2,1)
      go to 120
      endif
c     write(6,*)'xu=',xu,'hflux=',hflux
      endif
c ------------------------ test2 ------------------
      if (itest) 604,603,604
604   lab—6htest 2
      write(6,100) lab,press,dx,dpddx,pdgson
      lab=7hfs(1,i)
      write(6,100) lab,(fs(1,i),i=1,np3)
      lab=7hfs(2,i)
      write(6,100) lab,(fs(2,i),i=1,np3)
      lab=7hfs(3,i)
      write(6,100) lab,(fs(3,i),i=1,np3)
      lab=6hrho(i)
      write(6,100) lab,(rho(i),i=1,np3)
 603  continue
c ------------------------------- adjust r(1)
      if(kin.eq.2.and.krad.eq.1) r(1)=sqrt(abs(2.*psii/
     1 (rho(1)*u(1))))
c
c ----- stride1 -------- stride1 --------- stride1 -------
      call stride(1)
c
c ------------------------------------------------
chapter77777777777777777 forward step 777777777777777777
      if(istep.ge.ipyrol.and.abs(hflux).le.abs(href*fluxlim)
     1.and.abs(f(2,1)).le.yfw*fuellim.or.xu.ge.xlim) then
      write(6,*)'hf(',istep+1-ipyrol,')=',hf(istep+1-ipyrol)
      if(iwrite.eq.1) go to 120
      itno=itno+1
      write(6,*)'iteration number=',itno
      nend=istep
      nipyrol=ipyrol
      ll=1
      call wltemp
      lind=0
      open(unit=8,file= 'temp',status= 'unknown')
      write(8,*) nend,nipyrol
```

```
      do 19 ii=1,nend-nipyrol+1
      tsnt(ii)=tsn(ii)
      fuelt(ii)=fuel(ii)
      dut(ii)=du(ii)
      write(8,*) tsn(ii),fuel(ii),du(ii)
   19 continue
      close(8)
      write(6,*)'error=',error,'hflux=',hflux
      it=it+1
      if(it.ge.itmax.or.abs(error).le.abs(sumt*tlim))
     1 go to 120
      do 16 i=1,np3
      u(i)=ssu(i)
      f(1,i)=sf(1,i)
      su(2,i)=sus(2,i)
      sd(2,i)=sds(2,i)
      f(2,i)=sf(2,i)
      f(3,i)=sf(3,i)
   16 continue
      istep=isistep
      pei=spei
      bpi=sbpi
      bpe=sbpe
      xu=sxu
      taui=staui
      psii=spsii
      psie=spsie
      gi(1)=sgi
      fdifi(1)=sfdifi
      go to 60
      endif
      dx=fra*y(np3)
      do 667 i=1,np3
  667 yt(i)=y(i)
      if(lplot.eq.1.and.iiprint.eq.4.and.iprint.eq.2)
     1 go to 996
      if(iiprint.eq.1) go to 998
      if(xu.gt.xtry.and.iiprint.eq.3)go to 998
      if(xu.ge.xutest1.and.xu.le.xutest2.and.iiprint.eq.2
     1.and.it.eq.itmax-1) go to 996
      if(xu.ge.xuprint.and.iiprint.eq.3
     1.and.it.eq.itmax-1) go to 997
      go to 998
   997 continue
      xuprint=xuprint+xinc
   996 write(6,*)'xu=',xu
      write(6,*)'y','t','f','o','p','v','s','su(2,i)',
     1'sd(2,i)','f(3,i)','ddd(i)'
      do 999 i=1,np3
      write(6,995)y(i),fs(2,i),f(2,i),fs(1,i),fs(3,i),u(i),
     1 psi(i),su(2,i),sd(2,i),f(3,i),ddd(i)
  995 format(1x,11(1x,1pe11.3))
  999 continue
  998 continue
```

```
      lplot=0
      if(istep.ge.ipyrol.and.iprint.eq.2.and.
     1iwrite.eq.1)then
      call profile(xu)
      endif
      if(istep.lt.400) dx=.1*dx
      if(istep.ge.ipyrol.and.istep.le.ipyrol+lstep1)
     1 dx=.1*dx
      if(istep.gt.ipyrol+lstep1.and.istep.le.ipyrol+lstep2)
     1 then
      dx=frab*y(np3)
      endif
      if(istep.gt.ipyrol+lstep2)dx=fraa*y(np3)
      if(xu.ge.xu1.and.xu.le.xu2)then
      dx= frad*y(np3)
      endif
      if(istep.gt.ipyrol.and.(xpyrol/xu**2)*dx.ge.xadvance)
     1 then
      dx=(xu**2/xpyrol)*xadvance
      endif
      if(istep.ge.ipyrol) go to 73
      if(dx.lt.xpyrol-xu) go to 73
      dx=xpyrol-xu
      ipyrol=istep+1
      go to 73
      if(dx.gt.0.) go to 73
      write(6,*)'dx=',dx,'y(np3)=',y(np3),'fra=',fra
      ifin=1
      go to 1011
 73   xd=xu+dx
c-------- further adjustment to dx are made in chapters 8
c--------- and 9.
c
c ---------------------------------------------------
chapter88888888888 adjust longitudinal conditions 888888888
c
c ------- chapter 8a ---------- boundary conditions -----
c ---------------------------- i boundary
c 1    if(istep-iax) 8000,80,84
c8000 if(istep-iend) 8002,83,84
c ------------------------------------------------ wall
8002  kin=1
      u(1)=0.
c     rmi=0.
      if(istep.eq.0) rmi=0.0
      if(istep.eq.0) taui=0.
      ewall=9.
      if(istep.ge.ipyrol) go to 82
      do 81 j=1,nf
      indi(j)=1
      fs(2,1)=twall
      rmi=(rmin+rmi)*0.5
      f(1,1)=cmix*twall+hfu*yfw
      f(2,1)=yfw
```

```
      f(3,1)=-oxdfu*yfw
   81 continue
      go to 85
   82 indi(1)=1
      indi(2)=2
      indi(3)=2
      aji(2)=0.
      aji(3)=0.
      rmi=0.
      go to 85
c ------------------------------------------ free
   83 kin=2
      taui=0.
      u(1)=ua
      ru(1)=rho(1)*u(1)
      f(1,1)=f1a
      f(2,1)=f2a
      f(3,1)=f3a
      go to 84
c ------------------------------------------ symmetry axis
   80 kin=3
      rmi=0.
      r(1)=0.
      psii=0.
      taui=0.
c ------------------------------- e boundary
   84 if(istep-iout) 8004,85,85
 8004 kex=1
      u(np3)=0.
      rme=0.
      if(istep.eq.0) taue=0.
      ewall=9.
      do 892 j=1,nf
      inde(j)=2
  892 aje(j)=0.
      inde(1)=1
      fs(2,np3)=twall
      f(1,np3)=cmix*twall+float(masstr)*hfu*f(2,np3)
      go to 86
c ------------------------------------------ free
   85 kex=2
      taue=0.
      u(np3)=ud
      ru(np3)=rho(np3)*u(np3)
      f(1,np3)=f1d
      f(2,np3)=f2d
      f(3,np3)=f3d
      go to 89
c
c   chapter 8b ..................... duct geometry
   86 if(istep.ge.iout) go to 89
      if(istep.gt.0) go to 87
      rout=rd
      adud=(r(np3)**2-r(I)**2)*.5
```

```
   87 yduct=rout-r(1)
      aduu=adud
      ain=r(1)**2*.5*float(1/kin)
      if(istep.eq.iend) aduu=.5*rout**2
      aflu=r(np3)**2*.5-ain
      aex=aflu-aduu
      aexd=aex/aflu
      if(xd.eq.xend.or.xd.eq.xout.or.xd.eq.xu1ast.or.ia.x
     1.eq.istep+1) go to 88
      if(abs(aexd).gt.aexdlm) dx=dx*aexdlm/abs(aexd)
      xd=xu+dx
   88 rout=rout+tan*dx
      adud=rout**2*.5-ain
      da=afac*(adud-aflu)
c
c  chapter 8c ————  subsonic pressure gradient
c ------------------ ubar
   89 ubar=0.
      psi(1)=psii
      do 820 i=2,np1
      psi(i)=psii+pei*om(i)
  820 ubar=ubar+(u(i)+u(i+1))*omd(i)
      psi(np2)=psie
      psi(np3)=psie
      ubar= .5*ubar
      if(kin.eq.2) ubar=(ubar-ua)*pei/psie+ua
c     if(kin.eq.2) ubar=(ubar-u(1))*pei/psie+u(1)
c ---------------- subonic flow
c 803 if (istep-iout) 822,823,900
  803 if (istep-iout) 822,823,823
  823 dpddx=0.
      go to 824
c ------------------------- confined subsonic flow
  822 flotot=psie-psii*float(1/kin)
      dynhed=ubar*flotot/aflu
      dpddx=(dynhed*da/dx-taui*r(1)-taue*r(np3)+2.*rme*
     1 ubar)/adud
  824 dp=dpddx*dx
      do 825 i=1,np3
  825 dpdx(i)=dpddx
c ------------------------------------------ test 3
      if(itest) 802,801,802
  802 lab—6htest 3
      write(6,100) lab,ubar,dynhed,dx,da,dpddx,aexd,rmi
      write(6,101) lab,istep,kin,kex,iax,iend,iout
      lab—4hy(i)
      write(6,100) lab,(y(i),i=1,np3)
      lab=4hr(i)
      write(6,100) lab,(r(i),i= 1,np3)
      lab=5hru(i)
      write(6,100) lab,(ru(i),i=1,np3)
  801 continue
c
c ---------------------------------------------
```

```
chapter9999999 transport and entrainment properties 9999999
c  --- laminar viscosity according to square-root formula,
c  -- with weighting according to mass fraction.
  900 if(masstr.eq.1) go to 90
      do 98 i=1,np3
   98 emu(i)=vismix*fs(2,i)**0.8
      go to 99
   90 do 92 i=1,np3
   92 emu(i)=(visfu*f(2,i)+visox*fs(1,i)+vispr*fs(3,i))*
  1 fs(2,i)**0.8
   99 continue
      emu(2)=emu(1)
      emu(np2)=emu(np3)
c ---------- test 4 ----------
      if (itest) 902,901,902
  902 lab—6htest 4
      write(6,100) lab,rmi,rme,pei
      lab=6hemu(i)
      write(6,100) lab,(emu(i),i=1,np3)
  901 continue
c
c ------ aux ------- aux ------ aux ---------- aux ----
      call aux
c ------------------------------ entrainment control
      if(kin.ne.2) go to 94
      rat=abs((u(3)-u(1))/(u(np3)-u(1)+1.e-30))
      if(rat.lt.ulim) emau(2)=emau(2)*rat/ulim
      rmi=2.*emau(2)
   94 continue
      if(kex.ne.2) go to 97
      rat=abs((u(np1)-u(np3))/(u(np3)-u(1)+1.e-30))
      rme=-2.*emau(np1)
c     if(rme.ge.0.0)write(6,*)'rme=',rme
      if(ki.eq.1.and.rat.lt.ulim) rme=rme*(rat/ulim)**2
   97 if(xd.eq.xend.or.xd.eq.xout.or.xd.eq.xulast.or.
  1 ipyrol.eq.istep+1)        go to 96
c ------------------- limit on increment in pei.
      if((abs(rmi)+abs(rme))*dx.lt.pei*peilim) go to 96
      dx=pei*peilim/(abs(rmi)+abs(rme))
      xd=xu+dx
      write(6,*)'correct dx','xu=',xu
   96 continue
      if(istep.lt.ipyrol) go to 3
      if(ll.ne.1) then
      if(iinput.ne.1) then
      indi(1)=2
      aji(1)=0.0
      else
      write(6,*) 'read from file TEMP'
      open(unit=8,file= 'temp',status= 'unknown')
      read(8,*) nend,nipyrol
      do 9 ii=1,nend-nipyrol+1
      read(8,*) tsn(ii),fuel(ii),du(ii)
      tsnt(ii)=tsn(ii)
```

```
      fuelt(ii)=fuel(ii)
      dut(ii)=du(ii)
    9 continue
      close(8)
      write(6,*)'finish reading file TEMP'
      ll=1
      iinput=0
      endif
      endif
      if(ll.eq.1) then
      if(xd.gt.dut(nend+1-nipyrol)) then
      f(1,1)=cmix*tsnt(nend)+hfu*fuelt(nend)
      lind=1
      else
      do 13 ij=1,nend+0-nipyrol
      if(xd.ge.dut(ij).and.xd.le.dut(ij+1))then
      tsn(istep+2-ipyrol)=tsnt(ij)+(tsnt(ij+1)-tsnt(ij))
     1*(xd-dut(ij))/(dut(ij+1)-dut(ij))
      fuel(istep+2-ipyrol)=fuelt(ij)+(fuelt(ij+1)-fuelt(ij))
     1*(xd-dut(ij))/(dut(ij+1)-dut(ij))
      endif
   13 continue
      f(1,1)=cmix*tsn(istep+2-ipyrol)+hfu*fuel(istep+2-ipyrol)
      endif
      endif
    3 continue
c ---------- adjustment of dx to reach axis.----------
      if(kin.eq.1) go to 95
      if(istep.ge.iax) go to 95
      if(psii.gt.rmi*dx.or.iax.eq.istep+1) go to 95
      rmi=psii/dx
      iax=istep+1

c ------- stride2 --------- stride2 --------- stride2 ---
   95 call stride(2)

c ------------------------------------------------
chapter 10 10 10 10 10 10 10 10 10 10 10 10 10 10 10 10 10
 1000 if(istep.gt.0) go to 106
      anstat=nstat
      anprof=nprof
      anplot=nplot
chapter 10a ---- ---------- headings--
      re~=(floa+flob+floc)*4./emu(1)/r(np3)
      eqrat=0.0
      if(inert.ne.1) eqrat=flob*oxdfu/(floc+1.e-30)/oxc
      amach=ubar/sqrt(gamma*gascon*tb/wfu)
      write(6,*) kase,lesson,model,masstr,inert
      write(6,*) ua,ub,uc,ud,ta,tb,tc,td,ra,rb,rc,rd,
     1xend,xout,xulast,tan,press,preexp,rey,eqrat,amach
      lab=8homega(i)
      write(6,*) (om(i),i=1,np3)
      press1=press
  106 continue
```

```
c ---------------------------------------- test 5 --
      if(itest) 1002,1001,1002
 1002 lab—-6htest 5
      write(6,100) lab,rmi,rme,dx
 1001 continue
c
chapter lob —————————— test for printout
ciprint=0 gives no output, =1 gives single variables only,
c      =2 gives both single and array (profil) variables.
 101 1iprint=0
      if(float(istep/nstat).eq.float(istep)/anstat)iprint=1
      if(float(istep/nprof).eq.float(istep)/anprof)iprint=2
      if(istep.eq.iend.or.istep.eq.ipyrol.or.istep.eq.iout)
     1 iprint=2
      if(itest.ne.0.or.ifin.ne.0) iprint=2
c     ------ the next statement would be used for a typical
c     ------ plot control                                    a
c     if(float(istep/nplot).eq.float(istep)/anplot)iprint=3
c     ---- the next statement provides a plot just prior
c     ------ to termination
      if(xu.ge.xulast.or.ifin.ne.0.or.istep.eq.lastep)
     1 iprint=3
chapter 10c ---------- single station variables.
      if(iprint.eq.0) go to 110
      if(mm.eq.4) then
      write(6,*) istep,iax,iend,iout,kin,kex,dx,psii,psie,
     1rmi,rme,pei
       endif
      ubar=0.
      do 1020 j=1,nf
 1020 flux(j)=0.
      do 1021 i=2,np1
      ubar=ubar+omd(i)*(u(i)+u(i+1))
      do 1021 j=1,nf
 1021 flux(j)=flux(j)+omd(i)*(f(j,i)+f(j,i+1))
      ubar=.5*ubar
      uflux=pei*ubar
      do 1022 j=1,nf
 1022 flux(j)=.5*pei*flux(j)
c
      uref=ubar
      ruref=pei/.5/(r(1)+r(np3))/y(np3)
      do 1023 j=1,nf
      dfi(j)=flux(j)/pei-f(j,1)
 1023 dfe(j)=dfi(j)+f(j,1)-f(j,np3)
      uflux=uflux-psie*u(np3)+u(1)*psii
      go to (1041,1042,1043), nf
 1043 flux(3)=flux( 3)-psie*f3d+f3a*psii
 1042 flux(2)=flux(2)-psie*f2d+f2a*psii
 1041 flux(1)=flux(1)-psie*f1d+f1a*psii
      pressd=press/press1-1.
      if(mm.eq.4) then
      write(6,*) xu,uflux,pressd,aexd,(flux(j),j=1,nf)
      endif
```

```
      if(kin.ne.1) go to 1024
      tauid=taui/uref/ruref
      do 1025 j=1,nf
 1025 ajid(j)=aji(j)/ruref/dfi(j)
      if(mm.eq.4) then
      write(6,*) kin,tauid,(ajid(j),j=1,nf)
      endif
 1024 if (kex.ne.1) go to 1026
      taued=taue/uref/ruref
      do 1027 j=1,nf
 1027 ajed(j)=aje(j)/ruref/dfe(j)
      if(mm.eq.4) then
      write(6,*) kex,taued,(ajed(j),j=1,nf)
      endif
 1026 continue
chapter 10d ---------- profiles and other arrays
      if(iprint.eq.1) go to 110
      lab=6hr1,y 's
      div=1.
      do 1095 i=1,np3
 1095 out(i)=y(i)/div
      out(1)=r(1)
      out(np3)=y(np3)
      xaxis=4hy(i)
      do 1085 i=1,np3
 1085 xplot(i)=out(i)
      lab=5hu vel
      sub=0.
      div=1.
      do 1094 i=1,np3
 1094 outu(i)=(u(i)-sub)/div
      outu(1)=u(1)
      outu(np3)=u(np3)
      if(novel.ne.1) go to 2999
      ny=1
      yaxes(1)=8hvelocity
      symbol(1)=1hu
      do 1084 i=1,np3
 1084 yplot(1,i)=outu(i)
 2999 continue
      lab=4htemp
      sub=0.
      div=1.
      do 1093 i=1,np3
 1093 outt(i)=(fs(2,i)-sub)/div
      outt(2)=outt(1)
      outt(np2)=outt(np3)
      ny=2
      yaxes(2)=4htemp
      symbol(2)=1ht
      do 1083 i=1,np3
 1083 yplot(2,i)=outt(i)
      if(masstr.eq.0) go to 1009
      lab=4hfuel
```

```
      sub=0.
      div=1.
      do 1092 i=1,np3
 1092 outf(i)=(f(2,i)-sub)/div
      ny=3
      yaxes(3)=4hfuel
      symbol(3)= 1hf
      do 1082 i=1,np3
 1082 yplot(3,i)=outf(i)
      lab=6hoxygen
      sub=0.
      div=1.
      do 1091 i=1,np3
 1091 outo(i)=(fs(1,i)-sub)/div
      ny=4
      yaxes(4)=6hoxygen
      symbol(4)=1ho
      do 1081 i=1,np3
 1081 yplot(4,i)=outo(i)
 1009 continue
      if(iprint.eq.2) go to 110
      write(6,*) xu,istep
      call plots(xplot,93,np3,xaxis,yplot,10,ny,yaxes,symbol)
c ------------------------------------------------
chapter 11 11 11 1111 11 11 1111 11 11 end of main loop
  110 if(istep.ge.lastep.or.xu.ge.xulast.or.ifin.ne.0)
     1 go to 111
c --- stride3 --------- stride3 ---------- stride3 ----
      call stride(3)
      if(ifin) 1011,60,111
c
c ------------------------------- termination
  111 write(6,*) 'istep=',istep,'lastep=',lastep,
     1'xu=',xu,'xulast=',xulast,'ifin=',ifin
c ..........................................
  120 continue
      close(1)
      close(2)
      close(3)
      close(4)
      close(7)
      close(9)
      do 666 i=1,6
  666 write(6,*)'ifinal(',i,')=',ifinal(i)
      write(6,*)'it=',it,'itrmi=',itrmi,'error= ',error
      if(istep.ge.ipyrol)write(6,*)'href=',href,'sgi=',sgi
      stop
  100 format(1h ,a8,1p11e11.3/(9x,11e11.3))
  101 format(1h ,a8,11i11)
      end
```

```
      subroutine aux
c/--------- subroutine for program genmix 4a----------
c/------- D.B.Spalding, Imperial College, 1972 ---------
      dimension yedge(6),sau(5,93),sad(5,93)
      common/coma/a(93),aje(5),aji(5),b(93),c(93),csalfa,
     1 d(93),dpdx(93),dx,emu(93),f(5,93),fs(5,93),iax,iend
     2 ,ifin,inde(5),indi(5),iout,istep,itest,iutrap,js,
     3 jsw,jv,jy,kex,kin,krad,n,nd2,nf,novel,np1,np2,np3,
     4 om(93),omd(93),p(93),pei,pr(5),pref(5,93),psie,psii,
     5 r(93),rho(93),rme,rmi,ru(93),sd(5,93),su(5,93),taue,
     6 taui,u(93),xd,xu,y(93),ye,yi,emau(93),us(93)
      common/comb/ak,almg,arrcon,ewall,fr,h,hfu,inert,
     1 masstr,model,oxdfu,preexp,press,ubar,ufac
      common/comc/omi,bpi,ome,bpe,r25,rn15,yn15,thlp,gd4,
     1hlp,ttp,pd4,rmid2,fra
c  su(1,i) is used for dudy
c  su(2,i) indicates whether dudy excess a minimum value
c  su(3,i) is used for mixing length
c  sd(3,i) is used for r(i)*(y(i+1)-y(i-1))
c
c  1111111111111111111111111111111111111111111 mixing length
      if(model.eq.1) go to 200
      umax=0.
      umin=0.
      do 1 i=1,np3
      umax=amax1(umax,u(i))
    1 umin=amin1(umin,u(i))
      udmax=umax-umin
      dudymn=fr*udmax/y(np3)
      do 10 i=2,np1
      sau(1,i)=(u(i+1)-u(i))/(y(i+1)-y(i))
      if (abs(sau(1,i))-dudymn) 111,111,112
  111 sau(2,i)=0.
      go to 10
  112 sau(2,i)=1.
   10 continue
      if (kin.eq.1) sau(2,2)=1.
      if (kex.eq.1)sau(2,np1)=1.
      sau(2,1)=0.
c ---------- test 7
      if(itest) 17,16,17
   17 lab=6htest 7
      write(6,100) lab,dudymn,fr,ak,almg,ubar
      lab=8hsau(1,i)
      write(6,100) lab,(sau(1,i),i=1,np3)
      lab=8hsau(2,i)
      write(6,100) lab,(sau(2,i),i=1,np3)
   16 continue
c ------------------------------------
      k=1
      do 13 l=1,6
   13 yedge(l)=y(np3)
      do 11 i=2,np1
      if(sau(2,i)-sau(2,i-1)) 110,11,110
```

```
  110 yedge(k)=y(i)
      k=k+1
      if(k.gt.6) go to 14
   11 continue
   14 el12=(yedge(2)-yedge(1))*almg
      el34=(yedge(4)-yedge(3))*almg
      el56=(yedge(6)-yedge(5))*almg
      el23=.5*(el12+el34)
      el45=.5*(el34+el56)
c ---------------------------------- test 8
      if (itest) 19,18,19
   19 lab=6htest 8
      write(6,100) lab
      lab=4hel's
      write(6,100) lab,el12,el23,el34,el45,el56
      lab=7hyedge's
      write(6,100) lab,(yedge(i),i=1,6)
   18 continue
c ------------------------------------
      do 12 i=2,np1
      if(y(i)-yedge(1)) 120;121,121
  121 if(y(i)-yedge(2)) 122,123,123
  123 if(y(i)-yedge(3)) 124,125,125
  125 if(y(i)-yedge(4)) 126,127,127
  127 if(y(i)-yedge(5)) 128,129,129
  120 sau(3,i)=0.
      go to 130
  122 sau(3,i)=el12
      go to 130
  124 sau(3,i)=el23
      go to 130
  126 sau(3,i)=el34
      go to 130
  128 sau(3,i)=el45
      go to 130
  129 sau(3,i)=el56
c ..................... upper limits to mixing length
  130 s a 3(i)=amin1(sau(3,i),.5*udmax/(abs(sau(1,i))+
 1 1.e-30))
      if(kin-1) 131,132,131
  132 sau(3,i)=amin1(sau(3,i),ak*.5*(y(i)+y(i+1)))
  131 if(kex-1) 12,133,12
  133 sau(3,i)=amin1(sau(3,i),ak*(y(np3)-.5*(y(i)+y(i+1))))
   12 continue
c ---------------------- test 9
.     if(itest) 109,108,109
  109 lab=6htest 9
      write(6,100) lab
      lab=8hsau(3,i)
      write(6,100) lab,(sau(3,i),i= 1,np3)
  108 continue
c .....................................
c 22222222222222222222222222222222222222222222 viscosities
c -------laminar viscosities for cell boundaries ----------
```

```
  200 do 23 i=2,np1
   23 emu(i)=.5*(emu(i)+emu(i+1))
      if(model.eq.1) go to 29
c ------------------------------ turbulent contribution
      do 20 i=2,np1
      dudyl=abs(sau(1,i)*sau(3,i))
      udmin=ufac*.5*(u(i)+u(i+1))
      dudyl=amax1(dudyl,udmin)
      rhm=.5*(rho(i)+rho(i+1))
      emut=rhm*sau(3,i)*dudyl
c -------------- in this version, the turbulent and laminar
c              contributions are simply added. an
c              alternative would be to introduce the van
c              driest damping function.
      emu(i)=emu(i)+emut
   20 continue
c ------------------------------ test 10
      if(itest) 202,201,202
  202 lab=7htest 10
      write(6,100) lab
      lab=6hemu(i)
      write(6,100) lab,(emu(i),i=1,np3)
      lab=8hsad(1,i)
      write(6,100) lab,(sad(1,i),i=1,np3)
  201 continue
c ------------------------------ modification of emu array
   29 do 24 i=2,np1
   24 emau(i)=emu(i)/(y(i+1)-y(i))
      if(krad.eq.0) go to 25
      do 26 i=2,np1
   26 emau(i)=emau(i)*.5*(r(i)+r(i+1))
   25 if(istep) 28,28,300
c ------------------------------ initial pref s.
   28 do 27 j=1,nf
      do 27 i=1,np3
   27 pref(j,i)=pref(j,1)
c 33333333333333333333333333333333333333333333333333 sources
c ------------------------------ velocity
  300 do 307 i=2,np2
  307 sad(3,i)=pei*(om(i+1)-om(i-1))/rho(i)/u(i)
      go to (310,312,312), kin
  310 sad(3,2)=(r(1)+.5*(r(2)+r(3)))*yi
      go to 313
  312 sad(3,2)=pei*om(3)/rho(3)/u(3)
  313 go to (314,315,315), kex
  314 sad(3,np2)=(r(np3)+.5*(r(np1)+r(np2)))*ye
      go to 316
  315 sad(3,np2)=pei*(1.-om(np1))/rho(np1)/u(np1)
  316 continue
      do 308 i=2,np2
  308 us(i)=dpdx(i)*sad(3,i)
      if(nf.eq.0) return
c ..................... kinetic heating
c ------ temporary use of sd array
```

```
      go to (303,304), novel
  303 do 305 i=1,np3
      su(1,i)=0.
  305 sd(1,i)=0.
      go to 306
  304 do 30 i=2,np2
   30 sad(1,i)=u(i)*u(i)
      do 31 i=2,np1
   31 sad(1,i)=emau(i)*(sad(1,i+1)-sad(1,i))
      sad(1,1)=0.
      sad(1,np2)=0.
      do 32 i=2,np2
      t=( 1.-1./pref(1,i))*.5
   32 su(1,i)=(sad(1,i)-sad(1,i-1))*t
      do 33 i=2,np1
   33 sd(1,i)=0.
c ------------------------------ test 11
  306 if(itest) 302,301,302
  302 lab—7htest 11
      write(6,100) lab
      lab=7hsd(1,i)
      write(6,100) lab,(sd(1,i),i=1,np3)
      lab=7hsu(1,i)
      write(6,100) lab,(su(1,i),i=1,np3)
  301 continue
      if(nf.eq.1) return
c ------------------------------------------------ fuel
c     if(istep.gt.ipyrol.and.ll.ne.1) then
c     preexp—10.0
c     endif
      t1=.5*preexp*press**2
      do 40 i=2,np2
      if(inert-1) 45,41,45
   45 f2=f(2,i)
      f3=f(3,i)
      fs1=fs(1,i)
      fs2=fs(2,i)
      if(i-2) 42,46,42
   46 f2=f2+.25*(f(2,3)-f2)
      f3=f3+.25*(f(3,3)-f3)
      fs1=fs1+.25*(fs(1,3)-fs1)
      fs2=fs2+.25*(fs(2,3)-fs2)
   42 if(i-np2) 43,47,43
   47 f2=f2+.25*(f(2,np1)-f2)
      f3=f3+.25*(f(3,np1)-f3)
      fs1=fs1+.25*(fs(1,np1)-fs1)
      fs2=fs2+.25*(fs(2,np1)-fs2)
   43 fubrnt=.5*(abs(f3)-f3)/oxdfu
      expo=exp(-arrcon/fs2)
      if(f2-fubrnt) 44,41,44
   44 sd(2,i)=-t1*fs1*expo*sad(3,i)*f2/(f2-fubrnt)
      su(2,i)=-fubrnt*sd(2,i)
      go to 40
   41 su(2,i)=0.
```

```
      sd(2,i)=0.
   40 continue
c --  ---------- test 12
      if(itest) 402,401,402
  402 lab=7htest 12
      write(6,100) lab
      lab=7hsd(2,i)
      write(6,100) lab,(sd(2,i),i=1,np3)
      lab=7hsu(2,i)
      write(6,100) lab,(su(2,i),i=1,np3)
  401 continue
      if(nf.eq.2) return
c ------------------------------------- ox-fu*oxdfu
      do 50 i=2,np2
      su(3,i)=0.
   50 sd(3,i)=0.
c ------------------------------------- test 13
      if (itest) 502,501,502
  502 lab=7htest 13
      write(6,100) lab
      lab=7hsd(3,i)
      write(6,100) lab,(sd(3,i),i= 1,np3)
      lab= 7hsu(3,i)
      write(6,100) lab,(su(3,i),i= 1,np3)
  501 continue
      return
  100 format(1h ,a8,1p 11e11.3/(8x,11e11.3))
      end
            subroutine stride(isw)
c/---------- subroutine for program genmix 4a ----------
c/--------- D.B.Spalding, Imperial College,London --------
c/ this subroutine performs the same operations as the one
c  in genmix 4a but more economically. the a,b,c arrays are
c  one-dimensional. some c  often used functions of om are
c  stored, and a d array saves unnecessary arithematic in
c  the tdma operation.
c-------------------------------------------------
      dimension a2(5),anp2(5),b2(5),bnp2(5),c2(5),cnp2(5),
     1 d2(5),dnp2(5),ahlpt(93),bomt3(93),
     2 pbom(93),pgom(93),thlpt(93),ttpf(5)
      dimension bom(93),ompom(93)
      common/coma/a(93),aje(5),aji(5),b(93),c(93),csalfa,
     1 d(93),dpdx(93),dx,emu(93),f(5,93),fs(5,93),iax,iend,
     2 ifin,inde(5),indi(5),iout,istep,itest,iutrap,js,jsw,
     3 jv,jy,kex,kin,krad,n,nd2,nf,novel,np1,np2,np3,
     4 om(93),omd(93),p(93),pei,pr(5),pref(5,93),psie,psii,
     5 r(93),rho(93),rme,rmi,ru(93),sd(5,93),su(5,93),taue,
     6 taui,u(93),xd,xu,y(93),ye,yi,emau(93),us(93)
      common/comc/omi,bpi,ome,bpe,r25,rn15,yn15,thlp,gd4,
     1 hlp,ttp,pd4,rmid2,fra
      common/comd/gi(5),ge(5),fdifi(5),fdife(5)
      go to (1000,2000,3000,4000),isw
c**************************** stride1 ******************
 1000 if(istep) 1003,1003,1100
```

```
1003 omi=.5*om(3)
     ome=.5*(1.-om(np1))
     do 1002 i=2,np2
     bom(i)=om(i+1)-om(i-1)
     bomt3(i)=3.*bom(i)
     ompom(i)=om(i)+om(i+1)
1002 omd(i)=om(i+1)-om(i)
     omd(1)=bom(2)
     bpe=1.
     bpi= 1.
     y(1)=0.
     if(krad.eq.1) go to 1100
     do 1001 i=1,np3
1001 r(i)=1.
     r25=1.
     rn15=1.
     if(itest.ne.0) write(6,9010)(r(i),i= 1,np3),r25,rn15
c ---------- calculation of rho*u's ----------
1100 do 1101 i=1,np3
     if(rho(i).gt.0.) go to 1101
     write(6,1108) rho(i),i,rho(1)
1108 format(36h ********** negative or zero rho(i)=,
    1 1pe11.3,6h at i=,i3,6x,21hset to abs of rho(1)=,
    2 e11.3,17h ******** stride1)
     rho(i)=abs(rho(1))
1101 ru(i)=rho(i)*u(i)
     ru3=ru(3)
     run1=ru(np1)
     do 1102 i=2,np1
1102 ru(i)=.5*(ru(i)+ru(i+1))
     if(itest.ne.0) write(6,9010)(ru(i),i=1,np3),run1,
    1 ru3,pei
c ---------- calculation of y's and r's ----------
c ---------- y's for plane geometry
     yi=pei*omi/(bpi*ru(2))
     y(3)=yi+pei*om(3)/(ru(2)+ru3)
     y(2)=2.*yi-y(3)
     do 1103 i=4,np1
1103 y(i)=y(i-1)+pei*omd(i-1)/ru(i-1)
     yn15=y(np1)+pei*omd(np1)/(ru(np1)+run1)
     ye=pei*ome/(bpe*ru(np1))
     y(np3)=yn15+ye
     y(np2)=2.*yn15-y(np1)
     if(krad.eq.0) return
c---------- y's and r's for axisymmetrical geometry
     if(csalfa.eq.0.) go to 1110
c---------- csalfa ne zero
     cosd2=.5*csalfa
     if(r(1).ne.0.) go to 1105
c---------- r(1)=0.
     do 1106 i=2,np3
     y(i)=sqrt(abs(y(i)/cosd2))
1106 r(i)=y(i)*csalfa
     yi=sqrt(abs(yi/cosd2))
```

```
      yn15=sqrt(abs(yn15/cosd2))
      go to 1107
c-----------------------------------------------  r(1) ne 0.
 1105 r1d2=.5*r(1)
      r1d2sq=r1d2*r1d2
      do 1104 i=2,np3
      y(i)=y(i)/(r1d2+sqrt(abs(r1d2sq+cosd2*y(i))))
 1104 r(i)=r(1)+y(i)*csalfa
      yi=yi/(r1d2+sqrt(abs(r1d2sq+cosd2*yi)))
      yn15=yn15/(r1d2+sqrt(abs(r1d2sq+cosd2*yn15)))
 1107 r25=r(1)+yi*csalfa
      rn15=r(1)+yn15*csalfa
      ye=y(np3)-yn15
      return
c-------------------------------------  csalfa=0.
 1110 do 1111 i=2,np3
      y(i)=y(i)/r(1)
 1111 r(i)=r(1)
      yi=yi/r(1)
      yn15=yn15/r(I)
      r25=r(1)
      rn15=r(I)
      ye=y(np3)-yn15
      return
c************************ stride2 ************************
c-----------------------  preliminaries for coefficients
 2000 px=pei/dx
      pd8=.125*px
      pd4=pd8+pd8
      g=rmi-rme
      armi=abs(rmi)
      arme=abs(rme)
      gd4=.25*g
      pg=px+g
      pgd8=.125*pg
      pgd4=pgd8+pgd8
      rmid2=.5*rmi
      do 2004 i=2,np2
      pbom(i)=px*bom(i)
 2004 pgom(i)=pgd4*omd(i)
      p4omp=pd4*bom(2)
c-------------------------------------  grid point 2
c-------------------------------------  taui,bpi,t1
      if(kin.ne.1) go to 2001
      call wf(0,1,bpi,t1,taui)
      go to 2002
 2001 t1=0.
      if(krad.eq.0) bpi=.33333+.66667*ru(1)/ru(2)
      if(krad.eq.1)bpi=( r(1)*(5.*ru(1)+ru(2))+3.*r25*
     1              (ru(1)+ru(2)))/6./(r(1)+r25)/ru(2)
c-------------------  boundary coefficients for velocity
 2002 hlp=rmid2-gd4*ompom(2)
      ahlp=abs(hlp)
      thlp=hlp+hlp
```

```
      thlpt(2)= thlp
      tp=emau(2)
      ttp=tp+ahlp+abs(tp-ahlp)
      a(2)=ttp-thlp-t1-pgom(2)
      b(2)=2.*t1+rmi+armi
      c(2)=p4omp*(3.*u(2)+u(3))-us(2)
      d(2)=a(2)+b(2)+pbom(2)
c---------------------- boundary coefficients for f's
      if(nf.eq.0) go to 2304
      do 2300 j=1,nf
      tpf2=tp/pref(j,2)
      ttpf(j)=tpf2+ahlp+abs(tpf2-ahlp)
      if(kin.ne.1) go to 2301
      call wf(j,1,fdifi(j),t1f,gi(j))
      if(indi(j).eq.2) go to 2303
      aji(j)=gi(j)*(f(j,1)-.5*(f(j,2)+f(j,3))-fdifi(j))
      go to 2302
 2301 t1f=0.
      fdifi(j)=0.
 2302 a2(j)=ttpf(j)-thlp-t1f-pgom(2)+.5*sd(j,2)
      b2(j)=2.*t1f+rmi+armi
      d2(j)=a2(j)+b2(j)+pbom(2)-2.*sd(j,2)
      t=- t1f*fdifi(j)
      go to 2305
 2303 a2(j)=ttpf(j)-thlp-pgom(2)+.5*sd(j,2)
      b2(j)=0.
      d2(j)=a2(j)+pbom(2)-2.*sd(j,2)+rmi*2.
      t=rmi*f(j,1)+aji(j)*r(1)
 2305 tt=3.*f(j,2)+f(j,3)
 2300 c2(j)=p4omp*tt+2.*(t+su(j,2))
c  ----------------------------------grid point np2
c  ------------------------------taue, b e, tnp3
 2304 if(kex.ne.1) go to 2003
      call wf(0,np3,bpe,tnp3,taue)
      go to 2310
 2003 tnp3=0.
      if (krad.eq.0) bpe=.33333+.66667*ru(np3)/ru(np1)
      if(krad.eq.1)bpe=(r(np3)*(5.*ru(np3)+ru(np1))+3.*
     1rn15*(ru(np3)+ru(np1)))/6./(r(np3)+rn15)/ru(np1)
c  ------------------boundary coefficients for velocity
 2310 hlm=rmid2-gd4*ompom(np1)
      ahlm=abs(hlm)
      thlm=hlm+hlm
      tm=emau(np1)
      ttm=tm+ahlm+abs(tm-ahlm)
      p4omm=pd4*bom(np2)
      a(np2)=2.*tnp3-rme+arme
      b(np2)= ttm+thlm-tnp3-pgom(np1)
      c(np2)=p4omm*(3.*u(np2)+u(np1))-us(np2)
      d(np2)=a(np2)+b(np2)+pbom(np2)
      if (nf.eq.0) return
c ---------------------- boundary coefficients for f's
      do 2320 j=1,nf
      tmf=tm/pref(j,np1)
```

```
      ttmf=tmf+ahlm+abs(tmf-ahlm)
      if (kex.ne.1) go to 2311
      call wf(j,np3,fdife(j),tnp3f,ge(j))
      if(inde(j).eq.2) go to 2313
      aje(j)=ge(j)*(.5*(f(j,np2)+f(j,np1))+fdife(j)-
     1 f(j,np3))
      go to 2312
 2311 tnp3f=0.
      fdife(j)=0.
 2312 anp2(j)=2.*tnp3f-rme+arme
      bnp2(j)=ttmf+thlm-tnp3f-pgom(np1)+.5*sd(j,np2)
      dnp2(j)=anp2(j)+bnp2(j)+pbom(np2)-2.*sd(j,np2)
      t=-tnp3f*fdife(j)
      go to 2315
 2313 anp2(j)=0.
      bnp2(j)=ttmf+thlm-pgom(np1)+.5*sd(j,np2)
      dnp2(j)=bnp2(j)+pbom(np2)-2.*sd(j,np2)-rme*2.
      t=-rme*f(j,np3)-aje(j)*r(np3)
 2315 tt=3.*f(j,np2)+f(j,np1)
 2320 cnp2(j)=p4omm*tt+2.*(t+su(j,np2))
      return
c**********stride3**********
 3000 do 3005 i=3,np1
      thlm=thlp
      hlp=rmid2-gd4*ompom(i)
      thlp=hlp+hlp
      thlpt(i)=thlp
      ahlp=abs(hlp)
      ahlpt(i)=ahlp
      ttm=ttp
      tp=emau(i)
      ttp=tp+ahlp+abs(tp-ahlp)
      a(i)=ttp-thlp-pgom(i)
      b(i)=ttm+thlm-pgom(i-1)
      c(i)=pd4*(bomt3(i)*u(i)+omd(i)*u(i+1)+omd(i-1)*
     1 u(i-1))-us(i)
      d(i)=a(i)+b(i)+pbom(i)
 3005 continue
      go to (3021,3020), novel
 3020 if (itest) 3900,3905,3900
 3900 write(6,3901) (a(i),i=2,np2)
      write(6,3902) (b(i),i=2,np2)
      write(6,3903) (c(i),i=2,np2)
      write(6,3904) (d(i),i=2,np2)
 3901 format(7h  a(i) ,1p11e11.3/(7x,11e11.3))
 3902 format(7h  b(i) ,1p11e11.3/(7x,11e11.3))
 3903 format(7h  c(i) ,1p11e11.3/(7x,11e11.3))
 3904 format(7h  d(i) ,1p11e11.3/(7x,11e11.3))
 3905 continue
c-----------------------------------------------------
      if(kin.eq.2.and.ru(1).ne.0.) u(1)=u(1)-dpdx(1)*dx/
     I ru(1)
      if(kex.eq.2.and.ru(np3).ne.0.) u(np3)=u(np3)-
     1 dpdx(np3)*dx/ru(np3)
```

```
c-          ------ solve for downstream u's ----------
      b(2)=(b(2)*u(1)+c(2))/d(2)
      a(2)=a(2)/d(2)
      do 3048 i=3,np2
      t=d(i)-b(i)*a(i-1)
      a(i)=a(i)/t
 3048 b(i)=(b(i)*b(i-1)+c(i))/t
      do 3050 idash=2,np2
      i=n+4-idash
      u(i)=a(i)*u(i+1)+b(i)
c---------------------- test for negative u's ---------
c/iutrap=0,no action/ .gt.0,set to 1.e-30/ .gt.1,
c ifin=-1/ .gt.2,itest=1/
      if(iutrap.eq.0.or.i.eq.2.or.i.eq.np2) go to 3050
      if(u(i)) 3046,3046,3050
 3046 j=istep+1
      write(6,3047) u(i),i,j
 3047 format(25h ********** u (le zero) =,1pe10.3,6h at
     1i=,i3,8h, istep=,i6,34h, set u to 1.e-30 ***stride3)
      u(i)=1.e-30
      ifin=-iutrap/2
      itest=iutrap/3
 3050 continue
c-------------------------------------------------
      if (kin.eq.3) u(1)=.5*(u(2)+u(3))
      if (kex.eq.3) u(np3)=.5*(u(np1)+u(np2))
 3021 if (itest) 3011,3013,3011
 3011 write(6,3012) (u(i),i=1,np3)
 3012 format(3h u ,6x,1p11e11.3/(9x,11e11.3))
c-------------------- ---------- ---------------------
 3013 if(nf) 3060,3060,3014
 3014 do 3321 j=1,nf
c---------------- solve for downstream f's ----------
      a(2)=a2(j)
      b(2)=b2(j)
      c(2)=c2(j)
      d(2)=d2(j)
      a(np2)=anp2(j)
      b(np2)=bnp2(j)
      c(np2)=cnp2(j)
      d(np2)=dnp2(j)
      do 3002 i=3,np1
      ttmf=ttpf(j)
      tpf=emau(i)/pref(j,i)
      ttpf(j)= tpf+ahlpt(i)+abs(tpf-ahlpt(i))
      a(i)= ttpf(j)-thlpt(i)-pgom(i)
      b(i)=ttmf+thlpt(i-1)-pgom(i-1)
      c(i)=pd4*(bomt3(i)*f(j,i)+omd(i)*f(j,i+1)+omd(i-1)*
     1 f(j,i-1))+2.*su(j,i)
 3002 d(i)=a(i)+b(i)+pbom(i)-2.*sd(j,i)
      if(itest) 3906,3907,3906
 3906 write(6,3901) (a(i),i=2,np2)
      write(6,3902) (b(i),i=2,np2)
      write(6,3903) (c(i),i=2,np2)
```

```
      write(6,3904) (d(i),i=2,np2)
 3907 continue
c-----------------------------------------------
      b(2)=(b(2)*f(j,1)+c(2))/d(2)
      a(2)=a(2)/d(2)
      do 3148 i=3,np2
      t=d(i)-b(i)*a(i-1)
      a(i)=a(i)/t
 3148 b(i)=(b(i)*b(i-1)+c(i))/t
      do 3150 idash=2,np2
      i=n+4-idash
 3150 f(j,i)=a(i)*f(j,i+1)+b(i)
c---------- adjust f(j,1) and f(j,np3) ------
      go to (3210,3220,3230),kin
 3210 if(indi(j).eq.2) f(j,1)=fdifi(j)+.5*(f(j,2)+f(j,3))+
     1 aji(j)/gi(j)
      go to 3220
 3230 f(j,1)=.5*(f(j,2)+f(j,3))
 3220 go to (3310,3320,3330),kex
 3310 if(inde(j).eq.2) f(j,np3)=fdife(j)+.5*(f(j,np2)+
     1                 f(j,np1))-aje(j)/ge(j)
      go to 3320
 3330 f(j,np3)=.5*(f(j,np1)+f(j,np2))
 3320 if(itest) 3322,3321,3322
 3322 write(6,3323) j,(f(j,i),i=1,np3)
 3323 format(6H f, j=,i3,1p11e11.3/(9x,11e11.3))
 3321 continue
c-----------------------------------------------
 3060 xu=xd
      psii=psii-rmi*dx
      psie=psie-rme*dx
      pei=psie-psii
      istep=istep+1
      return
c********************** stride 4 ************************
 4000 continue
      nd2=n/2
      np1=n+1
      np2=n+2
      np3=n+3
      om(1)=0.
      om(np3)=1.
      istep=0
      iend=10000
      iax=10000
      iout=10000
      xu=-1.e-30
      dx=1.e-30
      ifin=0
      kin=1
      kex=1
      return
 9010 format(1h ,1p11e11.3)
      end
```

```
      subroutine wf(j,i1,out1,out2,out3)
c-----  subroutine for program genmix 4a ----------
c/------- D.B.Spalding, Imperial College, 1972 ----------
      common/coma/a(93),aje(5),aji(5),b(93),c(93),csalfa,
     1 d(93),dpdx(93),dx,emu(93),f(5,93),fs(5,93),iax,iend,
     2 ifin,inde(5),indi(5),iout,istep,itest,iutrap,js,jsw,
     3 jv,jy,kex,kin,krad,n,nd2,nf,novel,np1,np2,np3,om(93)
     4 ,omd(93),p(93),pei,pr(5),pref(5,93),psie,psii,r(93)
     5 ,rho(93),rme,rmi,ru(93),sd(5,93),su(5,93),taue,taui,
     6 u(93),xd,xu,y(93),ye,yi,emau(93),us(93)
      common/comb/ak,almg,arrcon,ewall,fr,h,hfu,inert,
     1 masstr,model,oxdfu,preexp,press,ubar,ufac
      common/comc/omi,bpi,ome,bpe,r25,rn15,yn15,thlp,gd4,
     1 hlp,ttp,pd4,rmid2,fra
c     effects of pressure gradient and mass transfer are included
c     effects of radius variation are neglected
c     for velocity        out1=bp,     out2=t,     out3=tau
c     for f's             out1=fidif,  out2=t,     out3=g
c
      data shalf/.04/, bplast/0.9/
      int=1/i1
      i2=i1-1+2*int
      i3=i1-2+4*int
      i25=i3-int
      if(j) 100,100,200
c------------------------- velocity ----------------
  100 uref=.5*(u(i2)+u(i3))
      rhoref=.5*rho(i1)+.25*(rho(i2)+rho(i3))
      ruref=rhoref*uref
      rref=.5*(r(i2)+r(i3))
      vref=emu(i1)
      yref=yi+(ye-yi)*om(i1)
      re=uref*rhoref*yref/vref
      rruref=rref*ruref
      am=(rmi-(rme+rmi)*om(i1))/rruref
      ef=yref*dpdx(i1)/ruref/uref
      if(model.eq.1) go to 110
c     write(6,*)'re=',re
      if(re.lt.132.25) go to 110

c------------------------- extended log law ---------
      er=re*ewall
      nit=0
  101 shalf1=shalf
      s=shalf**2
      sloc=s+am+ef
      if(sloc.gt.0.) go to 104
      sloc=1.e-30
      shalf=sqrt(abs(am+ef))
  104 bee=sqrt(sloc)/ak
      arg=er*(shalf+(am/(1.+bee)+.5*ef)/shalf)
      if (arg.gt.11.5*ewall) go to 106
      go to 110
  106 shalf=ak/alog(arg)
```

```
      if(abs(shalf-shalf1).lt..0001.or.nit.gt.10) go to 102
      nit=nit+1
      go to 101
  102 s=shalf**2
      out1=1./(1.+bee)
      emau(i25)=.25*rhoref*rref*abs(u(i3)-u(i2))*
     1 (ak/out1)**2
      go to 103
c------------------------------ laminar flow ---------
  110 amre=am*re
      fre=ef*re
      if(abs(amre).lt..01) go to 111
      amre=amax1(-60.,amin1(60.,amre))
      expmre=exp(amre)
      store=expmre-1.-amre
      amresq=amre*amre
      sre=amre*(1.-store*fre/amresq)/(expmre-1.)
      out1=sre*store/amresq+fre*(store-.5*amresq)/
     1 (amresq*amre)
      go to 112

  111 sre=(2.-fre*(1+amre/6.))/(2.+amre)
      out1=sre*(.5+amre/6.)+fre*(.16667+amre/24.)
  112 if(sre.gt.1.e-30) go to 113
      sre=1.e-30
      out1=.33333
  113 s=sre/re
      emau(i25)=vref*rref/abs(y(i3)-y(i2))
  103 out2=s*rruref
      out3=out2*uref/r(i1)
c------------------------------------ under-relax out1
      out1=.1*out1+.9*bplast
      bplast=outI
      return
c---------------- stagnation enthalpy, fuel, ox-fu/oxdfu
  200 continue
      if(re.lt.132.25) go to 210
      if(model.eq.1) go to 210
      prrat=pr(j)/pref(j,i25)
      pjay=9.*(prrat-1.)/prrat**.25
      s=sloc/pref(j,i25)/(1.+amax1(-.99999,pjay*
     1 sqrt(abs(sloc))))
      out1=0.
      if(j .eq. 1)out1=(h-1.)*.5*uref**2
      out2=s*rruref
      out3=out2/r(i1)
      return
  210 if(abs(amre).lt..01) go to 211
      s=am/(exp(pr(j)*amre)-1.)
      go to 212
  211 s=I./pr(j)/re/(I.+.5*pr(j)*amre)
  212 out1=0.
      if(j.eq.1) out1=(pr(j)-1.)*.5*uref**2
      out2=s*rruref
```

```
      out3=out2/r(i1)
      return
      end
c*************************************************************
      subroutine     profile(xu)
c-----------------------  ------  ----------------
      dimension save(93)
      common/comg/ftemp(6,93),peit,psit,np3t,ifinal(6),
     1 yt(93),tt,ff,oo,pp,vv,ss
      t=tt
      o=oo
      p=pp
      f=ff
      v=vv
      s=ss
      np3=np3t
      np2=np3-1
      tmax=-1.0e10
      fmax=-1.0e10
      omax=-1.0e10
      pmax=-1.0e10
      vmax=-1.0e10
      smax=-1.0e10
      tex= 300.0
      do 1 i=1,np3
      if(ftemp(1,i).gt.tmax) tmax=ftemp(1,i)
      if(ftemp(2,i).gt.fmax)  fmax=ftemp(2,i)
      if(ftemp(3,i).gt.omax) omax=ftemp(3,i)
      if(ftemp(4,i).gt.pmax) pmax=ftemp(4,i)
      if(ftemp(5,i).gt.vmax) vmax=ftemp(5,i)
      if(ftemp(6,i).gt.smax) smax=ftemp(6,i)
    1 continue
      nt=int((tmax-tex)/t+2.0)
      nf=int(fmax/f+2.0)
      no=int(omax/o+2.0)
      np=int(pmax/p+2.0)
      nv=int(vmax/v+2.0)
      nns=int(abs(psit)/s+1.0)
      ns=int(peit/s+2.0)
      do 2 l=1,6
      if(l.eq.1)then
                ii=nt
                store=t
                base= tex
                11= 1
                do 44 k=1,np3
   44            save(k)=ftemp(1,k)
               endif
      if(1.eq.2)then
                ii=nf
                store=f
                base=0.0
                ll=2
                do 5 k=1,np3
```

```
5           save(k)=ftemp(2,k)
           endif
  if(l.eq.3)then
           ii=no
           store=o
           base=0.0
           ll=3
           do 6 k=1,np3
6           save(k)=ftemp(3,k)
           endif.
  if(l.eq.4)then
           ii=np
           store=p
           base=0.0
           ll=4
           do 7 k=1,np3
7           save(k)=ftemp(4,k)
           endif
  if(l.eq.5)then
           ii=nv
           store=v
           base=0.0
           ll=7
           do 8 k=1,np3
8           save(k)=ftemp(5,k)
           endif
  if(1eq.6)then
           ii=ns
           store=s
           base=-s*nns
           ll=9
           do 9 k=1,np3
9           save(k)=ftemp(6,k)
           endif
  do 3 i=1,ii
      plot=store*float(i-1)+base
  do 4 j=1,np2
  if((plot-save(j))*(plot-save(j+1)).le.0.0)then
  if(plot.eq.save(j))then
  ytt=yt(j)
  plot=save(j)
  write(11,*)xu,ytt,plot
  go to 4
  endif
  if(plot.eq.save(j+1))then
  ytt=yt(j+I)
  plot=save(j+1)
  write(11,*)xu,ytt,plot
  go to 4
  endif
    ytt=yt(j)+(yt(j+1)-yt(j))*(plot-save(j))/
 1 (save(j+1)-save(j))
    ifinal(l)=ifinal(l)+1
    write(ll,*)xu,ytt,plot
```

```
      endif
    4 continue
    3 continue
    2 continue
      return
      end
c*******************************************************
                  subroutine wltemp
ccccccccccccccccccccccccccccccccccccccccccccccccccccccccc
cc                                                     cc
cc    this subroutine solves for the downstream        cc
cc    temperature distribution iteratively by using the cc
cc    previously calculated temperature distribution.  cc
cc    The initialtemperature distribution was calculated cc
cc    by assuming a downstream stagnation enthalpy     cc
cc    distribution.                                    cc
ccccccccccccccccccccccccccccccccccccccccccccccccccccccccc

      dimension d(10000),h1(10000),h2(10000),elta(10000)
      dimension temp1(10000),temp2(10000),temp3(10000)
      common/comf/hf(10000),tsn(10000),tso(10000),
     1 csi(10000),du(10000),ipyrol,nend,xpyrol,error,sumt,
     2 tlim,it,itmax,itchose
cc-----------------------------------------------------cc
      index=0
      h1int=0.0
      h2int=0.0
      n=nend-ipyrol+1
      error=0.0
      sumt=0.0
      alpha=1.0
      if(it.ge.itchose)alpha=0.5
      diffu=1.07573e-7
      twall=636.0
      tex=300.0
      conduc=2.678e-1
      psi=3.1415926
      do 1 istep=1,n
      temp1(istep)=hf(n+1-istep)
      tso(istep)=tsn(n+1-istep)
      if(tso(istep).le.tex) tso(istep)=tex
      if(tso(istep).ge.twall) tso(istep)=twall
      temp2(istep)=csi(n+1-istep)
    1 continue
      do 11 istep=1,n
      hf(istep)=temp1(istep)
      csi(istep)=temp2(istep)
      elta(istep)=csi(istep)
   11 continue
      do 3 istep=1,n
      d(istep)=hf(istep)/elta(istep)**0.5
      if(istep.eq.n) go to 3
      h2(istep)=d(istep)/(1.0-elta(istep))**0.5
    3 continue
```

```
      do 4 istep=1,n-2
      h2int=h2int+0.5*(h2(istep)+h2(istep+1))*
     1 (elta(istep+1)-elta(istep))
    4 continue
      h2int=h2int+(d(n-1)+d(n))*(1.0-elta(n-1))*0.5
      if(it.eq.itmax-1)then
      do 100 i=1,n
      storage1=xpyrol/elta(i)
      storage2=1.0/elta(i)
      write(6,*)elta(i),storage1,storage2,hf(i)
  100 continue
      endif
      do 5 istep=1,n
      if(istep.le.2) go to 10
      do 6 jstep=1,istep
      if(jstep.eq.istep) go to 6
      h1(jstep)=d(jstep)/(csi(istep)-elta(jstep))**0.5
    6 continue
      do 9 jstep=1,istep-2
      h1int=h1int+0.5*(h1(jstep)+h1(jstep+1))*
     1 (elta(jstep+1)-elta(jstep))
    9 continue
   10 continue
      if(istep.eq.1) go to 13
      h1int=h1int+(d(istep-1)+d(istep))*(elta(istep)-
     1elta(istep-1))**0.5
   13 cc=h1int/h2int
      if(cc.le.0.0) cc=0.0
      if(cc.ge.1.0) cc=1.0
      tsn(istep)=cc*(twall-tex)+tex
      tsn(istep)=alpha*tsn(istep)+(1.0-alpha)*tso(istep)
      if(tsn(istep).lt.tex) tsn(istep)=tex
      if(tsn(istep).gt.twall) tsn(istep)=twall
      error=abs(tsn(istep)-tso(istep))+error
      sumt=sumt+tsn(istep)
      temp3(n+1-istep)=tsn(istep)
      h1int=0.0
    5 continue
      do 12 istep=1,n
   12 tsn(istep)=temp3(istep)
      vp=(h2int/(twall-tex)/conduc)**2.0*diffu
     1*xpyrol/psi
      if(abs(error).le.abs(sumt*tlim)) index=1
      write(6,*)'vp=',vp,'index=',index
      return
      end
      subroutine plots (x,idim,imax,xaxis,y,jdim,jmax,
     1yaxes,symbol)
c*************************************************************
c                                                           c
c  xubroutine for plotting j curves of y(j,i) against x(i)c
c                                                           c
c  x and y are assumed to be in any range except that       c
c  negative values are plotted as zero. X and y are         c
```

```
c  scaled to the range 0, to 1. by division by the        c
c  maxima, which are also printed. idim is the variable   c
c  dimension for x. imax is the number of x values.       c
c  xaxis stores the name of the x-axis. jdim is           c
c  the variable dimension for y. jmax is the number of    c
c  curves to be plotted, (up to 10).The array yaxes(j)    c
c  stores the names of the curves. The array symbol(j)    c
c  stores the single characters used for plotting.        c
c                                                         c
c*********************************************************
      dimension x(idim),y(jdim,idim),yaxes(jdim),
     1 symbol(jdim),a(101),ymax(10),aa(11),ab(101)
      character*8 xaxis,yaxes(jdim),symbol(jdim)
      character*101 a(101)
      character*1 cross,dot,blank
      cross='+'
      blank=' '
      dot='.'
c******  scaling x array to the range 0 to 50
      xmax=1.e-30
      do 1 i=1,imax
    1 if(x(i).gt.xmax) xmax=x(i)
      do 2 i=1,imax
      x(i)=x(i)/xmax*50.
    2 if(x(i).lt.0.) x(i)=0.
c*****  scaling y array to the range 0 to 100
      do 3 j=1,jmax
      ymax(j)=1.e-30
      do 4 i=1,imax
    4 if(y(j,i).gt.ymax(j)) ymax(j)=y(j,i)
      do 3 i=1,imax
      y(j,i)=y(j,i)/ymax(j)*100.
    3 if(y(j,i).lt.0.) y(j,i)=0.
c*****  identifying the various curves to be plotted
      write(6,103) xaxis,xmax
      write(6,100) (yaxes(i),i=1,jmax)
      write(6,106) (symbol(i),i=1,jmax)
      write(6,102) (ymax(i),i=1,jmax)
      do 5 i=1,11
    5 aa(i)=0.1*float(i-1)
      write(6,101) (aa(i),i=1,11)
c*****  main loop. each pass produces an x-constant line.
      do 40 i=1,51
      if(i.eq.1.or.i.eq.51) go to 32
      go to 33
c*****  allocate. or + as marker on the y-axis
   32 do 30 k=1,101
   30 a(k)=dot
      do 31 k=11,101,10
   31 a(k)=cross
c***** allocate. or + mark of the x-axis, also the
c***** appropriate x value
   33 a(1)=dot
      a(101)=dot
```

```
      k=i-1
   46 k=k-5
      if (k)48,47,46
   47 a(1)=cross
      a(101)=cross
   48 xl=0.02*float(i-1)
c***** check if any y( x(i) ) calue lies on this
c***** x-constant line, if yes go to 41, otherwise
c***** go to 42
      do 43 k=1,imax
      if(ifix(x(k)+ 1.5)-i) 43,41,43
c***** locate y( x(i) )
   41 do 44 j=1,jmax
      ny=y(j,k)+ 1.5
      a(ny)=symbol(j)
   44 continue
      go to 42
   43 continue
c***** print x-constant line
   42 write(6,105) xl,(a(k),k=1,101),xl
c***** putting blanks into x-constant line
      do 49 k=1,101
   49 a(k)=blank
   40 continue
      do 50 i=1,11
   50 ab(i)=.1*float(i-1)
      write(6,104) (ab(i),i=1,11)
      return
  100 format(11h y-axes are,5x,10(1x,a10))
  101 format(1h0,2x,11f10.1)
  102 format(15h maximum values, 1p10e11.3)
  103 format(11hox-axis is ,a8,17h,maximum value =,1pe10.3)
  104 format(3x,11f10.1/1h1)
  105 format(2h x,f6.2,3x,101a1,f6.2)
  106 format(7h symbol,11x,10(1x,a10))
      end
```

Figure Captions

1-1 Schematic diagram of concurrent flow flame spread process.

2-1 Schematic diagram of the wind tunnel design.

2-2 Schematic diagram of the convergent nozzle.

2-3 Schematic diagram of the sonic nozzle orificies.

2-4 Calibrated velocity curve in the test chamber.

2-5 Schematic diagram of the thermally thick fuel (PMMA) arrangement.

2-6 Schematic diagram of the thermally thin fuel (Celluluous filter paper) arrangement.

2-7 Experimental apparatus for the study of flame spread over the surface of PMMA **0.0127** m thick.

2-8 Thermocouple measurements of the PMMA surface temperature histories.

2-9 Experimental data of the pyrolysis length versus time at various air velocities ranging from 0.5 m/s to **2.5** m/s.

2-10 Experimental data of the pyrolysis length versus time at $U_\infty = 1.5$ m/s and $Y_{o\infty}$ ranging from **0.20** to 0.50.

2-11 Experimental data of the rate of flame spread over the surface of PMMA in a concurrent gas flow of varied velocity and oxygen concentrations.

2-12 Coordinate system specified to solve equation **(2.4).**

2-13 Correlation of the PMMA experimental data with the flame spread rate of equation **(2.5)**

2-14 Experimental apparatus for the study of flame spread over thin filter paper sheets 0.3 mm thick.

2-15 Measurements of the variation with time of the pyrolysis, flame and burn-out distances for flames spreading over thin filter paper sheets in a

NIST-114A
(REV. 3-90)

U.S. DEPARTMENT OF COMMERCE
NATIONAL INSTITUTE OF STANDARDS AND TECHNOLOGY

BIBLIOGRAPHIC DATA SHEET

1. PUBLICATION OR REPORT NUMBER
NIST-GCR-92-603

2. PERFORMING ORGANIZATION REPORT NUMBER

3. PUBLICATION DATE
March 1992

4. TITLE AND SUBTITLE

Concurrent Flow Flame Spread Study

5. AUTHOR(S)

Hai-Tien Loh

6. PERFORMING ORGANIZATION (IF JOINT OR OTHER THAN NIST, SEE INSTRUCTIONS)

University of California
Dept. of Mechanical Engineering
Berkeley, CA 94720

7. CONTRACT/GRANT NUMBER
NIST Grant 60NANB7D737

8. TYPE OF REPORT AND PERIOD COVERED

9. SPONSORING ORGANIZATION NAME AND COMPLETE ADDRESS (STREET, CITY, STATE, ZIP)
U.S. Department of Commerce
National Institute of Standards & Technology
Gaithersburg, MD 20899

10. SUPPLEMENTARY NOTES

11. ABSTRACT (A 200-WORD OR LESS FACTUAL SUMMARY OF MOST SIGNIFICANT INFORMATION. IF DOCUMENT INCLUDES A SIGNIFICANT BIBLIOGRAPHY OR LITERATURE SURVEY, MENTION IT HERE.)

An experimental study has been performed of the spread of flames over the surface of thick PMMA and thin filter paper sheets in a forced gaseous flow of varied oxygen concentration moving in the direction of flame spread. It is found that the rate of spread of the PMMA pyrolysis front is time independent, linearly dependent on the gas flow velocity and approximately square power dependent on the oxygen concentration of the gas. The experimental data with thin filter paper sheets shows that the flame spread rate is independent of the flow velocity for forced flow conditions and linearly dependent on the oxygen concentration of the flow. In both experiments, it was found that the flame spread rate data can be correlated in terms of parameters deduced from heat transfer considerations only. This indicates that heat transfer from the flame to the condensed fuel is the primary mechanism controlling the spread of flame. Finite rate chemical kinetic effects have apparently a small influence on the flame process itself. Analytical and numerical methods were also employed to study theoretically the flame spread process over thermally thick fuel and the influence on the flow field behavio in the presence of a flame. It is found that an analytical model based on a quasi-steady analysis and the flame sheet approximation predicts a square power law dependence of the flame spread rate on the flow oxygen concentration and a linear dependence on the flow velocity. The correct and encouraging qualitative descriptions of the flow structure and surface fluxes in the region downstream from the pyrolysis front.

12. KEY WORDS (6 TO 12 ENTRIES; ALPHABETICAL ORDER; CAPITALIZE ONLY PROPER NAMES; AND SEPARATE KEY WORDS BY SEMICOLONS)

flame spread; oxygen concentration; paper; plastics; polymethylmethacrylate

13. AVAILABILITY

[X] UNLIMITED

[ ] FOR OFFICIAL DISTRIBUTION. DO NOT RELEASE TO NATIONAL TECHNICAL INFORMATION SERVICE (NTIS).

[ ] ORDER FROM SUPERINTENDENT OF DOCUMENTS, U.S. GOVERNMENT PRINTING OFFICE, WASHINGTON, DC 20402.

[X] ORDER FROM NATIONAL TECHNICAL INFORMATION SERVICE (NTIS), SPRINGFIELD, VA 22161.

14. NUMBER OF PRINTED PAGES
161

15. PRICE
A0

ELECTRONIC FORM